FACULDADE DE BIOCIÊNCIAS

PROGRAMA DE PÓS-GRADUAÇÃO EM BIOLOGIA CELULAR E MOLECULAR

DOUTORADO EM BIOLOGIA CELULAR E MOLECULAR

LEONARDO PEDRAZZA

USO DE CÉLULAS-TRONCO MESENQUIMAIS NO TRATAMENTO DA SEPSE E DA LESÃO PULMONAR AGUDA

Porto Alegre

2017

PONTIFÍCIA UNIVERSIDADE CATÓLICA DO RIO GRANDE DO SUL

FACULDADE DE BIOCIÊNCIAS

PROGRAMA DE PÓS-GRADUAÇÃO EM BIOLOGIA CELULAR E MOLECULAR

DOUTORADO EM BIOLOGIA CELULAR E MOLECULAR

USO DE CÉLULAS-TRONCO MESENQUIMAIS NO TRATAMENTO DA SEPSE E DA LESÃO PULMONAR AGUDA

Tese apresentada ao Programa de Pós-Graduação em Biologia Celular e Molecular da Pontifícia Universidade Católica do Rio Grande do Sul como requisito parcial para a obtenção do grau de Doutor em Biologia Celular e Molecular.

LEONARDO PEDRAZZA

ORIENTADOR: Prof. Dr. Jarbas Rodrigues de Oliveira

Porto Alegre

2017

Ficha Catalográfica

P371u Pedrazza, Leonardo

Uso de células-tronco mesenquimais no tratamento da sepse e da lesão pulmonar aguda / Leonardo Pedrazza . – 2017.
145 f.
Tese (Doutorado) – Programa de Pós-Graduação em Biologia Celular e Molecular, PUCRS.

Orientador: Prof. Dr. Jarbas Rodrigues de Oliveira.

1. Sepse. 2. infecção pulmonar aguda. 3. células-tronco. I. de Oliveira, Jarbas Rodrigues. II. Título.

Elaborada pelo Sistema de Geração Automática de Ficha Catalográfica da PUCRS
com os dados fornecidos pelo(a) autor(a).

“NOTHING IN LIFE IS TO BE FEARED, IT IS ONLY TO BE UNDERSTOOD. NOW IS THE TIME TO UNDERSTAND MORE, SO THAT WE MAY FEAR LESS.” – MARIE CURIE

Dedico aos meus pais, pelo amor

incondicional e por todo apoio nessa jornada.

AGRADECIMENTOS

Agradeço primeiramente ao Prof. Dr. Jarbas Rodrigues de Oliveira pela oportunidade de trabalhar em seu laboratório e me auxiliar no desenvolvimento deste trabalho.

Ao Prof. Dr. José Luis Rosa por me acolher em seu laboratório durante o período que estive em Barcelona, seus ensinamentos foram essenciais para a condução de todo o trabalho.

A todos meus colegas de laboratório, em especial a Fernanda Mesquita, Eduardo Caberlon, Gabriel Viegas e Taiane Schneider, pelo auxílio, paciência e companheirismo durante esta trajetória.

Agradeço a minha família pelo apoio, compreensão e amor durante esse período.

E por fim, um agradecimento muito especial às pessoas mais importantes neste trabalho que sempre estiveram comigo na bancada e me ajudaram nas situações mais complicadas, Carolina Luft e Monica Cubillos. Sem vocês este trabalho não seria possível.

RESUMO

As células-tronco mesenquimais (MSC) foram identificadas primeiramente por Friedenstein e Petrakova (1966), que isolaram estas células progenitoras a partir da medula óssea de rato e observaram serem capazes de se diferenciarem em linhagem de tecido conectivo, incluindo osso, tecido adiposo, cartilagem e músculo. As MSCs surgiram nos últimos anos como ferramentas terapêuticas baseadas em quatro características importantes: potencial de diferenciação, capacidade para modular a resposta imune, capacidades pró-angiogênicas promovendo regeneração tecidual, e baixa imunogenicidade, sendo que esta última característica pode permitir tratamentos alogênicos. Com base nas suas propriedades imunomoduladoras e efeitos parácrinos através de fatores tróficos com propriedades anti-fibróticas, anti-apoptóticas ou pró-angiogênicas, as MSCs são consideradas um instrumento promissor para a terapia celular, em particular para doenças inflamatórias. As MSCs regulam as funções de uma ampla gama de células imunes, e são ativadas por mediadores inflamatórios liberados de células imunes ativadas. Os mecanismos envolvidos na atividade imunorreguladora de MSCs estão ainda sob investigação. Desta forma, as células-tronco mesequimais se tornam uma potencial alternativa de tratamento para a sepse e para infecção pulmonar aguda, podendo levar a interrupção do curso da patogênese, e provocar a redução da mortalidade de ambas patologias. O principal objetivo deste trabalho foi avaliar o efeito terapêutico e imunomodulador de células-tronco mesenquimais no tratamento da sepse e da lesão pulmonar aguda e buscar os seus possíveis mecanismos de ação. Nossos resultados demonstraram pela primeira vez, que a redução da inflamação na sepse provocada pelo tratamento com células-tronco mesenquimais está diretamente envolvido a inibição da via das proteínas ativadas por mitógenos (MAPKs) e que as MSCs foram incapazes de modular a expressão de receptores do tipo toll. Durante a lesão pulmonar aguda (LPA) ficou evidente a imunomodulação provocada pelo tratamento e a diminuição do estresse oxidativo que consequentemente ocasionou a uma diminuição da formação das redes extracelulares de neutrófilos (NETs), levando a um aumento na sobrevida dos animais com LPA. Os resultados promissores obtidos neste estudo são encorajadores e sugerem que as MSCs podem ser uma opção terapêutica para tratar a sepse e a lesão pulmonar aguda em pacientes no futuro.

Palavras-chave: sepse, infecção pulmonar aguda, células-tronco mesenquimais, inflamação.

ABSTRACT

Mesenchymal stem cells (MSC) were first identified by Friedenstein and Petrakova (1966), who isolated these progenitor cells from rat bone marrow and found that these cells are able to differentiate into connective tissue lineage including bone, adipose tissue, cartilage and muscle. MSCs have emerged in recent years as therapeutic tools based on four important features: differentiation potential, capacity to modulate immune responses, pro-angiogenic and repair promoting capacities, and low immunogenicity, the latter feature may allow allogeneic treatments. Based on their immunomodulatory properties and paracrine effects through trophic factors with anti-fibrotic, anti-apoptotic or pro-angiogenic properties, MSCs are considered a promising instrument for cell therapy, in particular for inflammatory diseases. MSCs regulate the function of a broad range of immune cells, and are activated by inflammatory mediators released from activated immune cells. The mechanisms involved in the immunoregulatory activity of MSCs are still under investigation. Therefore, MSCs become a potential treatment alternative for sepsis and for acute lung infection, which may lead to the interruption of the sequence in the pathogenesis and cause mortality reduction of both pathologies. The principal objective of this study was to evaluate the therapeutic and immunomodulatory effect of MSCs in the treatment of sepsis and acute lung injury and search for their possible mechanisms of action. Our results demonstrated for the first time that the reduction of inflammation in sepsis caused by treatment with MSCs is directly involved in the inhibition of the pathway of mitogen-activated proteins (MAPKs) and that MSCs were unable to modulate the expression of toll-like receptors. During acute lung injury (ALI), the immunomodulation caused by the treatment and the decrease of the oxidative stress that consequently led to a decrease in the formation of extracellular neutrophil network (NETs), leading to an increase in the survival of animals with LPA. The promising results obtained in these studies are encouraging and suggest that MSCs might be a therapeutic option to treat sepsis and acute lung infection in patients in the future.

Keywords: Sepsis, acute lung injury, mesenchymal stem cells, inflammation.

LISTA DE FIGURAS

CAPÍTULO I

LISTA DE ABREVIATURAS

AMs - Antimicrobianos

CAT – Catalase

COX-2 – ciclooxigenase-2

DCF – Diclorofluoresceina

ERK – Quinase regulada por sinal extracelular

FGF – Fator de crescimento fibroblástico

FiO_2 – Fração inspirada de oxigênio

GPX – Glutationa Peroxidase

HGF – Fator de crescimento de hepatócitos

IGF-1 – Fator de crescimento semelhante à insulina

IL-1 – Interleucina 1

IL-4 – Interleucina 4

IL-6 – Interleucina 6

IL-8 – Interleucina 8

IL-10 – Interleucina 10

IL-13 – Interleucina 13

JNK – c-Jun N-terminal quinase

LPA – lesão aguda pulmonar

LPS – Lipopolissacarídeo

MAPK – Mitogen-Activated Protein Kinase

MSCs – Células-Tronco Mesenquimais

NETs – Redes neutrofílicas extracelulares

NF-κB – nuclear factor kappa B

PAF – Fator Ativador Plaquetário

PAM – Pressão Arterial Média

PaO_2 – Pressão Parcial de Oxigênio Arterial

PAs – Pressão Arterial Sistólica

PEEP – Pressão positiva expiratória final

RLs – Radicais Livres

ROS – Espécies Reativas de Oxigênio

SOD – Superóxido Dismutase

SOFA - Escore sequencial de falência orgânica

SDRA – Síndrome do desconforto respiratório agudo

TBARS – Espécies Reativas do Ácido Tiobarbitúrico

TGF-β – Fator de Crescimento Tumoral Beta

TNF-α – Fator de Necrose Tumoral Alfa

UTI – Unidade de Terapia Intensiva

SUMÁRIO

CAPÍTULO 1

INTRODUÇÃO

1. Introdução

1.1 Sepse

A sepse é uma síndrome complexa de origem infecciosa, ocasionando uma resposta inflamatória sistêmica descontrolada do indivíduo. É caracterizada por manifestações múltiplas que podem determinar disfunção ou até mesmo a falência de um ou mais órgãos, e consequentemente sua morte. Seus fatores fisiopatológicos incluem, principalmente, o local da infecção, sendo os sistemas da coagulação, fibrinolítico e inflamatório os determinantes de sua evolução[1].

O termo septicemia vem sendo usado desde a Grécia antiga para descrever casos onde havia putrefação associado com doença e morte[2]. Esta patologia foi descrita primeiramente por Tilney *et al*[3] em 1973, como "falência sistêmica seqüencial", abrangendo três pacientes que evoluíram para óbito por falência orgânica. Em 1975 Baue[4] descreveu três pacientes como "falência orgânica sistêmica progressiva, múltipla ou seqüencial".

Devido a esta grande quantidade de termos sinônimos para designar a mesma condição clínica e a sua gravidade, em agosto de 1991, uma nova definição foi estabelecida pelo *American College of Chest Physicians* e a *Society of Critical Care Medicine*, determinando assim um consenso sobre as definições e os critérios para o diagnóstico da sepse[5]. Em 2001, a *International Sepsis Definitions Conference* (Tabela 1), congregando um maior número de pesquisadores e peritos de várias partes do mundo, optou por não modificar as definições vigentes e sim por ampliar a lista de sinais e sintomas da sepse[6].

Tabela 1- Critérios para diagnóstico na sepse

Infecção documentada ou suspeita e algum dos seguintes critérios:

– Variáveis gerais

Febre (temperatura central > 38,3º C)

Hipotermia (temperatura central < 36º C)

Freqüência cardíaca > 90 bpm ou > 2 DP acima do valor normal para a idade

Taquipnéia

Alteração de sensório

Edema significativo ou balanço hídrico positivo (> 20 ml/kg/24 horas)

Hiperglicemia na ausência de diabete (glicemia > 120 mg/dl)

– Variáveis inflamatórias

Leucocitose (contagem leucócitos totais > 12.000 / mm^3)

Leucopenia (contagem leucócitos totais < 4.000 / mm^3)

Contagem de leucócitos totais normal com > 10% de formas imaturas

Proteína C-reativa no plasma > 2 DP acima do valor normal

Procalcitonina plasmática > 2 DP acima do valor normal

– Variáveis hemodinâmicas

Hipotensão arterial (PAs < 90 mmHg, PAM < 70 mmHg, ou

Redução da PAs > 40 mmHg em adolescentes, ou PAs / PAM < 2 DP abaixo do normal para idade)

Saturação de oxigênio venoso misto > 70% (não válido para crianças)

Índice cardíaco > 3,5 L/min (não válido para crianças)

– Variáveis de disfunção de órgãos

Hipoxemia arterial (PaO_2 / FiO_2 < 300)

Oligúria aguda (diurese < 0,5 mL/kg/h)

Creatinina > 0,5 mg/dL

Alterações de coagulação (INR > 1,5 ou TPPA > 60 s)

Íleo (ausência de ruídos hidroaéreos)

Trombocitopenia (contagem de plaquetas < 100.000 / mm^3)

Hiperbilirrubinemia (Bilirrubina total > 4 mg/dL)

– Variáveis de perfusão tecidual

Hiperlactatemia (> 1 mmol/L)

Enchimento capilar reduzido ou moteamento

BPM: batidas por minuto; DP: desvio padrão; PAs: pressão arterial sistólica; PAM: pressão arterial média; PaO_2: pressão parcial de oxigênio; FiO_2: fração inspirada de oxigênio; INR: razão normalizada internacional; TTPA: tempo de tromboplastina parcial ativada.

A *Society of Critical Care Medicine (SCCM)* e a *European Society of Intensive Care Medicine (ESICM)* convocaram uma força-tarefa internacional para revisar as definições de sepse e choque séptico em janeiro de 2014. Em fevereiro de 2016, este último consenso foi publicado no periódico JAMA[7,8] e posteriormente apresentado no *45th Critical Care Congress em 2016*. Para facilitar o diagnóstico da sepse, foi identificado um novo critério clínico que pode ser utilizado em emergênicas hospitalares, para rapidamente avaliar e diagnosticar pacientes com sepse.

A nova ferramente diagnóstica é denomida quickSOFA (escore sequencial de falência orgânica) ou qSOFA. Consiste em 3 testes clínicos que são conduzidos no leito

do paciente para identificar o risco para o desenvolcimento da sepse. O acesso ao qSOFA é feito por 3 sinais clínicos:

- Alteração do estado mental.

- Diminuição da pressão sistólica abaixo de 100 mmHg.

- Frequência respiratória maior que 22 respirações/min.

Dados indicam que pacientes com 2 ou mais destas condições tem um significante risco de prolongar sua estadia na UTI (3 ou mais dias) ou morrer no hospital. Para esses pacientes, recomenda-se aos médicos uma investigação maior sobre a disfunção orgânica, iniciem ou intensifiquem a terapia conforme apropriado e considerem o encaminhamento para cuidados intensivos ou aumentem a freqüência de monitoramento dos pacientes. Se os pacientes possuem 2 ou 3 componentes do qSOFA, devem ser examinados para falência orgânica e para tanto, dois novos critérios clínicos foram identificados e devem ser utilizados para o diagnóstico de pacientes com choque séptico, que são[7,8]:

- Persistente hipotensão requerendo vasopressores para manter Pressão Arterial Media ≥65 mmHg.

- Lactato sanguíneo ≥2 mmol/L, apesar de volume adequado de ressuscitação.

Os dados indicam que as taxas de mortalidade dos pacientes com estas duas condições são superiores a 40%, ou quatro vezes maior do que os pacientes com sepse. As novas recomendações representam um importante avanço, mas certamente não o último no estudo em evolução da sepse[7,8]. Essas definições atualizadas denominadas "Sepsis-3", devem oferecer maior consistência para estudos epidemiológicos e ensaios clínicos e facilitar o reconhecimento prévio e o manejo mais oportuno de pacientes com sepse ou com risco de desenvolver a sepse.

1.1.1 Epidemiologia

A sepse tem representado um grave problema epidemiológico para os sistemas de saúde em todo o mundo, tanto do ponto de vista econômico como social. Atualmente a sepse acomete cerca de 18 milhões de pessoas por ano no mundo. De acordo com um estudo epidemiológico nos EUA, a incidência da sepse aumentou de 82,7 para 240,4/100 mil habitantes, bem como as mortes relacionadas a ela, ainda que a taxa de mortalidade geral entre os pacientes com sepse tenha sido reduzida nesse período[9].

A incidência da sepse relatada na literatura pode variar de acordo com as características de cada região e local, sendo que nos EUA e Europa, a sepse é responsável por 2-11% das internações em UTI. Análise retrospectiva de Jacobs *et al*[10], em mais de 2.000 admissões de uma UTI pediátrica, identificou 42,5% de pacientes com doença infecciosa, dos quais 63% destes evoluíram para o estado de choque séptico. Proulx *et al*[11], avaliando 1.058 admissões em UTI pediátrica do hospital universitário canadense, identificaram 82% de síndrome da resposta inflamatória sistêmica (SRIS), sendo 23% de etiologia infecciosa (sepse), das quais 2% com choque séptico. No Brasil a incidência da mortalidade provocada pela sepse e suas conseqüências varia de 40 a 45%, conforme dados do *Brazilian Sepsis Epidemiological Study*[12.]

Estudos epidemiológicos mais recentes revelam que as bactérias Gram-positivas se tornaram a causa mais comum de sepse nos últimos 25 anos [13]. De acordo com as estimativas mais recentes na sepse, há cerca de 200.000 casos de sepsis Gram-positiva (maior incidência de *Staphylococcus aureus, Streptococcus pneumoniae, Enterococcus* spp) a cada ano, em comparação com aproximadamente 150.000 casos de sepsis Gram-negativa (maior incidência de *Escherichia coli, Pseudomonas aeruginosa, Klebsiella pneumonia*) nos EUA [14].

Embora as causas bacterianas da sepse tenham aumentado com o aumento geral da incidência, as causas fúngicas da sepse têm crescido a um ritmo ainda mais rápido. Isso pode representar um aumento geral nos casos de sepse nosocomial, promovendo assim infecções fúngicas para um papel mais importante[13].

1.1.2 Resposta do Organismo à Infecção na Sepse

A inflamação é uma resposta normal do hospedeiro contra agentes infecciosos. A sepse é caracterizada pela produção excessiva de mediadores inflamatórios, assim como pela expressiva ativação de células inflamatórias, resultando em uma anarquia metabólica[15].

Quando a infecção ou bacteremia ocorre, a primeira linha de defesa do hospedeiro é realizada por células fagocitárias (macrófagos, monócitos e granulócitos polimorfonucleares) e pela via alternativa do complemento, agindo de maneira não específica. Posteriormente, as imunoglobulinas e as células imunocompetentes iniciam à resposta imune específica[15,16].

Os componentes da parede bacteriana, onde se destacam as endotoxinas (lipopolissacárideos) dos microorganismos gram-negativos (principalmente o lipídio A) e o ácido teicóico dos microorganismos gram-positivo são os principais ativadores da resposta do hospedeiro. Eles desencadeiam a cascata inflamatória através da indução da produção de citocinas pelos macrófagos e monócitos, que, quando ativados, produzem sequencialmente, Fator de Necrose Tumoral Alfa (TNF-α), Interleucina-1 (IL-1), Interleucina-6 (IL-6) e a Interleucina-8 (IL-8) que interagem com outras células e elementos celulares (polimorfonucleares, células endoteliais, fibroblastos, plaquetas e os próprios monócitos), induzindo a produção e liberação de mediadores secundários, contribuindo para uma resposta inflamatória tardia[16,17] (Figura 1).

Paralelamente à liberação das citocinas pró-inflamatórias, o organismo responde a agentes infecciosos, liberando citocinas antiinflamatórias como Interleucina 4 (IL-4), Interleucina 10 (IL-10), Interleucina 13 (IL-13), Fator de Crescimento Tecidual Beta (TGF-β), entre outras. Estes mediadores parecem tanto contrabalançar as ações dos

mediadores pró-inflamatórios, através da redução da síntese e da liberação desses mediadores, quanto antagonizar seus efeitos [18,19].

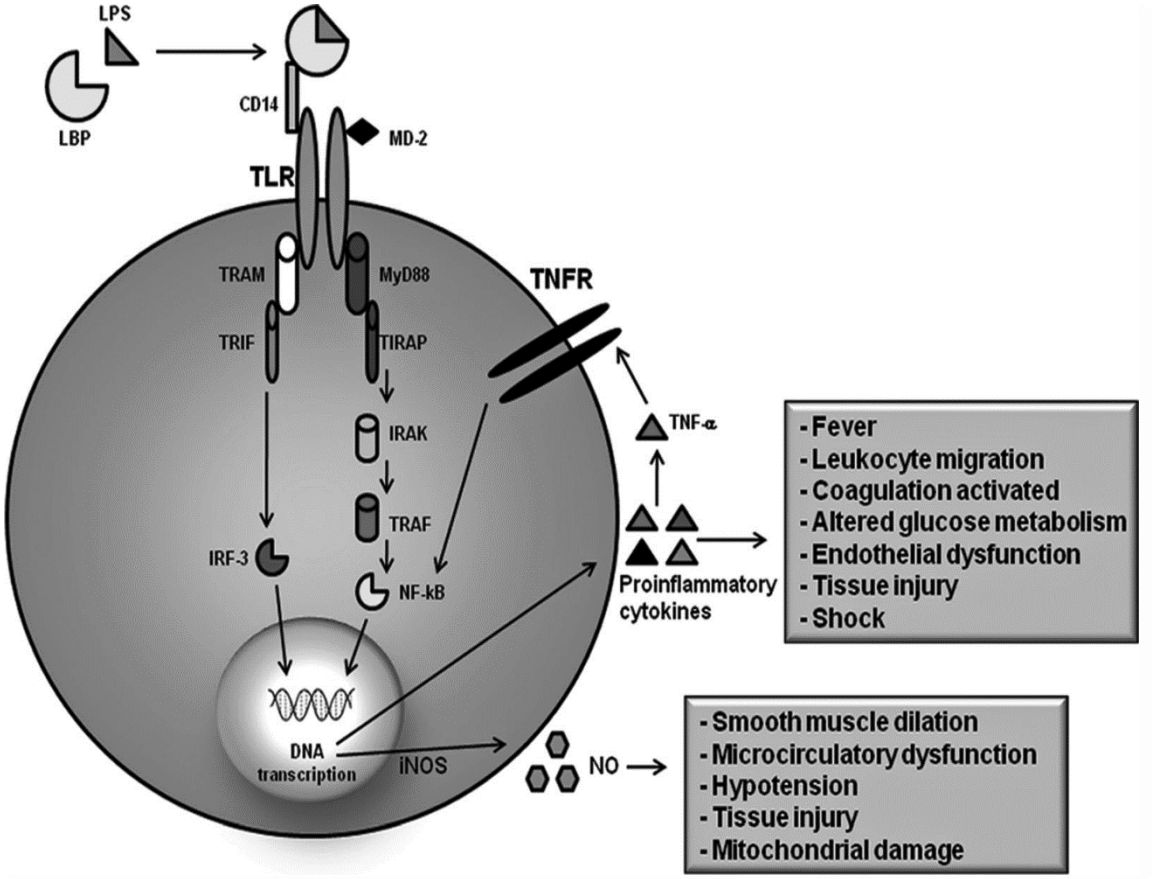

Figura 1 - **Início da resposta séptica.** Representação esquemática do reconhecimento do LPS e início da resposta séptica por células hospedeiras. LPS e outros padrões moleculares bacterianos são reconhecidos pelas células hospedeiras e produzem uma resposta via TLRs e suas vias descendentes. A ativação de vias associadas a TLR leva à ativação de factores de transcrição incluindo NF-κB e o fator de liberação de insulina (IRF-3). Isto resulta na produção de citocinas pró-inflamatórias e espécies reativas de oxigénio que desempenham um papel central na patogênese da sepse e podem propagar ainda mais a resposta inflamatória, por exemplo, através de receptores de factor de necrose tumoral [15].

As células endoteliais possuem um importante papel na homeostasia, regulação do tônus vascular e fibrinólise[20,21] e quando ativadas diretamente pelas endotoxinas ou citocinas, adquirem função pró-coagulante e protrombótica, provocadas pela liberação de tromboplastina, inibidor do ativador do plasminogênio e do fator ativador

plaquetário (PAF), além da diminuição da produção de trombomodulina. Elas também produzem mediadores inflamatórios, tais como as Interleucinas (IL-1, IL-6 e IL-8), prostaciclina, endotelina (capaz de aumentar o tônus vascular) e o óxido nítrico[22,23]. A destruição local do endotélio pela aderência de polimorfonucleares ativos causa aumento da permeabilidade e edema tecidual, que contribui para a ampliação da reação inflamatória[21].

Alterações nas dimensões dos pequenos vasos, juntamente com alterações bioquímicas e fisiológicas sangüíneas, prejudicam a homeostasia da microcirculação durante o choque séptico, sendo esse o principal sítio de ataque, podendo tornar-se uma área fértil para o crescimento bacteriano descontrolado[18]. Um importante fator precipitante é a diminuição da deformidade dos eritrócitos, que depende das propriedades viscoelásticas da membrana celular, viscosidade do citoplasma e da razão entre a área de superfície corpórea e o seu volume, podendo estar todos estes fatores alterados, devido à acidose, hipotermia e alterações na geometria da hemácia. Estas alterações, somadas a vasodilatação, levam à falta de oxigenação nos tecidos e à lesão celular[22].

1.1.3 MAPKs e Sepse

As proteínas quinases ativadas por mitógenos (MAPK) são um grupo de proteínas quinases serina/treonina que são altamente conservadas em todas as espécies eucarióticas. As MAPKs têm papel importante nos processos celulares, tais como proliferação, respostas ao estresse, apoptose e defesa imunológica. Em organismos multicelulares, MAPKs são necessários para diferenciação celular, desenvolvimento, aprendizagem, memória e secreção de fatores parácrinos e autócrinos. Em células de mamíferos, existem três vias de MAPK bem definidos: a via da quinase regulada por sinal extracelular (ERK), a via da c-JUN N-terminal quinase (JNK, também conhecida como MAPK8) e a p38 (também conhecida como MAPK14) [24].

As MAPKs ativadas podem fosforilar uma vasta gama de alvos '*downstream*', incluindo proteínas quinases e fatores de transcrição, que facilitam a transcrição de

genes regulados por MAPK. Além da regulação transcricional, as MAPKs também podem regular a expressão gênica de seus alvos, alterando a estabilidade, o transporte e a tradução do mRNA. Estas cascatas de sinalização não estão apenas envolvidas em processos celulares normais, mas também têm sido implicadas na patologia de muitas doenças, incluindo cancro, aterosclerose, diabetes, artrite e choque séptico[25].

A produção de muitos mediadores inflamatórios, tais como o fator de necrose tumoral (TNF), interleucina-1β (IL-1β) e a IL-6, bem como a prostaglandina e o óxido nítrico (sintetizados pela ciclooxigenase-2 (COX2) e óxido sintase (iNOS) respectivamente), são reguladas positivamente por MAPKs. Em vários modelos de inflamação sistémica, incluindo a modelos de sepse em camundongos, foi demosntrado que as MAPKs são mediadores chave que conduzem à produção de citocinas inflamatórias durante a sepse[26].

1.1.4 Tratamento da sepse

A resposta inflamatória sistêmica da sepse pode se restringir a um fenômeno auto-limitado ou pode progredir para quadros de maior gravidade, como sepse grave, choque séptico e disfunção ou falência de um ou mais órgãos. Apesar da grande quantidade de investigações e de relatos sobre sepse e síndromes correlatas nos últimos anos, o controle definitivo do foco infeccioso é imperativo no tratamento, sendo a primeira prioridade. Contudo, além das medidas de suporte de vida, quando indicadas, outras medidas devem ser tomadas de acordo com a gravidade de apresentação da respectiva síndrome[27].

Os antimicrobianos (AMs) são os agentes mais específicos e acessíveis para o tratamento do paciente com infecção, embora representem uma abordagem somente parcial do problema. Nas últimas quatro décadas, os estudos sobre o efeito do uso de AMs nas infecções graves por germes gram-positivos ou gram-negativos têm demonstrado uma considerável redução da morbidade e da mortalidade. Os AMs podem ser mais úteis no tratamento de estágios clínicos precoces da sepse ou bacteremia, antes que a produção seqüencial dos mediadores da inflamação do

hospedeiro determine estágios mais adiantados na cascata inflamatória, com eventuais danos teciduais graves[28]. Entretanto, alguns autores sustentam a idéia de que os AMs podem exacerbar a resposta inflamatória devido à lise dos microrganismos, com liberação de material de sua parede celular e consequente produção de mediadores inflamatórios endógenos[29].

Nos últimos 30 anos, 38 novos agentes terapêuticos experimentais foram submetidos a ensaios clínicos avançados de Fase II ou Fase III em doentes com sepse, mas nenhum resultou em quaisquer achados positivos significativos. Mais recentemente, a utilização de Drotrecogin alfa não confirmou os resultados positivos obtidos em estudos pré-clínicos[30]. Atualmente, vem sendo testadas estratégias para modular a excessiva geração ou ação de mediadores na sepse. A intervenção em qualquer passo da sequência dos eventos fisiopatológicos que caracterizam a resposta inflamatória sistêmica da sepse, no sentido de modificar (modular) essa reação do hospedeiro, parece ser a estratégia terapêutica com maiores perspectivas de mudar os resultados na terapia da sepse. Infelizmente, o uso clínico de terapias bloqueadoras de mediadores específicos tem falhado em reduzir a mortalidade geral associada à sepse. Contudo, a interrupção da seqüência, na patogênese, em múltiplos pontos, é a melhor chance na redução da alta mortalidade atual desta patologia[31].

1.1.5 Células-Tronco Mesenquimais (MSCs) e Sepse

As células-tronco mesenquimais foram identificadas primeiramente por Friedenstein e Petrakova (1966), que isolaram estas células progenitoras a partir da medula de ratos e observaram serem estas células capazes de se diferenciarem em linhagem de tecido conectivo, incluindo osso, tecido adiposo, cartilagem e músculo[32].

Nos últimos anos, foi descoberto que as células-tronco mesenquimais são potentes moduladoras da resposta imune. Estas células apresentam um elevado grau de quimiotaxia, baseado em citocinas pró-inflamatórias, localizando tecidos inflamados e neoplásicos[33,34,35]. Acredita-se que a capacidade proliferativa e pluripotente destas células seja independente do tecido de origem, desde que cultivadas em condições

adequadas. Morfologicamente, estas células apresentam-se fusiformes, assemelhando-se a fibroblastos[36,37].

O tecido adiposo representa uma fonte abundante e acessível de células-tronco adultas que podem se transformar em diversas linhagens celulares. As células derivadas do tecido adiposo possuem grande similaridade com células mesenquimais encontradas na medula óssea, e seu processo de coleta é menos invasivo[38].

Em situações clínicas agudas, como a sepse, poderia ser impossível a obtenção de células-tronco autólogas em número suficiente para ter um efeito terapêutico. Entretanto, evidências sugerem que as MSCs podem ser "imunoprivilegiadas" na medida em que estas células, mesmo alogeneticamente ou xenogênicas quando são transplantadas, podem ter uma habilidade inata para evitar a detecção pelo sistema imune do destinatário. Isto levanta a possibilidade para transplante não autólogos de MSCs como uma estratégia terapêutica. Embora mais pesquisas sobre o seu uso no tratamento em diferentes patologias sejam necessárias, é possível que MSC alogênicas possam ser mantidas em "bancos de células" e utilizadas terapeuticamente quando indicadas, eliminando assim a necessidade de obter células autólogas e expandi-las na fase aguda[39,40,41].

As células-tronco são potentes fontes de citocinas antiinflamatórias como fator de crescimento tecidual-β (TGF- β), IL-10 e IL-13. Além disso, atenuam a inflamação, causando uma diminuição de citocinas pró-inflamatórias como TNF-α, IL-1, IL-6[42,43,44].

Acredita-se que a sua propriedade antiinflamatória e citoprotetora aumenta para um grau ainda maior quando as células-tronco são expostas a ambientes nocivos semelhantes aos encontrados durante a sepse. Estas características das células-tronco podem ser úteis no seu uso como agentes terapêuticos da sepse (Figura 2).

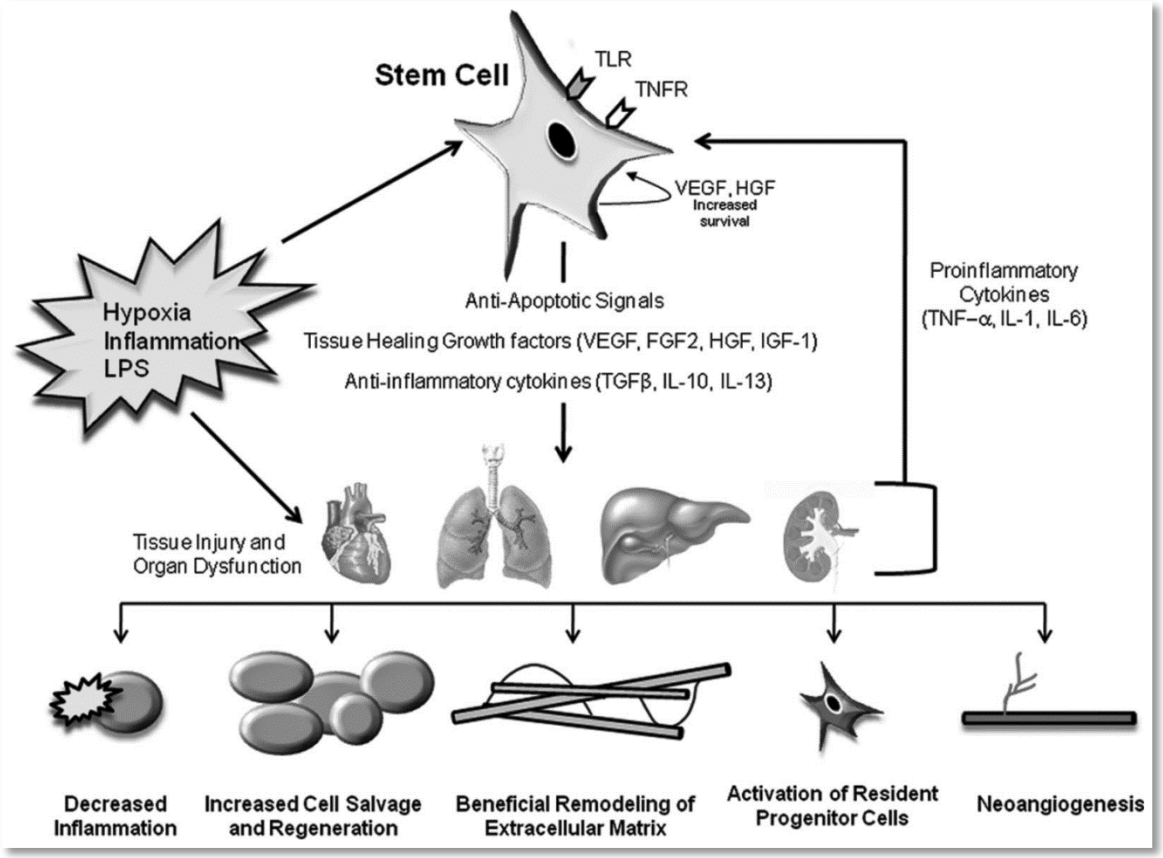

Figura 2 - **Atuação das células-tronco durante a sepse.** Mecanismos propostos pelos quais as células-tronco podem oferecer benefício terapêutico na sepse. As células-tronco transplantadas, estimuladas pelos ambientes nocivos encontrados na sepse, produzirão fatores citoprotetores, antiapoptóticos e anti-inflamatórios que podem desempenhar um papel na atenuação da resposta inflamatória do hospedeiro e da lesão tecidual resultante durante a sepse. Esta resposta pode ser mediada por TLRs e receptores de fator de necrose tumoral em superfícies de células-tronco. Os fatores de crescimento produzidos pelas células-tronco, incluindo VEGF, FGF2, IGF-1 e HGF, podem melhorar a vascularização do tecido hipóxico, melhorar a cicatrização e regeneração do tecido, estimular a proliferação de células estaminais residentes e promover a auto-sobrevivência. Os mediadores anti-inflamatórios produzidos pelas células-tronco tais como o TGFβ, IL-10 e IL-13 podem atenuar a inflamação e os seus efeitos potencialmente prejudiciais. Alem disso, as células-tronco podem causar uma diminuição da apoptose e melhor remodelação da matriz extracelular resultando em tecido mais saudável e viável[15].

Em um modelo de lesão pulmonar induzida por LPS, níveis reduzidos de citocinas pró-inflamatórias após o transplante de células-tronco foram associados com menor formação de edema pulmonar, redução da permeabilidade do epitélio alveolar, e um tempo de sobrevida maior. Estes benefícios são reforçados através de fatores citoprotetores e proangiogênicos, secretados pelas células-tronco como VEGF (fator de crescimento vascular endotelial), fator de crescimento de hepatócitos (HGF), fator de

crescimento semelhante à insulina (IGF-1), e fator de crescimento fibroblástico (FGF)[45,46].

A capacidade das células-tronco de reduzirem a apoptose celular pode conferir ainda uma outra fonte de benefício para o seu uso na sepse. As células-tronco têm demonstrado aumento da regulação de expressão de proteínas anti-apoptóticas, tais como a Bcl-2 e a diminuição da expressão de proteínas pró-apoptóticas, tais como caspases[47].

Estudos já demonstraram que em modelos experimentais de sepse, o tratamento com células-tronco mesenquimais foi efetivo. Os principais fatores positivos associados ao aumento da sobrevida animal durante a sepse nesses estudos estão relacionados ao fato destas células reduzirem a resposta inflamatória local e sistemicamente, inibirem a apoptose em tecidos lesados, estimulando a neoangiogênese, aumento da depuração bacteriana, redução da atividade deletéria dos neutrófilos em tecido lesados e o favorecimento à formação de linfócitos regulatórios, entre outros[33,48,49,50].

1.2 Lesão Pulmonar Aguda (LPA)

A lesão pulmonar aguda (LPA) e síndrome do desconforto respiratório agudo (SDRA) descrevem síndromes clínicas de insuficiência respiratória aguda com substancial morbidade e mortalidade. Mesmo em pacientes que sobrevivem à LPA, há evidências de que a sua qualidade de vida ao longo dos anos é adversamente afetada[51].

Ashbaugh e colaboradores em 1967 foram os primeiros a usar a síndrome do SDRA para descrever um estudo de coorte composto por 12 pacientes criticamente doentes com insuficiência respiratória aguda[52].

Em 1994, depois de décadas de diferentes definições foi estabelecida pelo American-European Consensus Conference Comittees, e essa foi amplamente adotada por clínicos e pesquisadores da área na identificação da LPA. Segundo o consenso, a LPA

foi conceituada como uma síndrome caracterizada por inflamação pulmonar aguda e persistente, com edema pulmonar devido ao aumento da permeabilidade vascular, associada a três achados clínicos[53]:

1. Infiltrado radiológico alveolar bilateral;

2. Relação entre a pressão parcial de oxigênio arterial e a fração inspirada de oxigênio (PaO2/FiO2) entre 201 e 300 mmHg, independente do valor da pressão positiva expiratória final (PEEP);

3. Ausência de evidência clínica de elevação da pressão atrial esquerda.

A SDRA, por sua vez, apresenta definição semelhante à LPA, exceto pela presença de hipoxemia grave, identificando-se uma relação entre PaO2/FiO2 igual ou menor a 200 mmHg, independente do valor PEEP. Portanto, considera-se que a SDRA representa o estágio mais grave do espectro da LPA[54].

A probabilidade de um paciente desenvolver LPA aumenta à medida que um ou mais fatores de risco estão presentes. Por essa razão, é de fundamental importância identificar o paciente de risco, pois quanto mais precocemente se intervém na causa de base, melhor será o prognóstico.

Os fatores de risco mais comumente relacionados à LPA são os seguintes [55]:

- Dano direto: aspiração, infecção pulmonar difusa (pneumonia), inalação tóxica, contusão pulmonar, embolia gordurosa e toxicidade pelo oxigênio.
- Dano indireto: sepse, politraumatismo, politransfusão, choque, queimaduras, pancreatite, “by-pass” cardiopulmonar, intoxicação exógena, coagulação intravascular disseminada e excesso de fluidos.

Histologicamente, a LPA é caracterizada pela presença de dano alveolar difuso. O padrão da lesão envolve três fases histopatológicas distintas[55]:

- Fase exudativa: caracterizada por edema intersticial e alveolar, bem como pela formação de membranas hialinas. Ocorre na primeira semana de evolução do quadro;

- Fase proliferativa: caracterizada pela melhora do edema pulmonar, pela proliferação de pneumócitos do tipo II, infiltração intersticial por miofibroblastos e deposição de colágeno;
- Fase fibrótica: ocorre em pacientes com doença prolongada, caracterizada por alteração da "arquitetura" pulmonar normal, fibrose difusa e formação de cistos.

É importante salientar que as três fases histológicas da lesão não necessariamente ocorrem em todos os pacientes com LPA.

A incidência de LPA é difícil de ser mensurada devido às definições não uniformes, variações etiológicas, variação geográfica, documentação inadequada e sub-reconhecimento da entidade da doença. A taxa de mortalidade dessa síndrome clínica chega a 40%, sendo que a maioria das mortes ocorre por disfunção de múltiplos órgãos e, apenas uma pequena porcentagem, morre propriamente por insuficiência respiratória[51,56].

1.2.1 Patogenicidade

A lesão pulmonar aguda é uma doença de inflamação aguda que provoca perturbações do endotélio pulmonar e das barreiras epiteliais. A membrana alveolo-capilar é formada pelo endotélio microvascular, interstício e epitélio alveolar. Características celulares da LPA incluem a perda da integridade da membrana alvéolo-capilar, a migração excessiva de neutrófilos transepiteliais, liberação de citocinas pró-inflamatórias e mediadores citotóxicos[57] (Figura 3).

Biomarcadores encontrados no epitélio e endotélio e que estão envolvidas nas cascatas de coagulação e inflamatórios são indicadores de morbilidade e mortalidade na LPA. Após uma infecção ou trauma, o aumento de citocinas pró-inflamatórias ocorre como uma resposta direta e/ou como um marcador de lesão celular em curso. Meduri e colaboradores descreveram que os níveis plasmáticos persistentemente elevados de interleucinas (IL-6 e IL-8) e do fator de necrose tumoral (TNF-α) estão fortemente

associados a um aumento da mortalidade. Na figura três podemos ver o processo inflamatório pulmonar na LPA[58,59,60].

Com a inflamação, as barreiras habitualmente responsáveis por impedir o edema alveolar são perdidas, havendo escape de proteínas do espaço intravascular em direção ao espaço intersticial, promovendo edema intersticial e alveolar. O influxo de líquido com elevada concentração de proteínas para o interior dos alvéolos altera a integridade do surfactante pulmonar, lesiona o tecido pulmonar e causa um colapso alveolar. Alterações na coagulação e na fibrinólise também ocorrem na lesão pulmonar, especificamente na proteína C e o no inibidor do ativador de plasminogênio tipo 1[61,62].

A migração de neutrófilos transepiteliais é uma característica importante de lesão pulmonar aguda pois os neutrófilos são os primeiros envolvidos na inflamação. A ativação excessiva e/ou prolongada de neutrófilos contribuem para a destruição da membrana basal e aumento da permeabilidade da barreira alvéolo-capilar. A migração de grupos de neutrófilos resulta na ampliação mecânica de rotas migratórias para neutrófilos paracelulares. Os neutrófilos também liberam mediadores pró-inflamatórios e pró-apoptóticos prejudiciais, que agem sobre as células adjacentes criando lesões ulcerosas[63].

1.2.2 Radicais Livres na LPA

Os radicais livres (RLs) são gerados em processos de oxidação biológica e exercem funções importantes no organismo. A redução do oxigênio à água forma radicais livres, sendo o $O2^-$ (superóxido) o primeiro radical livre formado nesse processo. A geração de RLs, como o $O2^-$, é outro importante mecanismo de lesão provocado pelos polimorfonucleares, principalmente pelos neutrófilos[64,65].

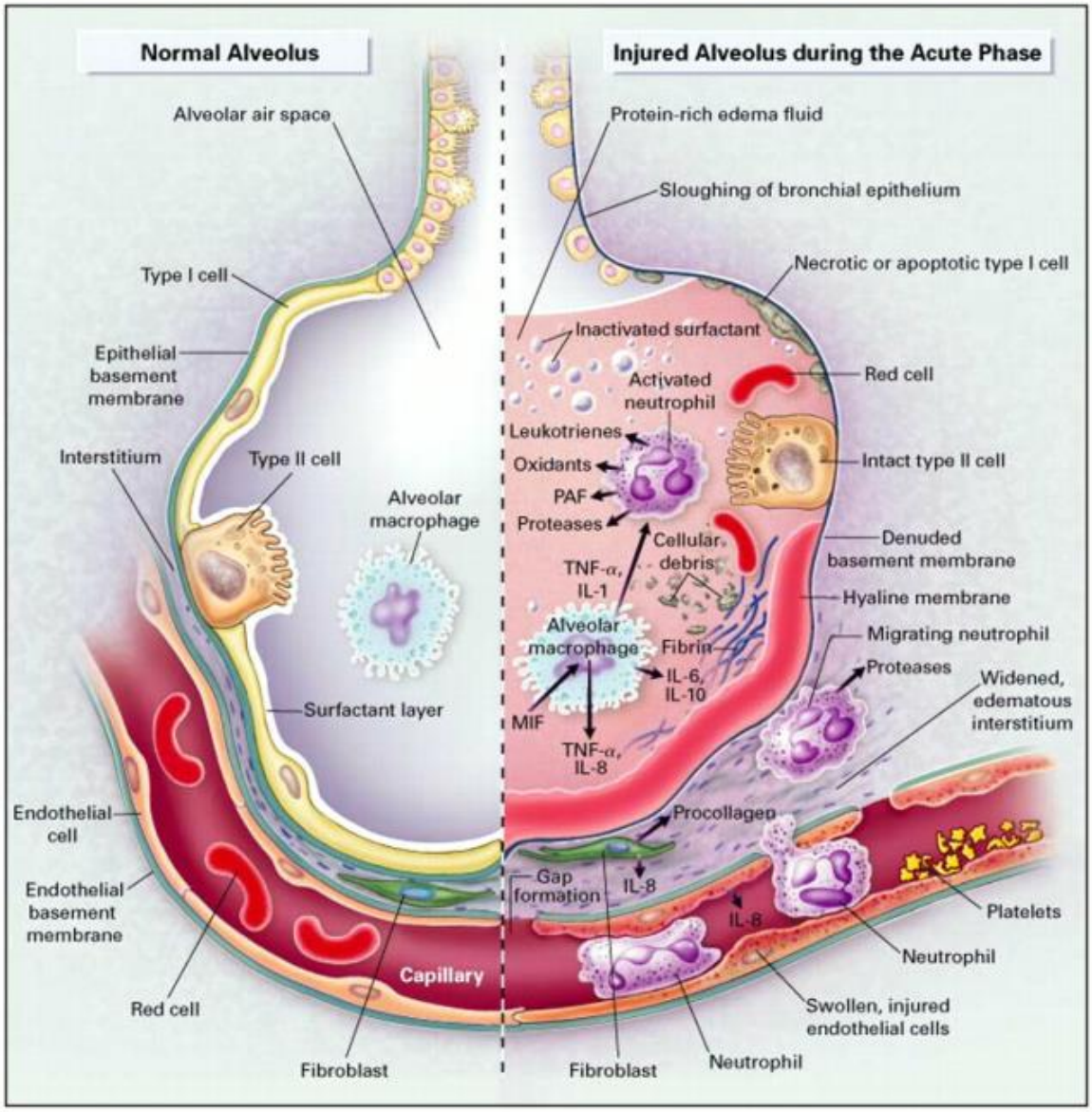

Figura 3. Processo inflamatório na LPA. O alvéolo normal (esquerda) e o alvéolo lesado na fase aguda da lesão pulmonar aguda (direita). Na fase aguda desta síndrome, há desprendimento das células epiteliais brônquicas e alveolares com a formação de membranas hialinas ricas em proteínas na membrana basal desnudada. Os neutrófilos são mostrados aderindo ao endotélio capilar machucado e marginando através do interstício para o espaço aéreo, que é preenchido com líquido edema rico em proteína [57].

Uma fonte importante de RLs é o sistema de transporte de elétrons mitocondrial, sendo seu principal sítio de formação o complexo citocromo b-ubiquinona. Na mitocôndria, a citocromo oxidase promove a redução completa de uma molécula de oxigênio (O_2) em uma molécula de água (H_2O) e, para isso, são necessários quatro elétrons. Contudo, nem sempre o O_2 origina H_2O diretamente. Como consequência de

sua configuração eletrônica, a molécula de O_2 tem forte tendência, durante as reações, de receber um elétron de cada vez, formando uma série de intermediários tóxicos e reativos, tais como: radical superóxido ($O2^-$), peróxido de hidrogênio (H_2O_2), e radical hidroxila (OH^-). O primeiro e o último destes apresentam elétrons desemparelhados e são classificados como RLs. Já o H_2O_2 não tem elétrons não-pareados na última camada e é classificado como uma espécie reativa de oxigênio (EROs)[66,67].

O O_2^- é o primeiro intermediário formado a partir da redução incompleta do oxigênio molecular na formação da H2O, e a partir dele podem se formar outras EROs como o OH^- e o H_2O_2. Muitos sistemas enzimáticos catalisam a redução do O_2 à O_2^-. Podemos citar como exemplos: xantina oxidase, flavina oxidase e peroxidases. Várias outras enzimas como aquelas que catalisam a formação de prostaglandinas (ciclooxigenases) e leucotrienos (lipooxigenases) também são fontes de O_2^-. Quando os RLs são produzidos em taxas que superam a capacidade antioxidante dos organismos ocasionam uma situação de estresse oxidativo[68,69].

A alteração no balanço antioxidante/oxidante parece ser muito importante na fisiopatologia da LPA. Concentrações diminuídas de antioxidantes (ácido úrico, glutationa, ascorbato) são observadas nas vias aéreas de pacientes com LPA. Concentrações elevadas de H_2O_2 bem como de produtos da peroxidação de fosfolipídeos de membrana foram observados no ar exalado por pacientes com LPA[68,70].

1.2.3 Redes neutrofílicas extracelulares (NETs)

Os neutrófilos, sob condições fisiológicas, têm meia vida curta, sendo comprometidos com a morte celular programada (apoptose). A apoptose é essencial para regulação das populações celulares adultas, porém em tecidos infectados pode ser atrasada por componentes microbianos e por estímulos pró-inflamatórios[71].

Durante a inflamação, quando os neutrófilos chegam ao local inflamado, já estão equipados com as proteínas necessárias para matar o microorganismo presente no tecido. O encontro com o patógeno causa a ativação de neutrófilos com a imersão do

microrganismo em um fagossomo. No fagossomo ocorrem dois eventos: primeiro, há grande geração de espécies reativas de oxigênio ROS e, segundo, os grânulos dos neutrófilos fundem-se ao fagossoma, descarregando peptídeos antimicrobianos e enzimas[72]. Juntos, estes dois eventos levam à morte microbiana. Além disso, estudos recentes mostram que os neutrófilos possuem outro mecanismo antimicrobiano, pois quando ativados por substâncias químicas tais como, acetato miristato de forbol, LPS, IL-8, por bactérias gram-positivas ou gram-negativas e fungos, liberam para o meio extraceluar a cromatina associada a diferentes proteínas, formando um complexo de armadilhas extracelulares chamadas redes neutrofílicas extracelulares (NETs). Estes NETs são abundantes em locais inflamados, como encontrado em pacientes com apendicite, pré-eclâmpsia e com infecção por Streptococcus pneumoniae[72,73].

Os NETs são importantes em proceder e matar as bactérias provocando o confinamento do patógeno no local da infecção. Entretanto, estudos recentes sugerem que esta ação pode provocar danos teciduais. A exposição do tecido às proteases associadas aos NETs podem provocar lesões celulares e por essa razão podemos ver que os NETs podem ter dois efeitos importantes. Em contrapartida, representam um mecanismo fundamental para a morte de microrganismos, prevenindo que se disseminem pelo organismo a partir do local da infecção. Por outro lado, a formação dos NETs pode ter efeitos deletérios para o hospedeiro devido à liberação de proteínas, como as proteases, que podem lesionar os tecidos adjacentes[73].

Estudos experimentais têm ligado os NETs à lesão pulmonar aguda. Um mecanismo importante parece ser a interação entre neutrófilos e de plaquetas, que induzem rapidamente a NETosis, conduzindo o aprisionamento de neutrófilos no endotélio, a ativação da coagulação, e aumento na permeabilidade vascular[74]. Estudo recente realizado por Rossaint e colaboradores, utilizando um modelo de LPIV (lesão pulmonar induzida por ventilação mecânica), demonstrou que a inibição da NETosis, bem como desintegração de redes por meio de tratamento com DNase, tinha função protetora contra a lesão pulmonar gerada pelo modelo de LPIV[75].

1.2.4 Tratamento da LPA e a Utilização de MSCs

O tratamento da lesão pulmonar aguda é baseado em estratégias ventilatórias e não ventilatórias. Até o presente momento, os avanços mais significativos no tratamento de suporte de pacientes com lesões pulmonares são associados com a melhoria do controle da ventilação mecânica[76].

Recentes avanços na compreensão da fisiopatologia da lesão pulmonar aguda levaram a investigações de vários potenciais tratamentos farmacológicos. Apesar das evidências pré-clínicas demonstrarem certa efetividade no tratamento da LPA, ensaios de fase clínica III não demonstraram efetividade necessária para o uso destas alternativas. Dentre eles estão: surfactante exógeno, o óxido nítrico inalado, prostaglandina E1 intravenosa, glicocorticóides, cetoconazol, lisofilina, N-acetilcisteína, e proteína C ativada[77,78,79,80,81,82,83].

Entretanto, um novo tratamento promissor para LPA é a utilização de células-tronco mesenquimais (MSCs). MSCs secretam fatores parácrinos que reduzem a gravidade da LPA, incluindo os fatores de crescimento, fatores que regulam a permeabilidade da barreira e citocinas anti-inflamatórias. Estudos demonstraram propriedades anti-inflamatórias das MSCs tanto in vivo como in vitro[84,85].

Em um modelo com camundongos, endotoxina de *Escherichia coli* foi instilada nos espaços aéreos distais do pulmão, seguido por administração intrapulmonar direta de MSC 4h após a instilação. As MSCs diminuíram o volume de líquido extravascular pulmonar, a permeabilidade alvéolo-capilar e a mortalidade. A resposta pró-inflamatória foi regulada negativamente, enquanto que a anti-inflamatória foi aumentada[86]. Atualmente diversos trabalhos estão sendo realizados a fim de agregar novos dados para que seja possível a condução de estudos experimentais e ensaios clínicos Fase I e II em pacientes com LPA grave.

2. Justificativa

Estudos recentes apontam, como uma alternativa promissora, a utilização de células-tronco mesenquimais no tratamento da lesão pulmonar aguda e da sepse. Seu potencial imunomodulador e angiogênico contribui na interrupção da seqüência da patogênese, reduzindo a mortalidade em modelos experimentais. Entretanto, os mecanismos de ação que essas células exercem durante ambas a patologias ainda são incertos. Desta forma, a concentração de esforços para desvendar como atuam estas células e qual sua influência sobre diferentes vias são essenciais, para que futuramente este tratamento possa ser utilizado como uma alternativa terapêutica para a sepse e para a LPA.

3. Objetivos

3.1 Objetivo Geral

Avaliar o efeito terapêutico e imunomodulador de células-tronco mesenquimais no tratamento da sepse e da infecção pulmonar aguda.

3.2 Objetivos Específicos

Sepse

- Avaliar a formação de edema através da análise histopatológica do tecido pulmonar nos diferentes grupos experimentais;

- Realizar análise *in vivo* dos mediadores inflamatórios (COX-2, NF-κB, IL-1, IL-6, TNF-α) e antiinflamatórios (IL-10) nos dos diferentes grupos experimentais;

- Realizar o cocultivo das MSCs com a linhagem de macrófagos pulmonares (RAW 264.7);

- Avaliar a capacidade de alteração da via das MAPKs e do NF-κB no cocultivo celular;

- Avaliar a expressão de mRNA mediadores inflamatórios (COX-2, IL-1β, IL-6) e antiinflamatórios (IL-10) no cocultivo celular;

- Avaliar a expressão de COX-2 e NF-κB no cocultivo em 24 e 48h;

- Avaliar a expressão de COX-2 e NF-κB nos macrófagos pré-tratados com inibidores específicos para MAPKs;

- Avaliar o perfil de expressão de mRNA de diferentes receptores tipo toll (TLR2, 3, 4 e 9) em córtex cerebral, cólon, fígado, rim e pulmão dos animais nos diferentes grupos experimentais *in vivo;*

Lesão Pulmonar Aguda (LPA)

- Avaliar a sobrevida dos animais nos diferentes grupos experimentais durante a LPA;

- Avaliar a formação de edema, através da análise histopatológica do tecido pulmonar nos diferentes grupos experimentais;

- Realizar a contagem total e diferencial de células no lavado bronco-alveolar dos animais estudados;

- Realizar análise dos mediadores inflamatórios (COX-2, NFκB, IL-1, IL-6, TNF-α) e antiinflamatórios (IL-10) nos dos diferentes grupos experimentais;

- Avaliar e comparar o dano oxidativo no soro e no tecido pulmonar através da determinação dos níveis de TBARS, DCF e grupos carbonil nos diferentes grupos experimentais;

- Avaliar e comparar as enzimas antioxidantes no tecido pulmonar através da determinação de alguns parâmetros como: catalase (CAT), superóxido dismutase (SOD) e glutationa reduzida (GSH);

- Avaliar o efeito das células-tronco sobre a formação dos NETs e sua quantificação nos diferentes grupos experimentais;

- Realizar a análise da função mecânica do sistema respiratório dos animais para determinar alterações na função pulmonar.

CAPÍTULO II

ARTIGO ORIGINAL I

[a]Os resultados do presente trabalho foram submetidos ao no ***Stem Cell Research & Therapy*** e está formatado de acordo com as normas do periódico.

Fator de Impacto: 4,504

4. Artigo Original I

CAPÍTULO III

ARTIGO ORIGINAL II

Mesenchymal stem cells improves survival in LPS-induced acute lung injury acting through inhibition of NETs formation[a]

[a]Os resultados do presente trabalho foram publicados no ***Journal of Cellular Physiology*** e está formatado de acordo com as normas do periódico.

Fator de Impacto: 4,155

5. Artigo Original II

Received: 6 December 2016 | Revised: 19 January 2017 | Accepted: 20 January 2017

DOI 10.1002/jcp.25816

ORIGINAL RESEARCH ARTICLE

WILEY Journal of Cellular Physiology

Mesenchymal stem cells improves survival in LPS-induced acute lung injury acting through inhibition of NETs formation

Leonardo Pedrazza[1] | Aline Andrea Cunha[2] | Carolina Luft[1,2] | Nailê Karine Nunes[2] | Felipe Schimitz[3] | Rodrigo Benedetti Gassen[4] | Ricardo Vaz Breda[5] | Marcio Vinícius Fagundes Donadio[1,2] | Angela Terezinha de Souza Wyse[3] | Paulo Marcio Condessa Pitrez[2] | Jose Luis Rosa[6] | Jarbas Rodrigues de Oliveira[1]

[1] Laboratório de Pesquisa em Biofísica Celular e Inflamação, Pontifícia Universidade Católica do Rio Grande do Sul (PUCRS), Porto Alegre, Rio Grande do Sul, Brazil

[2] Laboratório de Respirologia Pediátrica, Centro Infant, Instituto de Pesquisas Biomédicas (IPB), Pontifícia Universidade Católica do Rio Grande do Sul (PUCRS), Porto Alegre, Rio Grande do Sul, Brazil

[3] Laboratório de Neuroproteção e Doenças Metabólicas, Departamento de Bioquímica, Universidade Federal do Rio Grande do Sul, Porto Alegre, RS, Brazil

[4] Instituto do Cérebro (INSCER), Pontifícia Universidade Católica do Rio Grande do Sul (PUCRS), Porto Alegre, RS, Brazil

[5] Laboratório de Imunologia Celular e Molecular, Instituto de Pesquisas Biomédicas (IPB), Pontifícia Universidade Católica do Rio Grande do Sul (PUCRS), Porto Alegre, Rio Grande do Sul, Brazil

[6] Departament de Ciències Fisiològiques, IDIBELL, Campus de Bellvitge, Universitat de Barcelona, L'Hospitalet de Llobregat, Barcelona, Spain

Correspondence
Leonardo Pedrazza, Laboratório de Pesquisa em Biofísica Celular e Inflamação, Pontifícia Universidade Católica do Rio Grande do Sul (PUCRS), Porto Alegre, Rio Grande do Sul, CEP 90619-900, Brazil.
Email: leopedrazza@gmail.com

Funding information
Conselho Nacional de Desenvolvimento Científico e Tecnológico (CNPq), Grant number: 400422/2013-1

Acute lung injury (ALI) and acute respiratory distress syndrome (ARDS) are syndromes of acute hypoxemic respiratory failure resulting from a variety of direct and indirect injuries to the gas exchange parenchyma of the lungs. During the ALI, we have an increase release of proinflammatory cytokines and high reactive oxygen species (ROS) formation. These factors are responsible for the release and activation of neutrophil-derived proteases and the formation of neutrophil extracellular traps (NETs). The excessive increase in the release of NETs cause damage to lung tissue. Recent studies have studies involving the administration of mesenchymal stem cells (MSCs) for the treatment of experimental ALI has shown promising results. In this way, the objective of our study is to evaluate the ability of MSCs, in a lipopolysaccharide (LPS)-induced ALI model, to reduce inflammation, oxidative damage, and consequently decrease the release of NETs. Mice were submitted lung injury induced by intratracheal instillation of LPS and subsequently treated or not with MSCs. Treatment with MSCs was able to modulate pulmonary inflammation, decrease oxidative damage, and reduce the release of NETs. These benefits from treatment are evident when we observe a significant increase in the survival curve in the treated animals. Our results demonstrate that MSCs treatment is effective for the treatment of ALI. For the first time, it is described that MSCs can reduce the formation of NETs and an experimental model of ALI. This finding is directly related to these cells modulate the inflammatory response and oxidative damage in the course of the pathology.

KEYWORDS
acute lung injury, inflammation, mesenchymal stem cells, neutrophil extracellular traps, oxidative stress

1 | INTRODUCTION

Acute lung injury (ALI) and acute respiratory distress syndrome (ARDS) describe clinical syndromes of acute respiratory failure with substantial morbidity and mortality. Even in patients who survive ALI, there is evidence that their quality of life over the years is adversely affected (Dowdy et al., 2006; Johnson & Matthay, 2010; Rubenfeld et al., 2005). The mortality rate of this clinical syndrome reaches 40%, and

most of the deaths occur due to multiple organ dysfunction (Rubenfeld et al., 2005).

Biomarkers found in epithelium and endothelium are involved in coagulation and inflammatory cascades are indicators of morbidity and mortality in ALI. After an infection or trauma, increased proinflammatory cytokines occurs as a direct response and like a marker of cellular injury in progress. Meduri et al. have reported that persistently elevated plasma levels of interleukins 6 and 8 (IL-6 and IL-8) and tumor necrosis factor (TNF-α) are strongly associated with increased mortality (Levitt, Gould, Ware, & Matthay, 2009; Parsons et al., 2005; Stuber et al., 2002).

With inflammation, the barriers usually responsible for preventing alveolar edema are lost, with the escape of proteins from the intravascular space into the interstitial space, promoting interstitial and alveolar edema. The influx of fluid with a high concentration of proteins into the alveoli alters the integrity of the pulmonary surfactant, damages the lung tissue, and causes an alveolar collapse (Pugin, Verghese, Widmer, & Matthay, 1999; Ware et al., 2007). Migration of transepithelial neutrophils is an important feature of acute lung injury because neutrophils are the first involved in inflammation. Excessive and prolonged neutrophil activation contribute to the destruction of the basement membrane and increased permeability of the alveolar–capillary barrier. Neutrophils also release proinflammatory and pro-apoptotic mediators, which act on adjacent cells creating ulcerous lesions (Zemans, Colgan, & Downey, 2009).

It is believed that a key aspect of this pulmonary inflammatory response is mediated by increased levels of reactive species. Previous experimental studies demonstrate that mice subjected to pulmonary injury present an increase in lipid peroxidation, oxidative damage to the protein, and disrupted antioxidant defenses in the lung. Neutrophil activation generates high concentrations of antimicrobial reactive oxygen species (ROS) with superoxide anions (O_2^-) as the major component to create an environment that is toxic for pathogens (Cunha et al., 2015). In addition, high ROS concentrations are responsible for the release and activation of neutrophil-derived proteases and the formation of neutrophil extracellular traps (NETs) with expulsion of chromatin fibers from the nucleus of neutrophils as additional strategies to effectively combat and kill invading microorganisms (Jiang et al., 2016). However, when these mechanisms become overactivated either by persisting stimuli or by impeded resolution, they turn out to be highly destructive for the surrounding tissues and may cause severe damage and tissue break down as observed in neutrophil dominated diseases (Cohen, 2009; Coxon et al., 2001). A recent study by Rossaint et al. (2014) using an VILI (mechanical ventilation-induced lung injury) model demonstrated that inhibition of NETosis as well as disintegration of NETs by desoxyrribonuclease (DNase) treatment had a protective function against lung injury generated by the VILI model.

Recently Jiang et al. (2016) described the ability of MSCs to inhibit the formation and release of NETs, in a vasculitis model, based on the adaptive induction of antioxidant enzymes, particularly superoxide dismutase 3 (SOD3). Many studies have demonstrated that MSCs also release anti-inflammatory cytokines that can dampen the severity of inflammation in ALI (Geiser et al., 2001; González et al., 2013; Ortiz et al., 2003, 2007). These cells are potent modulators of the immune response and present a high degree of chemotaxis, based on proinflammatory cytokines, locating inflamed and neoplastic tissues (Arrieta, Ritz, & Silberstein, 2011; Horie & Laffey, 2016; Uccelli, Moretta, & Pistoia, 2008). MSCs also secrete paracrine factors that reduce the severity of ALI, including growth factors, factors that regulate barrier permeability, and anti-inflammatory cytokines (Rojas et al., 2005; Wang et al., 2014). However, little is unknown about others immunological mechanisms of MSCs during ALI.

In this study, we investigated the immunomodulatory and antioxidant effects of MSCs in an endotoxin model of ALI and try to demonstrate for the first time that these effects of this treatment may contribute decrease the release of NETs in this pathology.

2 | METHODS

2.1 | Animals

Male C57BL/6 mice (8–12 weeks old) were kept on shelves with ventilated cages that provide 60 air cycles per hour, relative humidity ranging between 55% and 65%, a 12 hr light–dark cycle, temperature of 22 ± 2°C with free access to food and water. The animals were maintained in accordance with the Guiding Principles in the Care and Use of Animals approved by the Council of the American Physiological Society. The experimental protocol was approved by the Ethics Research Committee of Pontifícia Universidade Católica do Rio Grande do Sul (protocol number 14/00403).

2.2 | MSC culture and characterization

Male C57BL/6 mice (8–12 weeks old) were MSC donors. Under sterile conditions, the animals were anesthetized (pentobarbital 50 mg/kg intraperitoneally) and after the collection of the adipose tissue, mice were killed by cervical dislocation. Adipose tissue was obtained from the epididymal adipose tissue, cut into small pieces, collagenase digested, filtered, and then cultured using DMEM Dulbecco's Modified Eagle Medium (Invitrogen Corporation, Carlsbad, CA) without ribonucleosides or deoxyribonucleosides containing 2 mM L-glutamine and 20% fetal bovine serum (FBS) (Invitrogen), with 1% penicillin–streptomycin. Cells were passaged every 3–4 days by trypsinization when they reached 70–80% confluence and were used for the experiments between passages 3 and 4. Between each passage, cell viability was measured using the trypan blue exclusion test. MSCs were cultured in a humidified incubator at 5% CO_2 and 37°C under sterile conditions. Before each experiment, cells were trypsinized, counted, washed twice with phosphate-buffered saline (PBS), and resuspended in PBS. MSCs were characterized by expression of cellular markers (CD 90$^+$, CD105$^+$, CD 34$^-$, and CD45$^-$) (Bio-Rad, Hercules, CA) was determined by flow cytometry analysis (Luna et al., 2014). MSCs were induced to differentiate into adipocytes, osteocytes, and chondrocytes by using cell differentiation kits from R&D Systems (Minneapolis, MN) in accordance with the recommendation of the manufacturer.

2.3 | Experimental procedures

Mice were anesthetized with a mixture of ketamine (80 mg/kg) and xylazine (20 mg/kg), intraperitoneally (IP), and lung injury was induced by intratracheal instillation of LPS (*Escherichia coli* 026:B6; Sigma Chemical, St. Louis, MO) at a dose of (200 μg/100 g) body weight. The LPS group, after LPS instillation, were treated with PBS (100 μl via retro-orbital injection). The LPS + MSC group, after the LPS instillation, were treated with MSCs (5×10^5/100 μl PBS via retro-orbital injection). In the Sham group, it was performed intratracheal instillation of PBS (50 μl) and subsequently treated with PBS (100 μl via retro-orbital injection). Subsequently, 12 hr after the LPS instillation, mice were anesthetized and bronchoalveolar lavage fluid (BALF) was collected with 1 ml of PBS. The final BALF lavage volume retrieved was approximately 0.7 ml. The BALF was then centrifuged (1,000*g* for 10 min) and the cell pellet was resuspended in 350 μl saline, and then diluted with Turk's solution and the total cell count was determined using a "Neubauer" counting chamber to confirm the lung injury induction. For the differential cell analysis, BALF suspension was centrifuged through a cytospin, and slides were stained with Hematoxylin and eosin—H&E (Panótico Rápido—Laborclin, Brazil). Four hundred cells were then counted under light microscopy. In order to estimate the alveolar cell injury and the alveolar-capillary membrane alterations, BALF total protein were measured using the commercial kit (Labtest Diagnóstica, Brazil) in a semi-automatic spectrophotometer (Spectronic/Genesis 8). Subsequently, the mice were killed by cervical dislocation and lung tissue was collected. One lung sample was isolated and fixed in a 4% formalin solution for histopathological analysis (see below) and the other was isolated and tissue homogenates were immediately stored at −70°C until assaying for oxidative stress.

2.4 | Survival curve

A survival curve for different experimental groups was performed. After 7 days, animals that were still alive were anesthetized with an IP solution of ketamine (100 mg/kg) and xylazine (50 mg/kg) and killed by cervical dislocation.

2.5 | Histological analysis

The superior lobe of the right lung was ligated and prepared for histological and morphological analysis. Lungs were perfused with 10% buffered formalin on a gravity column (20 mmHg). Tissue specimens were embedded in paraffin blocks, cut into 4-μm sections, stained with H&E and examined by light microscopy. Others sections were sequentially subjected to immunostaining analysis. After deparaffinization, the sections were sequentially treated with 1% H_2O_2 for 10 min and rinsed thoroughly with PBS. Sections were blocked with 2% normal blocking serum in PBS at room temperature for 60 min to suppress any nonspecific binding of IgG, followed by incubation with anti-COX-2 rabbit mAb (ciclooxygenase-2) (dilution 1:200; Merck Millipore, Darmstadt, GER), or NF-κB p65 rabbit mAb (dilution 1:200; Cell signaling, Danvers, MA). After being probed with the primary antibody, sections were washed in PBS for 3 × 10 min and then incubated with the suitable fluorochrome-labeled secondary antibody Goat anti-Mouse Alexa Fluor® 488 (1:200 Thermo Fisher Scientific, Waltham, MA). The cellular nucleus was stained using TO-PRO®3 (dilution 1:1000; Thermo Fisher Scientific). All of the slides were evaluated by confocal immunofluorescence microscopy a Zeiss LSM 5 Exciter (Zeiss, Oberkochen, Germany) with magnification 100×. The Zeiss ZEN 2008 Imaging Software (Zeiss) was used for microscopy analysis.

2.6 | Cytokines quantification

To determine cytokine levels, serum samples were collected from mice 12 hr after ALI induction. Multiple soluble cytokines: IL-6, TNF-α, and IL-10 were simultaneously measured using a Luminex Multiplex Assay kit (Thermo Fisher Scientific). We used a luminometer Luminex® 100/200 (Luminex Corporation, Austin, TX) and the results were analyzed using the software xPONENT® Solutions software (Luminex Corporation).

2.7 | Western blot analysis

Lung tissue were lysed in CHAPS lysis buffer (10 mM Tris–HCl, pH 7.5, 100 mM NaCl, 0.3% CHAPS, 50 mM NaF, 1 mM sodium vanadate, 1 mM phenylmethylsulfonyl fluoride, 5 μg/ml leupeptin, 5 μg/ml aprotinin, 1 μg/ml pepstatin A, 50 mM β-glycerophosphate, 100 μg/ml benzamidine) for 30 min at 4°C and equal amounts of proteins were separated by electrophoresis. We used Tris-Acetate PAGE systems as previously described (Casas-Terradellas, Tato, Bartrons, Ventura, & Rosa, 2008; Cubillos-Rojas et al., 2010). After running the gel, the proteins were transferred to polyvinylidene fluoride (PVDF) membranes and viewed by immunoblotting, as described elsewhere (Cubillos-Rojas et al., 2010). Band intensities were analyzed with a gel documentation system (LAS-3000 Fujifilm). The levels of COX-2 and NF-κB p65 were standardized with respect glyceraldehyde 3-phosphate dehydrogenase (GAPDH) levels and all was expressed as a percentage of controls. We used these antibodies for the experiments: anti-COX-2 rabbit mAb (1:1000 dilution), NF-κB p65 rabbit mAb (1:1000 dilution), and anti-GAPDH mouse mAb (1:3000 dilution) (Sigma–Aldrich, St. Louis, MO).

2.8 | Oxidative stress

For determination of oxidative stress parameters, the lung tissue was homogenized in 10 volumes (1:10, w/v) of 20 mM sodium phosphate buffer, pH 7.4, containing 140 mM KCl. The homogenate was centrifuged at 750*g* for 10 min at 4°C. The pellet was discarded, and the supernatant was immediately separated and used for the measurements of oxidative stress studied in this article (Cunha et al., 2015). Protein was measured according to Lowry, Rosebrough, Farr, and Randall (1951) for all techniques. Serum bovine albumin was used as standard.

2.8.1 | 2′7′Dichlorofluorescein fluorescence assay

Reactive species production was measured according to the method of LeBel, Ischiropoulos, and Bondy (1992) and based on the oxidation of 2′7′-dichlorofluorescein (H2DCF). The sample was incubated in a medium containing 100 μM 2′7′-dichlorofluorescein diacetate (H2DCF-DA) solution. The reaction produces the fluorescent compound dichlorofluorescein (DCF) which is measured at λ_{em} = 488 nm and λ_{ex} = 525 nm. Results were represented as nmol DCF/mg protein.

2.8.2 | Thiobarbituric acid-reactive substances (TBARS)

TBARS, an index of lipid peroxidation, were measured according (Ohkawa, Ohishi, & Yagi, 1979). Sample was incubated in a medium contained 8.1% SDS, 20% acetic acid, and 0.8% thiobarbituric acid. The mixture was vortexed and the reaction carried out in a boiling water bath for 1 hr. The resulting pink-stained TBARS were determined spectrophotometrically at 535 nm. A calibration curve was generated using 1,1,3,3-tetramethoxypropane as a standard and the results were represented as nmol TBARS/mg protein.

2.8.3 | Protein carbonyl content

Oxidatively modified proteins present an enhancement of carbonyl content. In this study, protein carbonyl content was assayed by a method based on the reaction of protein carbonyls with dinitrophenylhydrazine, forming dinitrophenylhydrazone, a yellow compound, measured spectrophotometrically at 370 nm (Reznick & Packer, 1994). Results were represented as protein carbonyl content (nmol/mg protein).

2.8.4 | Superoxide dismutase assay (SOD)

The SOD activity is based on the capacity of pyrogallol to autoxidize, a process highly dependent on superoxide, which is substrate for SOD (Aebi, 1984). The inhibition of autoxidation of this compound occurs in the presence of SOD, whose activity was then indirectly assayed at 420 nm. A calibration curve was performed with purified SOD as standard, in order to calculate the activity of SOD present in the samples. The results were represented as SOD units/mg protein.

2.8.5 | Catalase assay (CAT)

CAT activity was assayed using a SpectraMax M5/M5 Microplate Reader (Molecular Devices, MDS Analytical Technologies, Sunnyvale, CA). The method used is based on the disappearance of hydrogen peroxide (H_2O_2) at 240 nm in a reaction medium containing 20 mM H_2O_2, 0.1% Triton X-100, 10 mM potassium phosphate buffer pH 7.0, and 0.1–0.3 mg protein/ml. One CAT unit is defined as 1 µmol of H_2O_2 consumed per minute and the results were represented as CAT units/mg protein (Marklund, 1984).

2.8.6 | Glutathione peroxidase assay (GPx)

GPx activity was measured using tert-butyl-hydroperoxide as substrate. NADPH disappearance was monitored at 340 nm (Wendel, 1981). The medium contained 2 mM glutathione, 0.15 U/ml glutathione reductase, 0.4 mM azide, 0.5 mM tert-butyl-hydroperoxide, and 0.1 mM NADPH. One GPx unit is defined as 1 µmol of NADPH consumed per minute; the specific activity is represented as GPx units/mg protein.

2.9 | Quantification of NETs release, DNA quantification and apoptosis assay

NETs were quantified in BALF using Quant-iT dsDNA HS kit (Invitrogen), according to manufacturer's instructions. After the TCC count, BALF cells (2×10^5) were stimulated with PMA (50 nM) for 2 hr at 37°C, in 8-chamber culture slides (BD Bioscience, Franklin Lakes, NJ). After this period, cells were fixed in 4% paraformaldehyde, and stained with anti-myeloperoxidase mouse mAb (anti-MPO) (1:200; Life Technologies, Carlsbad, CA), followed by anti-mouse FITC antibody (1:500; Life Technologies) and Hoechst 33342 (1:2000; Invitrogen). Images were obtained with a Zeiss LSM 5 Exciter confocal microscope (Zeiss, Oberkochen, Germany). Cells isolated from BALF (1×10^5) were analyzed for apoptosis and necrosis with annexin-V and propidium iodide, respectively, according to manufacturer's instructions (BD PharmingenTM). Briefly, cells were washed twice, stained with annexin V-FITC, and propidium iodide for 15 min at room temperature and analyzed by flow cytometry (FACS Canto II, BD Bioscience) within 1 hr. Cells were then gated on both side scatter and forward scatter singlets, ensuring individual cell staining.

2.10 | Assessment of respiratory mechanics

Twelve hours after LPS instillation, the mice were anesthetized, as described above, tracheostomized and a rigid-type cannula was inserted into the trachea and firmly tied in place. The cannula was connected to a animal ventilator (flexi Vent, SCIREQ, Montreal, PQ, Canada). Lung mechanic was measured using a modification of the forced oscillation technique. During pauses in ventilation, an oscillatory signal containing frequencies (4–38 Hz) was generated by a loudspeaker and passed through a wave tube to the mouse via the tracheal cannula. The respiratory system impedance Zrs was measured as the load impedance on the wave tube. A four parameter model with constant phase tissue impedance was fitted to the Zrs data to obtain measures of Raw, the Newtonian resistance which is equivalent to airway resistance in the mouse due to the compliance of the chest wall, G (tissue damping), which represents the resistance of the small airways where air movement occurs primarily by diffusion, and H (tissue elastance), which is the stiffness of the lung parenchyma (Hantos, Daroczy, Suki, Nagy, & Fredberg, 1992; Zosky et al., 2008).

2.11 | Statistical analysis

The data were analyzed by one-way analysis of variance (ANOVA). For comparison of significance, Tukey's test was used as a post hoc test according to the statistical program GraphPad Prism. Survival data were presented as Kaplan–Meier curves and the statistical significance was assessed by Mantel-Cox test. Quantitative data are presented as means ± SEM. Differences were considered significant at $^*p < 0.05$, $^{**}p < 0.01$, and $^{***}p < 0.001$. Ns: no significant difference.

3 | RESULTS

3.1 | MSCs treatment improve survival

We wanted to know if the systemic treatment with MSCs could increase survival in the model studied. Over 72 hr, mice that received MSCs had a significantly higher survival rate compared to the LPS group (Figure 9). This difference between the two groups became apparent after the initial 36 hr. We followed the animals up to 120 hr to confirm that this result was maintained.

3.2 | MSCs treatment reduces cell migration to the lung during ALI

We investigated, using a model of endotoxin-induced acute lung injury, the disruption of the alveolar–capillary barrier. We evaluated parameters such as total cell count, differential count of cells, and total protein in BALF. We observed that the LPS group had a significant increase in the total cell count when compared with the Sham group. This increase found in the LPS group was reduced in the MSC-treated group (Figure 1A). In addition, MSCs were able to reduce the amount of macrophages, as well, the number of neutrophils in BALF when compared to the LPS group (Figure 1B and C). We also observed a reduction in the amount of total proteins in the LPS + MSC group when compared to the LPS group (Figure 2). No significant change in the number of lymphocytes was observed between the tested groups (Figure 1D).

3.3 | MSCs administration ameliorates inflammation in lung

Next, we tried to verify the ability of MSCs in decreasing the pulmonary inflammation. We perform the H&E staining 12 hr after ALI induction, it was observed that induction using only LPS was able to cause inflammation in the lung (Figure 3A). We calculated the score inflammatory lung tissue using the software Image-Pro Plus (Medical Cybernetics). It was possible evaluate in the LPS group that we had an increased in the inflammatory score, peribronchial and perivascular, when compared with the Sham group. The MSC-treated group had a reduced score when compared with the LPS group, demonstrating the ability of MSCs to decrease inflammation in the lung tissue (Figure 3B).

We measured the concentration of two inflammatory markers, IL-6 and TNF-α, and one anti-inflammatory, IL-10, in serum and BALF. The concentration of IL-10 in the LPS group had an increase when compared to the Sham group, however, a higher increase of this anti-inflammatory interleukin in the MSC group was not observed when compared to the LPS group in serum and BALF (Figure 4A and D). In addition, IL-6 and TNF-α were significantly increased in LPS group when compared with the Sham group and this increase was reduced in the ALI group treated with MSCs. The same profile was observed in the serum and in the BALF. These results demonstrate the immunomodulatory potential of these cells (Figure 4B, C, E, and F).

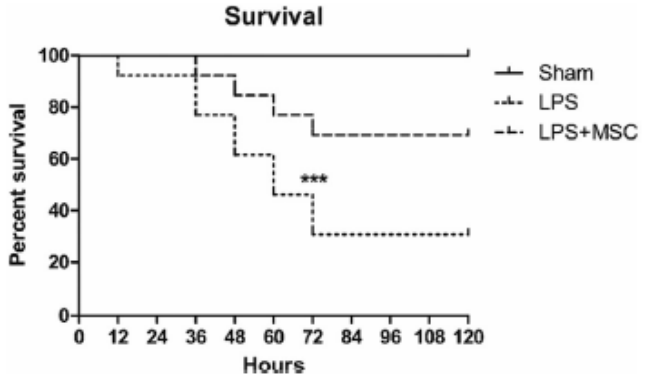

FIGURE 1 Administration of MSCs improved survival during ALI. MSCs was administered intravenous (i.v.) after instillation of endotoxin (2 mg/kg). Kaplan–Meier survival curve showed that the ALI-induced mice treated with MSCs had a significantly improved survival rate at 72 hr compared to the LPS group. Data represent the mean ±SEM, $n = 15$. ***Significant difference ($p < 0.001$) between the groups

3.4 | MSCs reduce COX-2 and NF-κB expression in lung tissue

Due to the results found in the inflammatory markers, we performed COX-2 and NF-κB analysis in ALI model. Expression of COX-2 mRNA and protein is often enhanced in various human cell types by inflammatory cytokines such as IL-1β and tumor TNF-α (Kuwano et al., 2004). We performed the COX-2 analysis through Western blot and observed a higher expression in the LPS group when compared to the Sham and LPS + MSC groups (Figure 5A). We also performed immunofluorescence staining and we observed the same expression profile (Figure 5B).

Subsequently we evaluated the expression of NF-κB, which is a transcriptional regulator and induces the expression of several genes including COX-2. When we performed the Western blot, we compared a reduction in the expression of NF-κB in the group treated with MSCs when compared to the LPS group (Figure 6A). We also conducted the immunofluorescence staining to confirm this decrease and obtained the same result (Figure 6B).

3.5 | Oxidative stress during ALI is attenuate by MSCs

Therefore, we resolved to investigate whether MSCs would be able to prevent the induction of oxidative stress in the lungs of mice. First, we evaluated the effect of ALI and the treatment with MSCs on reactive species production in lung, as indicated by DCF formed from the oxidation of H2DCF. The LPS group had an increased production of reactive species that was inhibited by treatment with MSCs (Figure 7A).

Next, we evaluated the effects of lung injury on lipid peroxidation, as measured by TBARS levels and damage to protein measured by carbonyl content. We observed that MSCs were able to prevent the increase in TBARS and carbonyl levels when compared to the LPS group (Figure 7B and C). The lung enzymatic antioxidant defense was evaluated by the activities of SOD, CAT, and GPx in the lung of mice submitted to ALI and treatment with MSCs. We observed a significant reduction in the SOD and CAT activity in LPS group when compared with the Sham group. However, the MSC-treated groups were not able to reverse this decrease found in the LPS group (Figure 7D and E). In addition, GPx activity was not altered in the lung of mice submitted to ALI and LPS-treated with MSCs (Figure 7F).

3.6 | NETs formation is reduced in ALI by MSCs

Extracellular deoxyribonucleic acid (DNA) forms NETs, which act like a danger-associated molecular pattern and are associated with inflammation and tissue injury (Huang et al., 2015). We conducted an investigation to find out if MSCs were able to reduce NETs formation during ALI. We performed an immunohistochemistry in BALF cells to

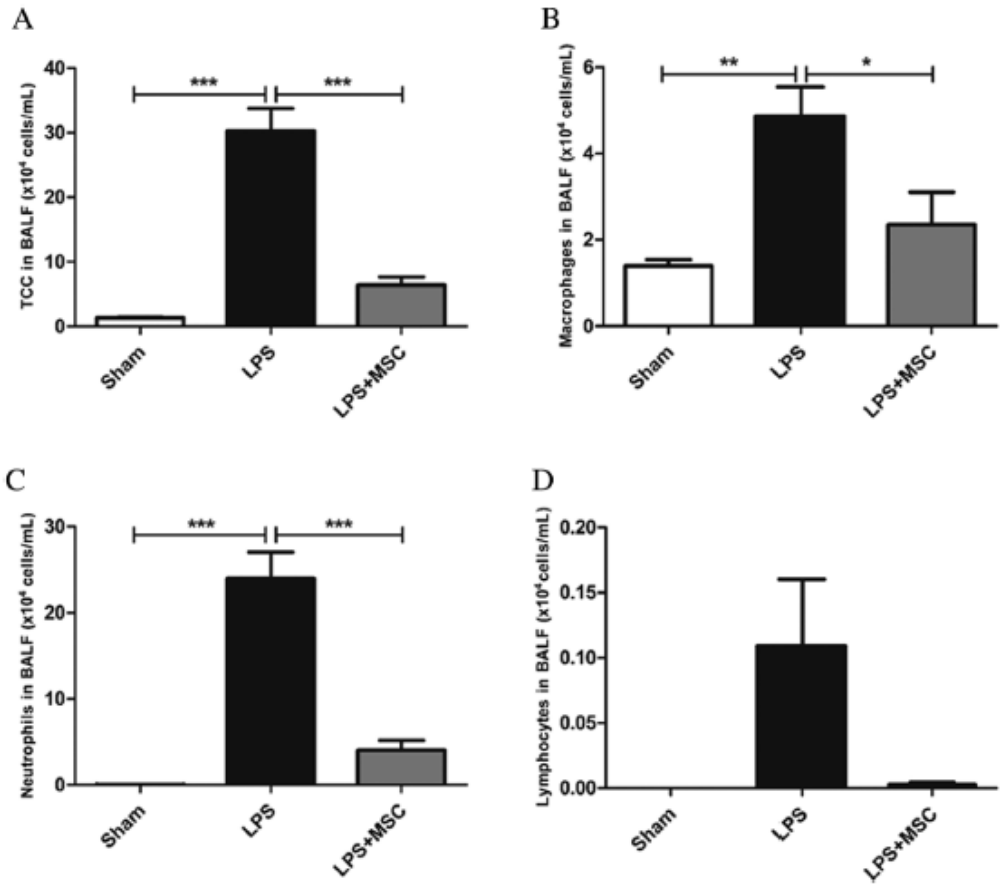

FIGURE 2 Mice treated with MSCs reduced cell infiltrate in lung. (A) Total cells count (TCC). (B–D) Differential cells counts (macrophages, neutrophils, and lymphocytes) in BALF of mice. The total cell count after 12 hr showed a significant increase in the number of cells in the LPS group compared with the levels in the Sham group. A significant decrease in number of cells was observed in the LPS + MSC group compared with the levels in the LPS group. Also, the differential cells count showed a significant increase in the number of neutrophils and macrophages in the LPS group compared with the levels in the Sham group and a reduction in the LPS + MSC group when compared with the LPS group. Data represent the mean ±SEM, $n = 10$. *Significant difference ($p < 0.05$), **significant difference ($p < 0.01$), and ***significant difference ($p < 0.001$) between the groups

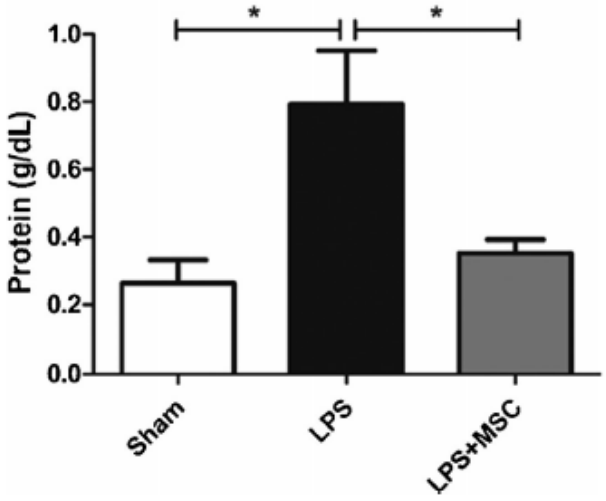

FIGURE 3 Mice treated with MSCs show reduced protein concentration in BALF. BALF levels protein were measured using the commercial kits in a semi-automatic spectrophotometer after 12 hr. There was a significant increase in protein concentration in the LPS group compared with the Sham group. Protein concentration was decreased in the LPS + MSC group compared with the LPS group. Data represent the mean ± SEM, $n = 10$. *Significant difference ($p < 0.05$)

see if we had less formation of these traps in treated animals with MSCs. The results show that the LPS + MSC group has a great reduction in the formation of NETs when compared to the LPS group, indicating a possible action of MSCs via neutrophils (Figure 8A). To confirm this result, a DNA extracellular assay was performed on the BALF and the results demonstrate that the LPS group had a significant increase of DNA extracellular when compared to the Sham group. This increase is severely reduced in the group treated with MSCs, corroborating the results founded in confocal microscopy (Figure 8B).

To discard the possibility of this DNA extracellular found in BALF to be derived from a larger number of cells in apoptosis, we performed flow cytometric analysis of the Annexin V labeling assay to identify the percentage of cells in apoptosis in all groups (Figure 8C). No difference in the number of cells in apoptosis was found between the groups, indicating that the large amount of DNA extracellular found in the LPS group possibly comes from the release of the NETs.

3.7 | Respiratory mechanics are not affected during ALI

Finally, we evaluated whether the treatment was capable of improving respiratory mechanics during acute lung injury. Three parameters were

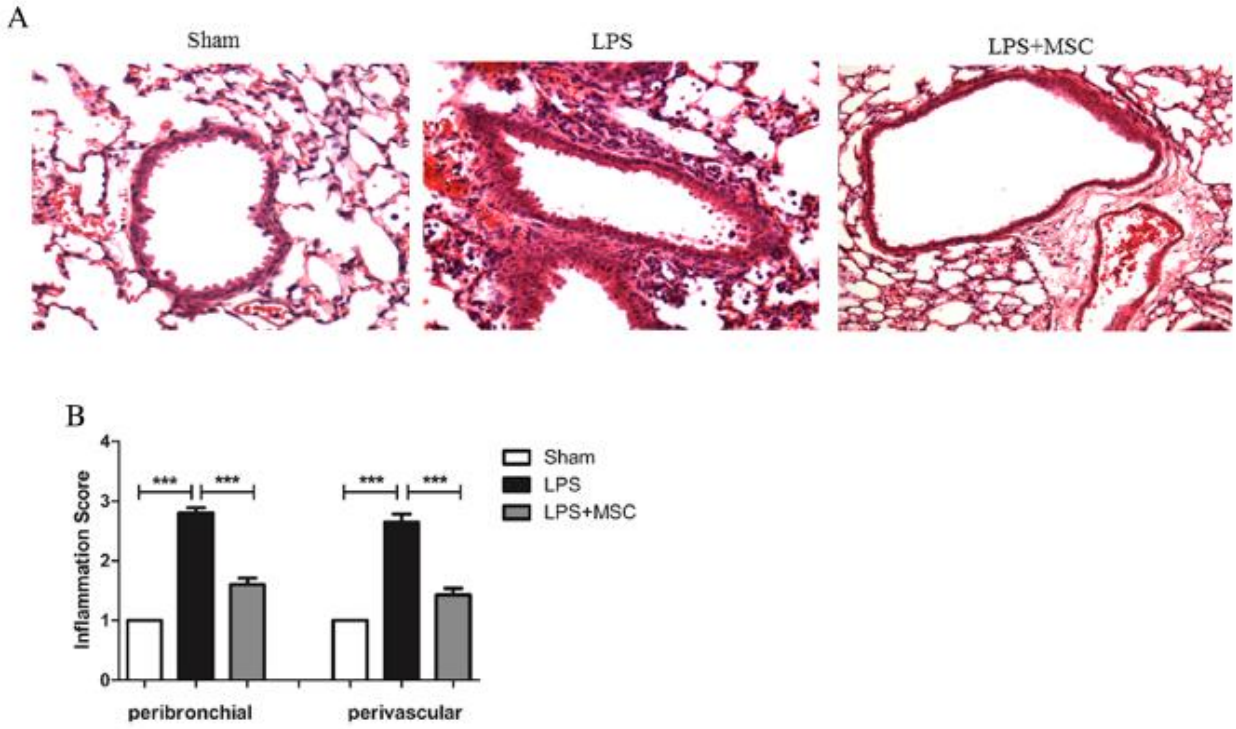

FIGURE 4 Mice treated with MSCs show reduced inflammation score in lung. (A) Lung sections were subjected to H&E staining. (B) The inflammatory cells infiltrated into the peribronchial and perivascular lung tissues in the LPS group were ameliorated after MSC administration (×200 magnification). After 12 hr data represent the mean ± SEM, $n = 5$. ***Significant difference ($p < 0.001$) between the groups

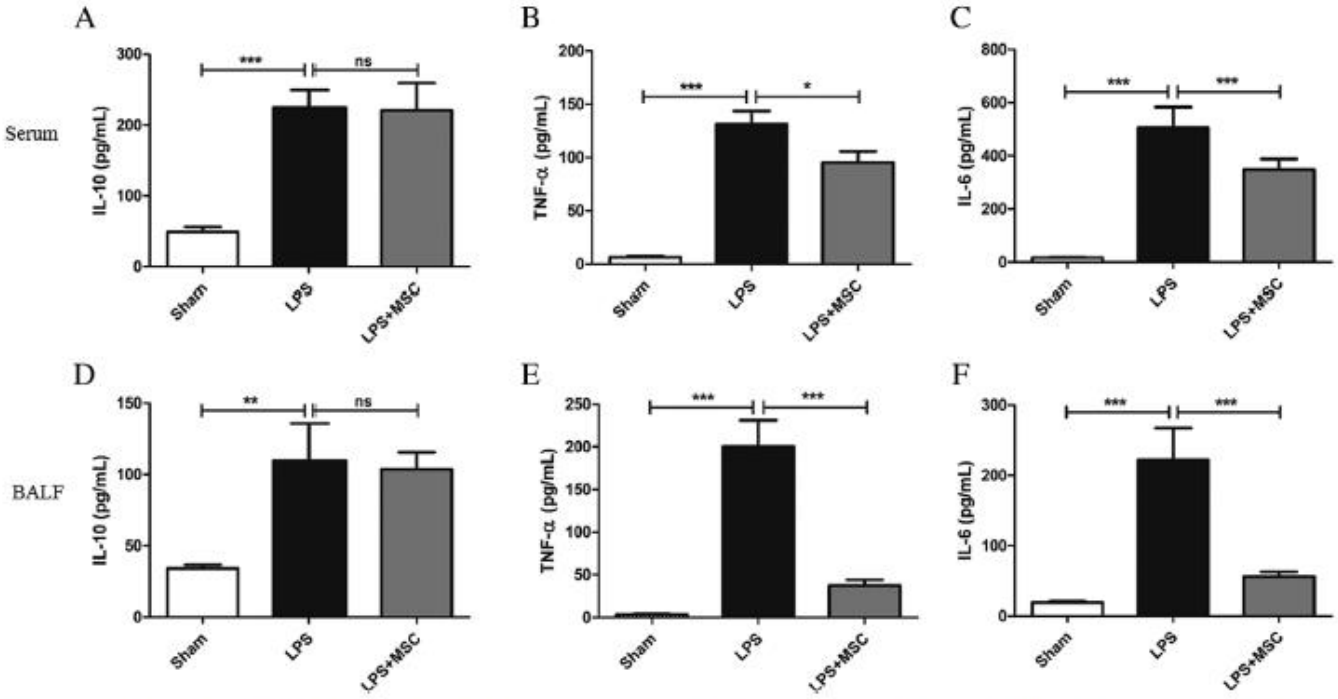

FIGURE 5 Mice treated with MSC show reduced inflammatory markers. The proinflammatory factors TNF-α, IL-6 and the anti-inflammatory IL-10 in the serum and BALF were detected by luminescence after 12 hr. (A and D) We had a significant increase in IL-10 in the LPS group compared with the levels in the Sham group. This profile was also observed in both, serum and BALF. No significant difference was observed between the LPS group and the ALI + MSC group at IL-10 levels. (B, C, E, and F) The results showed a significant increase in TNF-α, IL-6 in the sepsis group compared with the levels in the Sham group, in both, serum and BALF. A significant decrease in TNF-α and IL-6 was observed in the LPS + MSC group compared with the levels in the LPS group, in both, serum and BALF. Data represent the mean ±SEM, $n = 10$. Ns:non significant difference, *significant difference ($p < 0.05$), **significant difference ($p < 0.01$), and ***significant difference ($p < 0.001$) between the groups

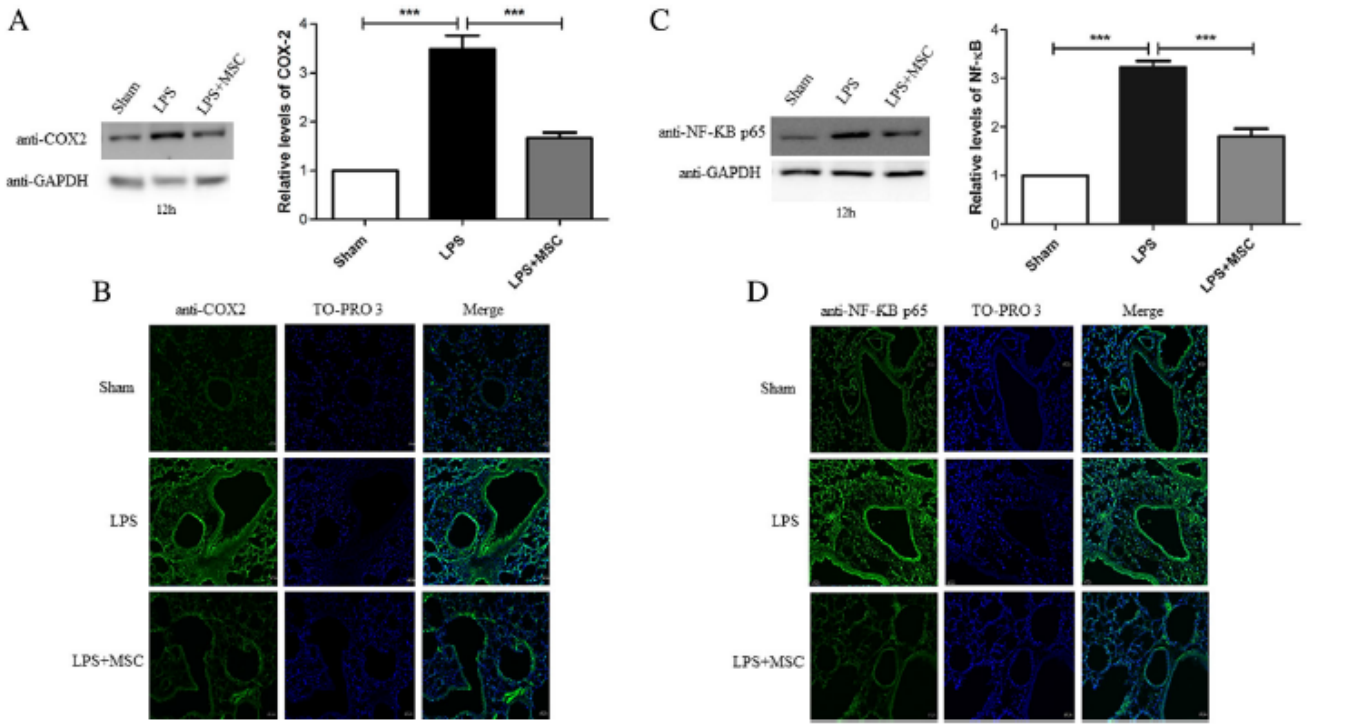

FIGURE 6 MSCs administration reduced elevated COX-2 and NF-κB p65 in lung tissue. (A and B) Lung tissues were scraped into a homogenate and analyzed by Western blotting for the expression of COX-2 and NF-κB p65. COX-2 and NF-κB p65 expression were increased in the LPS group and decreased after MSC administration. All experiments were realized after 12 hr after ALI induction. Data represent the mean ± SEM, $n = 5$. ***Significant difference ($p < 0.001$) between the groups. (C and D) Lung sections were prepared and immunofluorescence was used to assess the expression of COX-2 and NF-κB p65 using a fluorescence microscopy. TO-PRO 3-staining nuclei (blue) were also shown. Images showed representative data from one of four individual experiments. The COX-2 and NF-κB in lung tissue were measured by immunohistochemistry assay. There were increases in COX-2 and NF-κB p65 immunoreactivity in the LPS group compared with the Sham group. The immunoreactivity of COX-2 and NF-κB p65 were decreased in the ALI = MSC group compared with the LPS group ($n = 4$, per group, ×100 magnification)

evaluated: airway resistance, tissue elastance, and tissue damping. Surprisingly, none of the studied parameters were altered in the LPS group when compared to the Sham group, in the same way no difference was found in the LPS + MSC group when compared with the LPS group (Figure 9A–C). These results may be related to the time (12 hr) used to perform this analysis in this model.

4 | DISCUSSION

ALI and its more severe form, ARDS, are syndromes of acute hypoxemic respiratory failure resulting from a variety of direct and indirect injuries to the gas exchange parenchyma of the lungs (Mei et al., 2007). In the present study, we demonstrate in a murine model of ALI that systemic administration of MSCs prevented LPS-induced lung inflammation, oxidative stress, and NETs formation.

First we perform the survival curve. After 72 hr we can observe a large difference in the percentage of live animals treated with MSCs when compared to ALI. The MSCs-treated animals present a survival of around 70% and untreated 35%, demonstrating the full potential of these cells during acute lung injury. Through this result we began to investigate the beneficial effects and possible pathways of action of MSCs during ALI.

We evaluate the lung cell migration during ALI to determine if MSCs were able to inhibit this process and maintain endothelial barrier. When we analyzed cell count, a massive decrease in the number of total cell counts in BALF was evident. In the differential count, it was evident the decrease of the cellular infiltrate of neutrophils and macrophages in the group treated with MSCs. In addition, we found an increase in protein concentration in BALF demonstrating loss of endothelial and epithelial barriers. Edema accumulates in the alveoli through some combination of increased permeability to protein of the endothelial and epithelial barriers, and reduced (or insufficient) alveolar fluid clearance (AFC) (Gotts & Matthay, 2011). A number of groups have reported that MSCs reduce the increase in endothelial permeability associated with ALI and our results corroborate with these findings.

The beneficial effect of MSCs appears to derive more from their homing capacity to injured tissue, interact with injured host cells, and secrete paracrine soluble factors that modulate immune responses as well as alter the responses of endothelium or epithelium to injury through the release of growth factors and antimicrobial peptides (Leea, Fang, Krasnodembskaya, Howard, & Matthay, 2011). Many studies have demonstrated that MSCs also release anti-inflammatory cytokines that can dampen the severity of inflammation in ALI (Wang, Li, & Wang, 2013; Xu et al., 2007). We evaluated proinflammatory cytokines (IL-6 and TNF-α) and IL-10

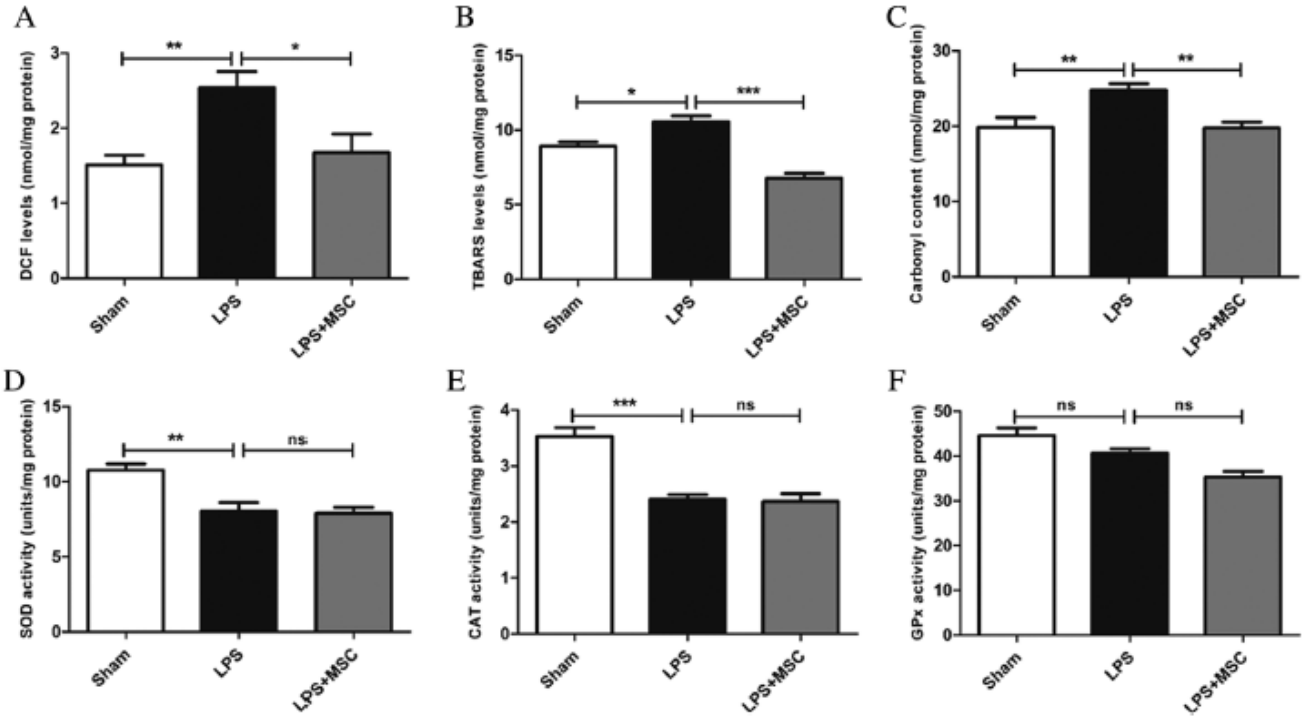

FIGURE 7 MSCs treatment reduced oxidative stress in lung during acute lung injury. Lung sections were collected 12 hr after ALI induction and all the measured were performed as previously described using a spectrophotometer. We evaluated reactive species production by DCF the lipid peroxidation by TBARS and damage to proteins by carbonyl levels. The activity of antioxidant enzymes were also measured: (A–C) DCF, TBARS, and carbonyl levels were increased in the LPS group and decreased after MSCs administration. (D) Superoxide dismutase activity (E) Catalase activity. (F) Glutathione peroxidase activity. No significant change in GPx activity was observed between groups. However, a significant decrease in catalase and superoxide dismutase activity in the LPS group compared with the Sham group. Data represent the mean ±SEM, $n = 10$. Ns:non significant difference, *significant difference ($p < 0.05$), **significant difference ($p < 0.01$), and ***significant difference ($p < 0.001$) between the groups

anti-inflammatory cytoline. It was possible to observe a decrease in the production of the inflammatory cytokines in the group treated with stem cells, demonstrating the anti-inflammatory potential of these cells during the course of the ALI. However, we did not observe a greater increase of IL-10 in the treated group when compared to the LPS group and this result is somewhat controversial when compared with other studies, it is possible that in the evaluated time (12 hr) we do not yet have a peak IL-10 stimulated by stem cells.

Due to this immunomodulation caused by stem cells, we decided to evaluate two factors directly involved in the production of inflammatory mediators: NF-κB and COX-2. Cyclooxygenase (COX), the prostaglandin H synthase enzyme, has been implicated in the mechanisms of a wide variety of inflammatory diseases, including lung injury. COX-2, as the inducible isoform of COX, is found to be increased markedly during inflammation (Minghetti, 2004). COX-2 could be upregulated by proinflammatory cytokines and further aggravates the inflammatory immune response in lung injury (Wang et al., 2014). In addition, pharmacologic inhibition of COX-2 has been proven to be able to decrease the proinflammatory cytokines and chemokines and thus protect against ALI (Sio, Ang, Lu, Moochhala, & Bhatia, 2010). Our, Western blot and immunohistochemistry, results demonstrate that MSCs can inhibit the expression of COX-2 by ameliorating the inflammatory condition during ALI.

Another important mediator of the inflammatory process is the NF-κB. This nuclear transcription factor is a regulator of inflammatory processes and plays an important role in the pathogenesis of lung diseases (Lawrence, 2009). When evaluated their expression we also observed a decrease in its expression. Expression of NF-κB is required for maximal transcription of numerous cytokines, including TNF-α, IL-1β, and IL-6 (Yang et al., 2012). In this way, the correlation between the reduction of the inflammatory cytokines in the animals treated with MSCs and the decrease of the expression of this factor is evident.

It is believed that a key aspect of this pulmonary inflammatory response is mediated by increased levels of reactive species (Bowler et al., 2003). In this framework experimental demonstrate that mice subjected to pulmonary injury present an increase in lipid peroxidation, oxidative damage to the protein and disrupted antioxidant defenses in the lung. The presence of these antioxidant enzymes and reducing factors in lung illustrates how the lung adapts to maintain a redox balance and can respond to oxidizing conditions that may threaten the structural and functional integrity of the lung (Cunha et al., 2013).

When we observed our results on oxidative stress, an increase in the amount of carbonyls in the LPS group is evident, demonstrating that we have damage to proteins in addition to an increase in the production of TBARS, which demonstrates a greater damage to membrane lipids. In addition, the number of reactive species, mostly ROS, is also increased and can be observed through DCF.

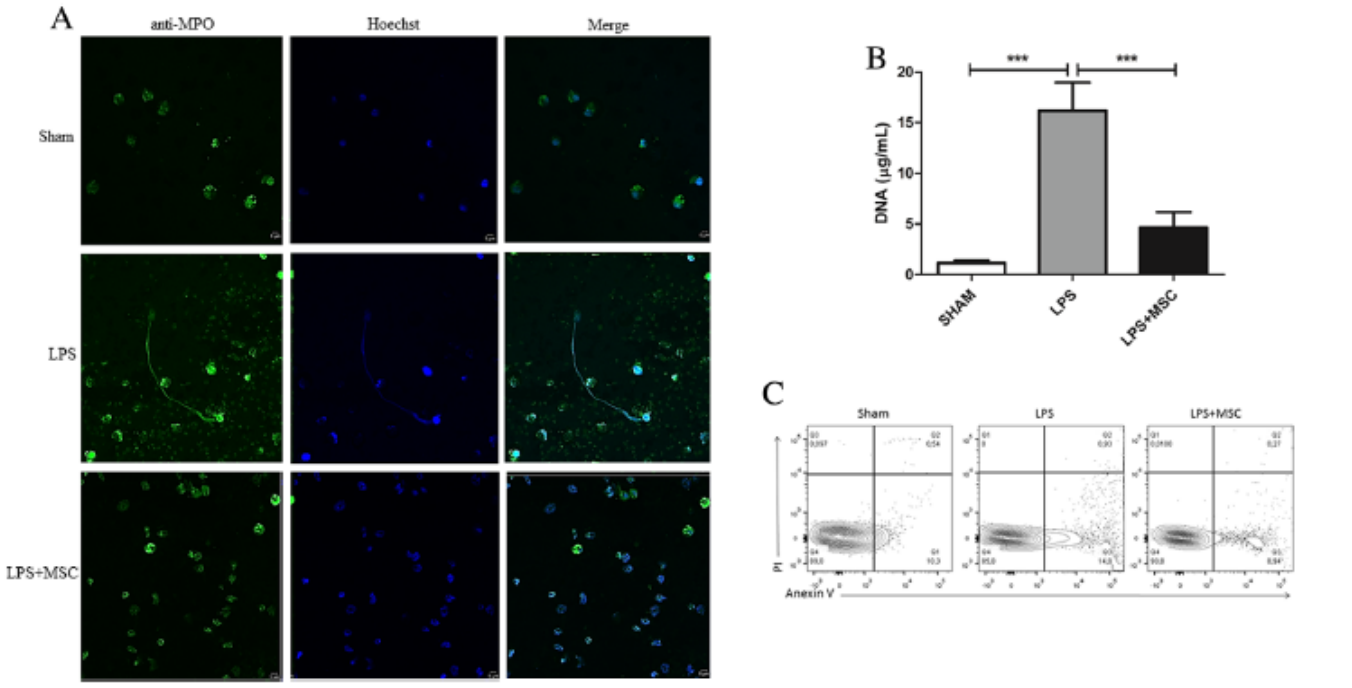

FIGURE 8 MSCs reduce the release of neutrophil extracellular traps. (A) Cells isolated from BALF 12 hr after ALI induction were incubated in eight-chamber culture slides, fixed with 4% paraformaldehyde stained with anti-MPO, followed by anti-mouse FITC antibody and Hoechst 33342. Images are representative of at least three independent experiments. Images were taken with a Zeiss LSM 5 Exciter microscope. Scale bars = 10 µm. (B) Extracellular DNA quantification in BALF supernatants from the all groups was performed with Qubit dsDNA HS assay kit. Data represent the mean ± SEM, $n = 10$. ***Significant difference ($p < 0.001$) between the groups. (C) Flow cytometric analysis of annexin-V binding and propidiumiodide uptake in BALF cells from the all groups. Data are representative of four separate experiments with similar results. There was a significant increase in NETs release and concentration of DNA in BALF in the LPS group compared with the Sham group. MSC-treated group when compared to the LPS group demonstrated a reduction in the release of NETs and a decrease in circulating DNA in BALF. The number of cells in apoptosis had no difference between the groups

The increase in the number of reactive species leads to an increase in the consumption of the SOD enzyme to detoxify the excess of O_2^- formed, which would justify the decrease found in the LPS group. The detoxification caused by SOD can generate large amount of H_2O_2, which, the CAT enzyme is able to neutralize. In the same way as SOD, the CAT enzyme is also decreased in the LPS group, possibly because it is being consumed in this process. We did not have significant changes in the GPx enzyme, this antioxidant enzyme is the most expressed and most active in the lung and possibly does not change like the others (Asikainen, Raivio, Saksela, & Kinnula, 1998; Lubos, Loscalzo, & Handy, 2011). Treatment with MSCs was not able to alter or improve the activity of antioxidant enzymes, however, it was able to decrease ROS production, damage to membrane lipids, and carbonyl proteins indicating that MSCs can prevent LPS-induced lung injury by from ROS exposure.

These results on oxidative stress and massive neutrophil migration led us to perform experiments to evaluate whether MSCs could reduce the formation of NETs during ALI. Experimental studies have linked

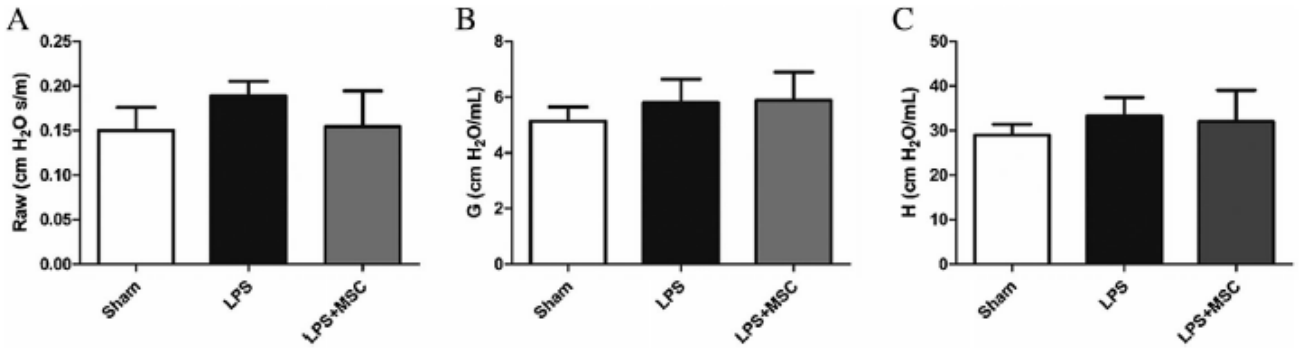

FIGURE 9 Pulmonary function parameters in ALI are not affected. Animals exposed to LPS-induced ALI after 12 hr were submitted a small animal ventilator (flexi Vent, SCIREQ, Montreal, PQ, Canada) for assessment of respiratory mechanics. The evaluation of three parameters was performed: (A) airway resistance (Raw); (B) tissue elastance (H); (C) tissue damping (G). Data represent the mean ± SEM, $n = 6$. We did not observe any significant change between the groups

acute lung injury to NETs formation and their ROS-dependent production (Chen et al., 2014). High ROS concentrations are responsible for the activation and release of neutrophil-derived proteases and the formation of NETs (Amulic, Cazalet, Hayes, Metzler, & Zychlinsky, 2012; Rayment, Upton, & Shooter, 2008).

Recently, it has been described in a vasculitis model that MSCs were able to inhibit the formation of these networks. Based on the adaptive induction of antioxidant enzymes, particularly SOD3, MSCs were able to efficiently dampen the oxidative burst outcome of neutrophils, to suppress their release of destructive enzymes, such as peroxidases and proteases, and to inhibit NETs formation (Jiang et al., 2016). In experimental transfusion-related acute lung injury (TRALI) in vivo degradation of NET-derived DNA structures using DNAse1 reduced the severity of lung injury and mortality in the murine TRALI model (Abrams et al., 2013). Another study using blocking antibodies against histones H2A and H4 and also disrupting the NET scaffold with DNase were effective in reducing lung injury and mortality (Caudrillier et al., 2012). We conducted the evaluation of NETs in the BALF to verify if we had a higher formation in the LPS group when compared to the MSCs-treated group. It was evident the decrease in the formation of these NETs in the LPS + MSC group when we made the evaluation by immunofluorescence The decrease of these networks is a positive point, because it reduces the tissue damage caused by the excess formation of the same ones during the ALI.

We also performed the DNA extracellular assay on BALF to confirm that we had an increase in circulating DNA extracellular by the lung and that it was possibly from the NETs. The result shows a massive increase of DNA extracellular in LPS group that is not found in the group treated with MSCs. The count of cell numbers on apoptosis in BALF was also analyzed to confirm that this DNA extracellular found was not derived from the increase of dead cells circulating in the lung. No difference was observed in the number of cells in apoptosis between the groups demonstrating that the DNA found in BALF possibly comes from the release of NETs.

Finally, we conclude that lung injury is accompanied by impaired respiratory mechanics and edema formation, which contribute to the respiratory failure. In this way, we have extended our investigation to evaluate if treatment could lead to an improvement of lung mechanical parameters. However, despite all the benefits of the treatment, when we performed the analysis of elastance, airway resistance and tissue resistance, it was not possible to verify any significant alterations in the LPS group and also in the group treated with MSCs. It is possible that in the short time of 12 hr it is still not possible to identify any changes in these parameters, perhaps in the long term it is possible to better evaluate changes in pulmonary mechanics.

5 | CONCLUSIONS

In conclusion, our study demonstrates the effectiveness of MSCs in the treatment of ALI decreasing oxidative stress and inflammation. Through our experiments it was possible to demonstrate for the first time that MSCs treatment can reduce the formation of NETs during ALI, and thus contribute to a better prognosis in the course of the disease. Further efforts to elucidate the various mechanisms to which MSCs are involved during ALI are essential to take this promising treatment to clinical stage.

ACKNOWLEDGMENT

This study was supported by grant from the Conselho Nacional de Desenvolvimento Científico e Tecnológico (CNPq, 400422/2013-1), from the Ministry of Science, Technology and Innovation Education of Brazil.

AUTHORS' CONTRIBUTIONS

LP conceived the work, acquired data, drafted the article, and approved the final version. MVTD, ATSW, PMCP, JLR, and JRO, conceived the work, revised the article, and approved the final version. AAC designed the work, revised the article, and approved the final version. CL, NKN, FS, RBG, and RVB acquired data, revised the article, and approved the final version.

CONFLICTS OF INTEREST

The authors declare that they have no competing interests.

REFERENCES

Abrams, S. T., Zhang, N., Manson, J., Liu, T., Dart, C., Baluwa, F., ... Toh, C. H. (2013). Circulating histones are mediators of trauma-associated lung injury. *American Journal of Respiratory and Critical Care Medicine*, *187*(2), 160–169.

Aebi, H. (1984). Catalase in vitro. *Methods in Enzymology*, *105*, 121–126.

Amulic, B., Cazalet, C., Hayes, G. L., Metzler, K. D., & Zychlinsky, A. (2012). Neutrophil function: From mechanisms to disease. *Annual Review of Immunology*, *30*, 459–489.

Arrieta, C. N., Ritz, J., & Silberstein, L. E. (2011). The elusive nature and function of mesenchymal stem cells. *Nature Reviews Molecular Cell Biology*, *12*(2), 126–131.

Asikainen, T. M., Raivio, K. O., Saksela, M., & Kinnula, V. L. (1998). Expression and developmental profile of antioxidant enzymes in human lung and liver. *American Journal of Respiratory Cell and Molecular Biology*, *19*, 942–949.

Bowler, R. P., Velsor, L. W., Duda, B., Chan, E. D., Abraham, E., Ware, L. B., ... Day, B. J. (2003). Pulmonary edema fluid antioxidants are depressed in acute lung injury. *Critical Care Medicine*, *31*(9), 2309–2315.

Casas-Terradellas, E., Tato, I., Bartrons, R., Ventura, F., & Rosa, J. L. (2008). ERK and p38 pathways regulate amino acid signalling. *Biochimica et Biophysica Acta*, *1783*, 2241–2254.

Caudrillier, A., Kessenbrock, K., Gilliss, B. M., Nguyen, J. X., Marques, M. B., Monestier, M., ... Looney, M. R. (2012). Platelets induce neutrophil extracellular traps in transfusion-related acute lung injury. *The Journal of Clinical Investigation*, *122*(7), 2661–2671.

Chen, G., Zhang, D., Fuchs, T. A., Manwani, D., Wagner, D. D., & Frenette, P. S. (2014). Heme-induced neutrophil extracellular traps contribute to the pathogenesis of sickle cell disease. *Blood*, *123*(24), 3818–3827.

Cohen, P. R. (2009). Neutrophilic dermatoses: A review of current treatment options. *American Journal of Clinical Dermatology*, *10*, 301–312.

Coxon, A., Cullere, X., Knight, S., Sethi, S., Wakelin, M. W., Stavrakis, G., ... Mayadas, T. N. (2001). Fc gamma RIII mediates neutrophil recruitment to immune complexes. A mechanism for neutrophil accumulation in immunemediated inflammation. *Immunity*, *14*, 693–704.

Cubillos-Rojas, M., Amair-Pinedo, F., Tato, I., Bartrons, R., Ventura, F., & Rosa, J. L. (2010). Simultaneous electrophoretic analysis of proteins of very high and low molecular mass using tris-acetate polyacrylamide gels. *Electrophoresis*, *31*, 1318–1321.

Cunha, M. J., Cunha, A. A., Ferreira, G. K., Baladão, M. E., Savio, L. E. B., Reichel, C. L., … Wyse, A. T. S. (2013). The effect of exercise on the oxidative stress induced by experimental lung injury. *Life Sciences*, *92*(3), 218–227.

Cunha, M. J., Cunha, A. A., Loureiro, S. O., Machado, F. R., Schmitz, F., Kolling, J., … Wyse, A. T. S. (2015). Experimental lung injury promotes changes in oxidative/nitrative status and inflammatory markers in cerebral cortex of rats. *Molecular Neurobiology*, *52*(3), 1590–1600.

Dowdy, D. W., Eid, M. P., Dennison, C. R., Mendez-Tellez, P. A., Herridge, M. S., Guallar, E., … Needham, D. M. (2006). Quality of life after acute respiratory distress syndrome: A meta-analysis. *Intensive Care Medicine*, *32*, 1115–1124.

Geiser, T., Atabai, K., Jarreau, P. H., Ware, L. B., Pugin, J., & Matthay, M. A. (2001). Pulmonary edema fluid from patients with acute lung injury augments in vitro alveolar epithelial repair by an IL-1beta-dependent mechanism. *American Journal of Respiratory and Critical Care Medicine*, *163*, 1384–1388.

González, I. M., Roca, O., Masclans, J. R., Moreno, R., Salcedo, M. T., Baekelandt, V., … Aran, J. M. (2013). Human mesenchymal stem cells overexpressing the IL-33 antagonist soluble IL-1 receptor-like-1 attenuate endotoxin-induced acute lung injury. *American Journal of Respiratory Cell and Molecular Biology*, *49*(4), 552–562.

Gotts, J. E., & Matthay, M. A. (2011). Mesenchymal stem cells and acute lung injury. *Critical Care Clinics*, *27*(3), 719–733.

Hantos, Z., Daroczy, B., Suki, B., Nagy, S., & Fredberg, J. J. (1992). Input impedance and peripheral inhomogeneity of dog lungs. *Journal of Applied Physiology*, *72*, 168–178.

Horie, S., & Laffey, J. G. (2016). Recent insights: Mesenchymal stromal/stem cell therapy for acute respiratory distress syndrome. *F1000 Research*, *5*, 1532.

Huang, H., Tohme, S., Al-Khafaji, A. B., Tai, S., Loughran, P., Chen, L., … & Tsung, A. Hepatology. (2015). Damage-associated molecular pattern-activated neutrophil extracellular trap exacerbates sterile inflammatory liver injury. *Critical Care Medicine*, *62*(2), 600–614.

Jiang, D., Muschhammer, J., Qi, Y., Kügler, A., Vries, J. C., Saffarzadeh, M., … Kochanek, K. S. (2016). Suppression of neutrophil-mediated tissue damage – a novel skill of mesenchymal stem cells. *Stem Cells*, *34*, 2393–2406.

Johnson, E. R., & Matthay, M. A. (2010). Acute lung injury: Epidemiology, pathogenesis, and treatment. *Journal of Aerosol Medicine and Pulmonary Drug Delivery*, *23*(4), 243–252.

Kuwano, T., Nakao, S., Yamamoto, H., Tsuneyoshi, M., Yamamoto, T., Kuwano, M., & Ono, M. (2004). Cyclooxygenase 2 is a key enzyme for inflammatory cytokine-induced angiogenesis. *FASEB Journal*, *18*, 300–310.

Lawrence, T. (2009). The nuclear factor NF-kB pathway in inflammation. *Cold Spring Harbor Perspectives in Biology*, *1*(6), 1–11.

LeBel, C. P., Ischiropoulos, H., & Bondy, S. C. (1992). Evaluation of the probe 2′,7′-dichlorofluorescin as an indicator of reactive oxygen species formation and oxidative stress. *Chemical Research in Toxicology*, *5*, 227–231.

Leea, J. W., Fang, X., Krasnodembskaya, A., Howard, J. P., & Matthay, M. A. (2011). Concise review: Mesenchymal stem cells for acute lung injury: Role of paracrine soluble factors. *Stem Cells*, *29*(6), 913–919.

Levitt, J. E., Gould, M. K., Ware, L. B., & Matthay, M. A. (2009). Analytic review: The pathogenetic and prognostic value of biologic markers in acute lung injury. *Journal of Intensive Care Medicine*, *24*, 151–167.

Lowry, O. H., Rosebrough, N. J., Farr, A. L., & Randall, R. J. (1951). Protein measurement with the Folin phenol reagent. *The Journal of Biological Chemistry*, *193*, 265–275.

Lubos, E., Loscalzo, J., & Handy, D. E. (2011). Glutathione peroxidase-1 in health and disease: From molecular mechanisms to therapeutic opportunities. *Antioxidants Redox Signaling*, *15*(7), 1957–1997.

Luna, A. C. L., Madeira, M. E. P. P., Conceição, T. O., Moreira, J. A. L. C., Laiso, R. A. N., & Maria, A. D. (2014). Characterization of adipose-derived stem cells of anatomical region from mice. *BCM Research Notes*, *7*, 552.

Marklund, S. L. (1984). *Handbook for oxygen radical research*. Boca Raton: CRC Press.

Mei, S. H. J., McCarter, S. D., Deng, Y., Parker, C. H., Liles, W. C., & Stewart, D. J. (2007). Prevention of LPS-induced acute lung injury in mice by mesenchymal stem cells overexpressing angiopoietin 1. *PLoS Medicine*, *4*(9), e269.

Minghetti, L. (2004). Cyclooxygenase-2 (COX-2) in inflammatory and degenerative brain diseases. *Journal of Neuropathology and Experimental Neurology*, *63*(9), 901–910.

Ohkawa, H., Ohishi, N., & Yagi, K. (1979). Assay for lipid peroxides in animal tissues by thiobarbituric acid reaction. *Analytical Biochemistry*, *95*, 351–358.

Ortiz, L. A., Dutreil, M., Fattman, C., Pandey, A. C., Torres, G., Go, K., & Phinney, D. G. (2007). Interleukin 1 receptor antagonist mediates the antiinflammatory and antifibrotic effect of mesenchymal stem cells during lung injury. *Proceedings of the National Academy of Sciences of the United States of America*, *104*, 11002–11007.

Ortiz, L. A., Gambelli, F., McBride, C., Gaupp, D., Baddoo, M., Kaminski, N., & Phinney, D. G. (2003). Mesenchymal stem cell engraftment in lung is enhanced in response to bleomycin exposure and ameliorates its fibrotic effects. *Proceedings of the National Academy of Sciences of the United States of America*, *100*, 8407–8411.

Parsons, P. E., Eisner, M. D., Thompson, B. T., Matthay, M. A., Ancukiewicz, M., Bernard, G. R., & Wheeler, A. P. Network NARDSCT. (2005). Lower tidal volume ventilation and plasma cytokine markers of inflammation in patients with acute lung injury. *Critical Care Medicine*, *33*, 1–6.

Pugin, J., Verghese, G., Widmer, M. C., & Matthay, M. A. (1999). The alveolar space is the site of intense inflammatory and profibrotic reactions in the early phase of acute respiratory distress syndrome. *Critical Care Medicine*, *27*, 304–312.

Rayment, E. A., Upton, Z., & Shooter, G. K. (2008). Increased matrix metalloproteinase-9 (MMP-9) activity observed in chronic wound fluid is related to the clinical severity of the ulcer. *British Journal of Dermatology*, *158*, 951–961.

Reznick, A. Z., & Packer, L. (1994). Oxidative damage to proteins: Spectrophotometric method for carbonyl assay. *Methods in Enzymology*, *233*, 357–363.

Rojas, M., Xu, J., Woods, C. R., Mora, A. L., Spears, W., Roman, J., & Brigham, K. L. (2005). Bone marrow-derived mesenchymal stem cells in repair of the injured lung. *American Journal of Respiratory Cell and Molecular Biology*, *33*, 145–152.

Rossaint, J., Herter, J. M., Van Aken, H., Napirei, M., Döring, Y., Weber, C., … Zarbock, A. (2014). Synchronized integrin engagement and chemokine activation is crucial in neutrophil extracellular trap-mediated sterile inflammation. *Blood*, *123*, 2573–2584.

Rubenfeld, G. D., Caldwell, E., Peabody, E., Weaver, J., Martin, D. P., Neff, M., … Hudson, L. D. (2005). Incidence and outcomes of acute lung injury. *New England Journal of Medicine*, *353*, 1685–1693.

Sio, S. W., Ang, S. F., Lu, J., Moochhala, S., & Bhatia, M. (2010). Substance P upregulates cyclooxygenase-2 and prostaglandin E metabolite by activating ERK1/2 and NF-kappaB in a mouse model of burn induced remote acute lung injury. *Journal of Immunology*, *185*, 6265.

Stuber, F., Wrigge, H., Schroeder, S., Wetegrove, S., Zinserling, J., Hoeft, A., & Putensen, C. (2002). Kinetic and reversibility of mechanical ventilation-associated pulmonary and systemic inflammatory response in patients with acute lung injury. *Intensive Care Medicine*, *28*, 834–841.

Uccelli, A., Moretta, L., & Pistoia, V. (2008). Mesenchymal stem cells in health and disease. *Nature Reviews Immunology*, *8*, 726–736.

Wang, J., Liu, Y. T., Xiao, L., Zhu, L., Wang, Q., & Yan, T. (2014). Anti-inflammatory effects of apigenin in lipopolysaccharide-induced inflammatory in acute lung injury by suppressing COX-2 and NF-kB pathway. *Inflammation*, *37*(6), 2085–2090.

Wang, Y. Y., Li, X. Z., & Wang, L. B. (2013). Therapeutic implications of mesenchymal stem cells in acute lung injury/acute respiratory distress syndrome. *Stem Cell Research & Therapy*, *4*, 45.

Ware, L. B., Matthay, M. A., Parsons, P. E., Thompson, B. T., Januzzi, J. L., Eisner, M. D., National Heart, Lung, and Blood Institute, & Acute Respiratory Distress Syndrome Clinical Trials Network. (2007). Pathogenetic and prognostic significance of altered coagulation and fibrinolysis in acute lung injury = acute respiratory distress syndrome. *Critical Care Medicine*, *35*, 1821–1828.

Wendel, A. (1981). Glutathione peroxidase. *Methods in Enzymology*, *77*, 325–333.

Xu, J., Woods, C. R., Mora, A. L., Joodi, R., Brigham, K. L., Iyer, S., & Rojas, M. (2007). Prevention of endotoxin-induced systemic response by bone marrow-derived mesenchymal stem cells in mice. *American Journal of Physiology – Lung Cellular & Molecular Physiology*, *293*, L131–L141.

Yang, R., Yang, R., Shen, X., Cheng, W., Zhao, B., Ali, K. H., . . . Ji, H. (2012). Suppression of NF-κB pathway by crocetin contributes to attenuation of lipopolysaccharide-induced acute lung injury in mice. *European Journal of Pharmacology*, *674*, 391–396.

Zemans, R. L., Colgan, S. P., & Downey, G. P. (2009). Transepithelial migration of neutrophils: Mechanisms and implications for acute lung injury. *American Journal of Respiratory Cell and Molecular Biology*, *40*, 519–535.

Zosky, G. R., Janosi, T. Z., Adamicza, A., Bozanich, M. E., Cannizzaro, V., Larcombe, A. N., . . . Hantos, Z. (2008). The bimodal quasi-static and dynamic elastance of the murine lung. *Journal of Applied Physiology*, *105*, 685–692.

How to cite this article: Pedrazza L, Cunha AA, Luft C, et al. Mesenchymal stem cells improves survival in LPS-induced acute lung injury acting through inhibition of NETs formation. *J Cell Physiol.* 2017;9999:1–13. https://doi.org/10.1002/jcp.25816

CAPÍTULO IV

ARTIGO ORIGINAL III

Mesenchymal stem cells cannot affect mRNA expression of toll-like receptors in different tissues during sepsis[a]

[a]Os resultados do presente trabalho foram publicados no periódico ***Inflammation Research*** e está formatado de acordo com as normas do periódico.

Fator de Impacto: 2,557

6. Artigo Original III

Inflamm. Res.
DOI 10.1007/s00011-017-1042-6

Inflammation Research

SHORT COMMUNICATION

Mesenchymal stem cells cannot affect mRNA expression of toll-like receptors in different tissues during sepsis

Leonardo Pedrazza[1] · Talita Carneiro Brandão Pereira[2] · Ana Lucia Abujamra[3] · Fernanda Bordignon Nunes[1] · Maurício Reis Bogo[2] · Jarbas Rodrigues de Oliveira[1]

Received: 8 March 2017 / Revised: 31 March 2017 / Accepted: 3 April 2017

Abstract

Objective and design Experimental animal models and human clinical studies support a crucial role for TLRs in infectious diseases. The aim of this study was to test the ability of MSCs, which have immunomodulatory effects, of altering the mRNA expression of toll-like receptors during a experimental model of sepsis in different tissues.

Materials and methods Three experimental groups (male C57BL/6 mice) were formed for the test: control group, untreated septic group and septic group treated with MSCs (1×10^6 cells/animal). Lungs, cortex, kidney, liver and colon tissue were dissected after 12 h of sepsis induction and TLR2/3/4/9 mRNA were evaluated by RT-qPCR.

Results We observed a decrease of TLR2 and 9 mRNA expression in the liver of the sepsis group, while TLR3 was decreased in the lung and liver. No change was found between the sepsis group and the sepsis + MSC group.

Conclusions In this model of experimental sepsis the MSCs were unable to modify the mRNA expression of the different toll-like receptors evaluated.

Responsible Editor: John Di Battista.

✉ Leonardo Pedrazza
leopedrazza@gmail.com

[1] Laboratório de Pesquisa em Biofísica Celular e Inflamação, Pontifícia Universidade Católica do Rio Grande do Sul (PUCRS), Porto Alegre, Rio Grande do Sul CEP 90619-900, Brazil

[2] Laboratório de Biologia Celular e Molecular, Pontifícia Universidade Católica do Rio Grande do Sul (PUCRS), Porto Alegre, Rio Grande do Sul CEP 90619-900, Brazil

[3] Programa de Graduação de Biotecnologia, Centro Universitário Univates, Lajeado, Rio Grande do Sul CEP 95900-000, Brazil

Published online: 08 April 2017

Keywords Sepsis · Toll-like receptors · Mesenchymal stem cells

Introduction

Septic syndromes are defined as the presence of infection associated with a systemic inflammatory response. The initial phase of the disease is dominated by an exacerbated inflammatory response responsible for successive organ failures and ultimately refractory hypotension leadin to shock [1].

Sepsis is one of the leading causes of death worldwide. Incidence of severe sepsis is increasing and mortality rates remain significantly high despite early care management. Moreover, more than 30% of survivors develop long-term functional disabilities and cognitive impairments [2, 3].

Based on their immunomodulatory properties, adult mesenchymal stem or stromal cells (MSCs) can be a novel therapeutic tool to treat sepsis [4]. MSCs reduce mortality in experimental models of sepsis by modulating the dysregulated inflammatory response against bacteria through the regulation of multiple inflammatory networks, the reprogramming of macrophages and neutrophils towards a more anti-inflammatory phenotype and the release of antimicrobial peptides [5].

Toll-like receptors (TLRs) are pattern recognition receptors playing a fundamental role in sensing microbial invasion and initiating innate and adaptive immune responses. The discovery of TLRs and their involvement in innate immune responses has attracted much interest into the development of drugs for controlling infections and improving sepsis management [7].

TLR expression is not exclusively limited to immune cells (i.e., macrophages, dendritic cells, neutrophils, T cells, and B cells) but has also been reported in multiple

other cell types under physiological conditions, including nervous, muscular, reproductive, colonic, adipose, renal, hepatic, and alveolar tissue [8]. Thus, the objective of our study was to evaluate the expression of four toll-like receptors (TLR2, 3, 4, 9) in a sepsis model and the ability of the treatment with MSCs modify the mRNA expression of these receptors in different tissues.

Materials and methods

Animals

Male C57BL/6 mice (8–12 weeks old) were kept on shelves with ventilated cages that provide 60 air cycles per hour, relative humidity ranging between 55 and 65%, a 12 h light–dark cycle, temperature of 22 ± 2 °C with free access to food and water. The animals were maintained in accordance with the Guiding Principles in the Care and Use of Animals approved by the Council of the American Physiological Society. The experimental protocol was approved by the Ethics Research Committee of Pontifícia Universidade Católica do Rio Grande do Sul (protocol no. 14/00403).

Cell culture

MSCs were characterized by expression of cellular markers (CD 90+, CD105+, CD 34−, and CD45−) (Bio-Rad, Hercules, CA) was determined by flow cytometry analysis [9]. MSCs were induced to differentiate into adipocytes, osteocytes, and chondrocytes by using cell differentiation kits from R&D Systems (Minneapolis, MN) in accordance with the recommendation of the manufacturer. Prior to the collection of the adipose tissue, mice were killed by cervical dislocation.

Adipose tissue was obtained from the epididymal adipose tissue, cut into small pieces, collagenase digested, filtered and then cultured using DMEM Dulbecco's Modified Eagle Medium (Invitrogen Corporation, California, USA) without ribonucleosides or deoxyribonucleosides containing 2 mM L-glutamine and 10% fetal bovine serum (FBS) (Invitrogen, USA), with 1% penicillin–streptomycin. Cells were passaged every 3–4 days by trypsinization when they reached 70–80% confluence and were used for the experiments between passages 3 and 4. Between each passage, cell viability was measured using the trypan blue exclusion test. MSCs were cultured in a humidified incubator at 5% CO2 and 37 °C under sterile conditions. Before each experiment, cells were trypsinized, counted, washed twice with PBS and resuspended in phosphatebuffered saline (PBS) (Gibco, USA). In all in vivo experiments, MSCs were used between passages 3 and 4.

Sepsis induction and treatment

The animals were weighed and then anesthetized with a mixture of ketamine (80 mg/kg) and xylazine (20 mg/kg) intraperitoneally (i.p). The abdomen of each animal was shaved and cleaned with povidone–iodine solution. A 1 cm midline abdominal incision was made to expose the linea alba. The peritoneum was opened by blunt dissection. Sepsis was induced by introducing a sterile gelatin capsule size "1" in the peritoneal cavity containing another sterile capsule size "2" with the Escherichia coli (3 µL, ATCC 25922) suspension and a non-sterile fecal content (20 mg). This experimental model was developed by our laboratory [10, 11]. The animals were then divided into three groups: (1) sham (mice were implanted with an empty capsule and received retro-orbital injection of 100 µL PBS), (2) sepsis (sepsis-induced and received retro-orbital injection of 100 µL PBS), (3) sepsis + MSC (sepsis-induced and treated with 1×10^6 MSCs in retro-orbital injection of 100 µL PBS at the time of induction).

RT-qPCR analysis of gene expression

Lungs, cortex, kidney, liver and colon tissue were dissected and store in 300l of TRIzol Reagent (Sigma; St Louis, USA) at −80 °C until use. The total RNA was isolated with Trizol reagent (Invitrogen, Carlsbad, California, USA) in accordance with the manufacturers' instructions. The total RNA was quantified by spectrophotometry and the cDNA was synthesized with ImProm-II Reverse Transcription System (So Paulo, Brazil, Promega) from 1 µg of total RNA, following the manufacturers' instructions. Quantitative PCR was performed using SYBR Green I (Invitrogen; Carlsbad, USA) to detect double-strand in a final volume of 25 µl using 12.5 µl of diluted cDNA and containing a final concentration of 0.2 × SYBR Green I, 100 µM dNTP, 1 PCR Buffer, 3 mM MgCl2, 0.25 U Platinum Taq DNA Polymerase (Invitrogen; Carlsbad, USA) and 200 nM of each reverse and forward primers. The primers used were TLR-2 (forward 5′-TGCTTTCCT GCTGGAGATTT-3′; reverse 5′-TGTAACGCAACAGCT TCAGG-3′) [12], TLR-3 (forward 5′- AGCTTTGCTGGG AACTTTCA-3′, reverse 5′-GAAAGATCGAGCTGGGTG AG-3′) [13], TLR-4 (forward 5′-ATGGAAAAGCCTC-GAATCCT-3′; reverse 5′- CTTAGCAGCCATGTGTTCC A-3′) [14], TLR-4 (forward 5′-CTTTGGCCTTTCACTCT TG-3′; reverse 5′-ACCACGAAGGCATCATAAGG-3′) [15, 16] Hprt1 (forward 5′-CTCATGGACTGATTATG-GACAGGAC-3′; reverse 5′- CAGGTCAGCAAAGAACT TATAGCC-3) [17] (GenBankTM accession number NM_013556) and TBP (forward5- CCGTGAATCTTGGC TGTAAACTTG -3; reverse 5′- GTTGTCCGTGGCTCTC TTATTCTC-3′) [17] (GenBankTM accession number

NM_013684). The PCR cycling conditions started with an initial polymerase activation step for 5 min at 95 °C for denaturation, and four cycles 15 s at 95 °C for denaturation, 35 s at 6 °C for annealing and 15 s at 72 °C for elongation. At the end of the cycling protocol, a melting curve analysis was included and fluorescence measured from 60 °C to 99 °C.

Relative expression levels were determined with 7500 fast real-time system sequence detection software v.2.0.5 (Applied Biosystems; Carlsbad, USA) and were analyzed by the $2^{-\Delta\Delta CT}$ method using tbp and hprt as reference genes. The efficiency per sample was calculated using *LinRegPCR Software* v20161 (http://LinRegPCR.nl).

Statistical analysis

The data were analyzed by one-way analysis of variance (ANOVA). For comparison of significance, Tukey's test was used as a post hoc test according to the statistical program GraphPad Prism. Quantitative data are presented as mean ± SEM. Differences were considered significant at $*p < 0.05$ between the sham and sepsis group and $\#p < 0.05$ between the sham group and sepsis + MSC group.

Results

Twelve hours after the treatment with MSCs, we performed the tissue collection to evaluate the mRNA expression of four different TLRs (TLR2, 3, 4, 9). When we analyzed the level of expression in the cerebral cortex and the colon (Table 1A, B), we found no significant change between the groups studied.

However, when we performed the expression analysis of the receptors in the kidney of the mice, we observed a decrease in TLR2 expression in the sepsis group when compared to the sham group (Table 1C). No significant difference was found between the sepsis group and the sepsis + MSC group.

We also evaluated the mRNA expression in the liver, and it was possible to observe a decrease in TLR3 and TLR9 in the sepsis group compared to the sham group and no change between the sepsis group and the MSCs-treated group. In contrast, we had an increase in the expression of TLR4 in the sepsis group relative to the sham group and no significant difference between the sepsis group when compared to the sepsis + MSC group (Table 1D).

Finally, in the lung, our analyses indicated a decrease in TLR3 in the sepsis group compared to the sham group, and no significant difference between the sepsis group and the MSCs-treated group (Table 1E).

Discussion

This is the first report of mRNA expression profile in a sepsis model and the possible influence of MSCs in different tissues. Mesenchymal stem cells have immunomodulating properties and inhibit function of immune cells [18]. There is evidence that the capability to modulate immune responses rely on both cell contact-dependent mechanisms and paracrine effects through the release of soluble factors. Several studies have reported beneficial effects of MSC treatment in animal models of sepsis [11, 19–21].

TLRs play a fundamental role in the primary response against invaders connecting both innate and adaptive immune responses [6]. Activation of TLRs in inflammatory diseases underpins their pathophysiology via aberrant secretion of pro-inflammatory cytokines and chemokines, which in turn creates an inflammatory feedback loop. Breakage of this feedback loop should dampen the inflammation and reestablish an appropriate immune response to pathogens [22].

Targeting TLRs is a promising field for sepsis management and infection control. In general, strategies utilized to downmodulate the overactivation of TLRs involve the use of antagonists that block the binding of ligands or protein–ligand complexes to the receptors, or antagonists that interfere with the intracellular adaptor molecules of the common signaling pathways, neutralizing their effects and blocking the activation of TLR signaling cascade. Given their pivotal role in orchestrating the immune response, the main challenge for the development of TLR-blocking agents is to reduce the excessive inflammation without affecting innate immunity [6].

In our work we observed a decrease in mRNA expression of different TLRs in different organs; however, we found an increase in TLR4 in the liver. Under normal circumstances, the liver negatively regulates TLR4 signaling at different levels, contributing to a process known as "liver tolerance" [23]. Our results show a breakdown of liver tolerance by increased exposure of TLR4 to LPS, from septic induction, with a increased expression of TLR4. These results suggest that the liver may react to LPS infection and aggravate inflammatory conditions.

We found no evidence that MSCs could modulate the expression of these receptors in this preclinical model in any way. It is possible that TLRs are up-regulated in different tissues in early stages. However, our model of sepsis is very severe, the animals begin to die in 15 h [11] and we perform the tissue collection at 12 h. Probably, in this period the animals are in a very advanced phase of the sepsis course. Previously studies with severely septic patients, especially patients with APACHE II scores

Table 1 TLR2, TLR3, TLR4 and TLR9 relative expression levels of mRNA determined 12 h after sepsis induction in (A) cerebral cortex, (B) colon, (C) kidney, (D) liver and (E) lung. The experimental conditions are described under "Materials and Methods"

	TLR2	TLR3	TLR4	TLR9
(A). Cer.cortex				
Sham	1.45 ± 0.05	1.46 ± 0.05	1.11 ± 0.03	1.32 ± 0.05
Sepsis	1.35 ± 0.02	1.35 ± 0.02	1.12 ± 0.03	1.14 ± 0.01
Sepsis + MSC	1.30 ± 0.15	1.39 ± 0.20	1.21 ± 0.07	1.52 ± 0.19
(B). Colon				
Sham	1.26 ± 0.10	–	1.18 ± 0.12	0.73 ± 0.17
Sepsis	1.17 ± 0.10	–	1.11 ± 0.07	0.73 ± 0.16
Sepsis + MSC	1.12 ± 0.11	–	1.12 ± 0.11	1.09 ± 0.18
(C). Kidney				
Sham	1.15 ± 0.21	0.97 ± 0.03	0.68 ± 0.12	0.94 ± 0.02
Sepsis	0.41 ± 0.05*	0.99 ± 0.02	0.36 ± 0.07	1.18 ± 0.07
Sepsis + MSC	0.53 ± 0.12*	0.92 ± 0.03	0.43 ± 0.11	1.12 ± 0.09
(D). Liver				
Sham	1.09 ± 0.04	2.04 ± 0.19	0.81 ± 0.02	1.71 ± 0.16
Sepsis	0.96 ± 0.02	1.28 ± 0.09*	1.02 ± 0.02*	1.12 ± 0.28*
Sepsis + MSC	0.97 ± 0.04	1.31 ± 0.12*	0.96 ± 0.05*	1.21 ± 0.05*
(E). Lung				
Sham	1.08 ± 0.02	1.35 ± 0.09	1.09 ± 0.03	1.02 ± 0.04
Sepsis	0.97 ± 0.01	1.16 ± 0.06*	1.01 ± 0.02	1.03 ± 0.02
Sepsis + MSC	0.96 ± 0.02	1.22 ± 0.07*	0.97 ± 0.05	0.94 ± 0.03

Data represent the mean ± SEM, $n = 5$

*$p < 0.05$ between the sham and sepsis group or between the sham group and sepsis + MSC group

greater than 20 and an unfavorable clinical outcome, did not have increased expression of TLRs relative to less severely injured patients. The association between TLR expression and the severity of illness in septic patients, however, remains elusive, and further investigations will be necessary [24].

Further investigation in experimental animal models is required to clarify the correlation between TLRs and MSCs during sepsis. This work opens new ways for future research and elucidations about this promising treatment for sepsis.

References

1. Hotchkiss RS, Nicholson DW. Apoptosis and caspases regulate death and inflammation in sepsis. Nature. 2006;6:813–22.
2. Gaieski DF, Edwards JM, Kallan MJ, Carr BG. Bench marking the incidence and mortality of severe sepsis in the United States. Crit Care Med. 2013;41:116774. doi:10.1097/CCM.0b013e31827c09f8.
3. Iwashyna TJ, Ely EW, Smith DM, Langa KM. Long-term cognitive impairment and functional disability among survivors of severe sepsis. JAMA. 2010;304:178794. doi:10.1001/jama.2010.1553.
4. Lalu MM, Sullivan KJ, Mei SHJ, Moher D, Straus A, Fergusson DA, et al. Evaluating mesenchymal stem cell therapy for sepsis with preclinical meta-analyses prior to initiating a first-in-human trial. eLife. 2016;5:e17850. doi:10.7554/eLife.17850.
5. Lombardo E, van der Poll T, DelaRosa O, Dalemans W. Mesenchymal stem cells as a therapeutic tool to treat sepsis. World J Stem Cells. 2015;7(2):368–79.
6. Savva A, Roger T. Targeting toll-like receptors: promising therapeutic strategies for the management of sepsis-associated pathology and infectious diseases. Front Immunol. 2013;4:387. doi:10.3389/fimmu.2013.00387.
7. Hennessy EJ, Parker AE, Oneill LA. Targeting toll-like receptors:emerging therapeutics? Nat Rev Drug Discov. 2010;9:293307. doi:10.1038/nrd3203.
8. Asma A, Yesudhas D, Choi S. Toll-like receptors: promising therapeutic targets for inflammatory diseases. Arch Pharm Res. 2016;39:1032–49. doi:10.1007/s12272-016-0806-9.
9. Alvarado G, Lathia JD. Review taking a toll on self-renewal TLR-mediated innate immune signaling in stem cells. Trends Neurosci. 2016;39(7):463–71. doi:10.1016/j.tins.2016.04.005.
10. Luna ACL, Madeira MEPP, Conceio TO, Moreira JALC, Laiso RAN, Maria AD. Characterization of adipose-derived stem cells of anatomical region from mice. BCM Res Notes. 2014;7:552.
11. Nunes FB, Pires MGS, Filho JCFA, Wachter PH, Oliveira JR. Physiopathological studies in septic rats and the use of fructose-1,6-bisphosphate as cellular protection. Crit Care Med. 2002;30(9):2069–74.
12. Pedrazza L, Lunardelli A, Luft C, Cruz CU, Mesquita FC, et al. Mesenchymal stem cells decrease splenocytes apoptosis in a sepsis experimental model. Inflamm Res. 2014;2014(63):719–28.
13. Lim JY, Im KI, Lee ES, Kim N, Nam YS, Jeon YW, Cho SG. Enhanced immunoregulation of mesenchymal stem cells by IL-10- producing type 1 regulatory T cells in collagen-induced arthritis. Sci Rep. 2016;6:26851. doi:10.1038/srep26851.

14. Rolls A, Shechter R, London A, Ziv Y, Ronen A, Levy R, Schwartz M. Toll-like receptors modulate adult hippocampal neurogenesis. Nat Cell Biol. 2007;9(9):1081–8.
15. Pope MR, Hoffman SM, Tomlinson S, Fleming SD. Complement regulates TLR4-mediated inflammatory responses during intestinal ischemia reperfusion. Mol Immunol. 2010;48(1–3):356–64. doi:10.1016/j.molimm.2010.07.004.
16. Shechter R, Ronen A, Rolls A, London A, Bakalash S, Young MJ, Schwartz M. Toll-like receptor 4 restricts retinal progenitor cell proliferation. J Cell Biol. 2008;183(3):393–400. doi:10.1083/jcb.200804010.
17. Arciero J, Bard Ermentrout G, Siggers R, Afrazi A, Hackam D, Vodovotz Y, Rubin J. Modeling the interactions of bacteria and toll-like receptor-mediated inflammation in necrotizing enterocolitis. J Theor Biol. 2013;321:83–99. doi:10.1016/j.jtbi.2012.12.002.
18. Pernot F, Dorandeu F, Beaup C, Peinnequin A. Selection of reference genes for real-time quantitative reverse transcription-polymerase chain reaction in hippocampal structure in a murine model of temporal lobe epilepsy with focal seizures. J Neurosci Res. 2010;88(5):1000–8. doi:10.1002/jnr.22282.
19. Gao F, Chiu SM, Motan DAL, Zhang Z, Chen L, Ji HL, et al. Mesenchymal stem cells and immunomodulation: current status and future prospects. Cell Death Dis. 2016;7(1):e2062. doi:10.1038/cddis.2015.327.
20. Németh K, Leelahavanichkul A, Yuen PST, Mayer B, Parmelee A, Doi K, et al. Bone marrow stromal cells attenuate sepsis via prostaglandin E2-dependent reprogramming of host macrophages to increase their interleukin-10 production. Nat Med. 2009;15:42–9.
21. Mei SH, Haitsma JJ, Dos Santos CC, Deng Y, Lai PF, Slutsky AS, et al. Mesenchymal stem cells reduce inflammation while enhancing bacterial clearance and improving survival in sepsis. Am J Respir Crit Care Med. 2010;182:1047–57.
22. Basith S, Manavalan B, Lee G, Kim SG, Choi S. Toll-like receptor modulators: a patent review (2006–2010). Expert Opin Ther Pat. 2011;21:927–44.
23. Soares JB, Nunes PP, Albuquerque RR Jr, Moreira AL. The role of lipopolysaccharide/toll-like receptor 4 signaling in chronic liver diseases. Hepatol Int. 2010;4:659–72. doi:10.1007/s12072-010-9219-x.
24. Tsujimoto H, Ono S, Efron PA, Scumpia PO, Moldawer LL, Mochizuki H. Role of toll-like receptors in the development of sepsis. Shock. 2008;29(3):315–21. doi:10.1097/SHK.0b013e318157ee55.

CAPÍTULO V

CONSIDERAÇÕES FINAIS

7. Considerações Finais

Alertado nos últimos anos pela morbidade e mortalidade decorrentes da sepse e da LPA, principalmente por deficiências dos atuais regimes terapêuticos, pesquisadores se voltaram à terapia baseada em células como uma nova abordagem para o tratamento destas patologias. Embora inicialmente acreditava-se que o maior potencial de células-tronco residia na sua capacidade de enxertar e se diferenciar em tipos de células de órgãos lesados, elas também exibem uma gama de habilidades benéficas, incluindo migração para locais lesionados, modulação da cascata inflamatória, prevenção de apoptose celular nos tecidos, promoção da neoangiogênese, ativação de células-tronco residentes e a modulação da atividade de vários tipos celulares do sistema imunológico.

Considerando nossa experiência em estudos anteriores[50] utilizando estas células como tratamento em modelo experimental de sepse, este trabalho teve como objetivo elucidar mecanismos aos quais estas células estão envolvidas durante a sepse e durante a lesão pulmonar aguda.

Trabalhos anteriores demonstraram que as células-tronco eram capazes de reprogramar macrófagos de um estado pró-inflamatório a um estado anti-inflamatório, provocando um aumentando a liberação da interlecuina anti-inflamatória IL-10[33]. Entretanto, os mecanismos alterados nas células efetoras do sistema imune não estão completamente elucidados.

Desta forma, o primeiro objetivo do nosso trabalho foi identificar um modelo pelo qual nós poderíamos verificar de que maneira as células-tronco mesenquimais afetam os macrófagos do hospedeiro modulando a resposta inflamatória a ponto de diminuírem a liberação de mediadores inflamatórios.

Primeiramente, nós testamos dois modelos de sepse, um deles utilizando apenas LPS e outro, desenvolvido pelo nosso laboratório [50,87], utilizando uma cápsula contendo suspensão de Escherichia coli e fezes. Os nossos primeiros resultados indicavam que o modelo utilizando apenas LPS não era capaz de provocar uma inflamação pulmonar concisa e que o modelo desenvolvido pelo laboratório

apresentava melhores resultados para a sequência do trabalho. Ficou evidenciado também que as MSCs eram efetivas na redução do score inflamatório peribronquial e perivascular durante a sepse.

Subsequentemente para verificar se as células MSCs possuíam efeito importante sobre o quadro inflamatório, nós avaliamos diversos marcadores inflamatórios e anti-inflamatórios envolvidos durante a sepse. O tratamento com as MSCs foi efetivo na redução dos marcadores inflamatórios (IL-6 e TNF-α) e aumento na produção da interleucina anti-inflamatória IL-10, o que apenas corroborava com resultados anteriores. Nós ainda realizamos a análise da COX-2 e do NF-κB que estão diretamente envolvidos na estimulação da produção dos mediadores inflamatórios e ficou evidente a capacidade destas células em inibirem a expressão de ambos.

Estes resultados iniciais nos conduziram a buscar o mecanismo pelo qual isto ocorria durante nosso modelo experimental. Desta forma, nós resolvemos iniciar o trabalho *in vitro* que nos possibilitava estudar com mais clareza o que observávamos *in vivo*. Neste momento do trabalho nós iniciamos a colaboração com o laboratório de biologia molecular do Centro de Ciências Fisiológicas da Universidade de Barcelona.

Incialmente o nosso objetivo era retirar os macrófagos pulmonares e conduzi-los para a cultura celular e dar sequência aos experimentos *in vitro*. Entretanto devido a limitações das técnicas e ao número elevado de experimentos que queríamos realizar se tornou inviável ao longo do tempo dar sequência ao trabalho dessa forma. Então, nós optamos por utilizar uma linhagem celular de macrófagos pulmonares de camundongos (RAW 264.7) o que possibilitou o melhor desenvolvimento do trabalho.

Sabe-se que as MAPKs estimulam produção de muitos mediadores inflamatórios, tais como o fator de necrose tumoral (TNF-α), interleucina-1β (IL-1β), IL-6, COX-2 e do NF-κB[25]. Desta maneira, nós resolvemos investigar se as células-tronco poderiam de alguma forma influenciar a fosforilação de duas vias das MAPKs (ERK 1/2, p38) e diminuir a produção dos mediadores inflamatórios.

O primeiro passo dos nossos experimentos *in vitro* foi verificar se nosso modelo era efetivo em ativar a via das MAPKs nos macrófagos e encontrar o melhor tempo para que pudéssemos identificar possíveis alterações. Nossos resultados indicaram que o

modelo utilizando LPS era efetivo e que tempos curtos eram mais efetivos para verificação das fosforilações, o que nos fez optar pelos tempos de 15', 30' e 60'.

Dando sequência ao trabalho, para verificarmos se as MSCs eram capazes de influenciar a rota das MAPKs, nós realizamos o cocultivo celular entre os macrófagos e as MSCs. Nós tentamos de duas maneiras, contato direto , célula-célula, e o contato indireto através da utilização de uma membrana denominada *'trans-well'* o que impedia o contato entre as células, permitindo apenas a troca de fatores liberados no meio de cultivo. O contato direto se mostrou mais efetivo e continuamos os experimentos com este modelo.

Nos primeiros experimentos realizados com o cocultivo é visível a capacidade das MSCs em diminuir a fosforolição das MAPKs, tanto para ERK como para p38. Além disso, é possível observar a redução de RSK (substrato da ERK) e de NF-κB. Estes resultados indicavam que possivelmente as células-tronco agiam por essa rota para diminuir a produção e liberação de mediadores inflamatórios provenientes dos macrófagos. Para maior robustez dos resultados nós analisamos por duas metodologias diferentes (western blot e imunofluorescência) e em ambas obtivemos resultados semelhantes.

Antes de darmos sequência à investigação para verificar se os mediadores inflamatórios estavam realmente diminuindo, nós decidimos realizar todos os experimentos de cocultivo novamente e incluir um grupo apenas com MSCs para verificar se a expressão de cada proteína analisada era apenas dos macrófagos e não das MSCs. O resultado demonstra que a influência da expressão proveniente das MSCs no western blot é mínima e que o que tínhamos encontrado anteriormente realmente era proveniente dos macrófagos.

Prosseguindo com a nossa investigação, nós procuramos identificar se a inibição da via das MAPKs provocada pelas MSCs em tempos curtos poderia influenciar a expressão de COX-2 e NF-κB em períodos longos de tempo, portanto, nós resolvemos avaliar a expressão de mediadores inflamatórios a longo prazo (24 e 48h). Nossos experimentos demosntram uma clara diminuição na expressão destes marcadores nas células que são cocultivadas com MSCs. Além disso, nós realizamos a análise de outros mediadores inflamatórios (IL-1β e IL-6) e anti-inflamatório (IL-10) e fica evidente a

imunomodulação provocada pelas MSCs nos macrófagos cocultivados, corroborando com os resultados encontrados in vivo.

Entretanto, apesar de todos estes nossos esforços, de alguma maneira faltava demonstrar que realmente a inibição dessa via pelas MSCs estava diretamente envolvida na diminuição da liberação de fatores pro-inflamatórios dos macrófagos e que isto poderia contribuir para o controle da inflamação no decorrer da sepse. Sendo assim, nós resolvemos realizar um experimento diferente substituindo o cocultivo celular e tratando os macrófagos com dois inibidores de MAPKs diferentes (SB203580 para p38 e U0126 para ERK 1/2) que mimetizassem o papel que nós achávamos que as MSCs estavam desempenhando. Quando observamos a expressão de COX-2 e NF-κB pós tratamento com ambos inibidores, foi possível observar que há uma diminuição significativa quando comparado com as células não tratadas, demonstrando que a inibição desta rota possivelmente é capaz de modular a inflamação e que os resultados obtidos com as MSCs provavelmente são devido a sua capacidade de inibir a via das MAPKs.

Terminado este primeiro trabalho nós resolvemos investigar outros possíveis mecanismos das MSCs no processo inflamatório. Os resultados obtidos no primeiro artigo avaliando a diminuição do edema pulmonar e o domínio das técnicas para estudo desse tecido nos fez optar por investigar a atuação das células em um modelo agudo e pontual no pulmão, desta maneira optamos por utilizar a LPA induzida por LPS.

No primeiro momento realizamos uma curva de sobrevida e identificamos que as MSCs aumentavam a sobrevida dos animais quando comparado com o grupo não-tratado. Este primeiro resultado promissor nos conduziu a investigar o que levava a esse aumento na sobrevida dos animais.

Nós iniciamos realizando um experimento semelhante ao do artigo anterior, verificando se nosso modelo era efetivo e se poderíamos novamente observar a efetividade das MSCs na modulação da inflamação pulmonar. Os primeiros resultados indicavam que sim, porque o tratamento sistêmico com as células foi capaz de diminuir o score inflamatório peribronquial e perivascular no tecido pulmonar. Além disso, foi possível observar que os animais tratados tinham menos migração celular, já que,

tínhamos uma redução significativa na contagem de células totais, macrófagos e neutrófilos além da diminuição das proteínas no lavado bronco-alveolar.

Dando sequência aos nossos experimentos, nós resolvemos confirmar se a redução de células efetoras do sistema imune no tecido pulmonar e diminuição na formação do edema se refletia nos marcadores inflamatórios. Nossos resultados indicaram que sim, como na sepse aqui também temos a redução de IL-6 e TNF-α tanto sistemicamente (soro) quanto local (BALF). Entretanto, não observamos alterações na IL-10, anti-inflamatória, o que diferencia dos nossos resultados obtidos na sepse.

Como já se sabe que a resposta inflamatória pulmonar é mediada por níveis aumentados de espécies reativas, nós resolvemos avaliar parâmetros de estresse oxidativo no pulmão e verificar se as MSCs poderiam estar alterando essa via. O tratamento com MSCs não foi capaz de alterar ou melhorar a atividade de enzimas antioxidantes, no entanto, foi capaz de diminuir a produção de ROS, danos aos lípidos de membrana e de proteínas carbonil, indicando que MSCs podem prevenir a lesão pulmonar induzida por LPS.

As concentrações elevadas de ROS são responsáveis pela liberação e ativação de proteases derivadas de neutrófilos e pela formação de armadilhas extracelulares de neutrófilos (NETs) com a expulsão de fibras de cromatina do núcleo de neutrófilos como estratégias adicionais para combater e matar eficazmente microorganismos invasores[88]. No entanto, quando esses mecanismos estão excessivamente ativados tornam-se altamente destrutivos para os tecidos. Desta forma, todos experimentos iniciais serviram de base para chegarmos na hipótese central deste segundo artigo, que foi verificar se as MSCs poderiam influenciar a formação dos NETs, e que até o momento não se tinha descrito na lesão pulmonar aguda.

Quando nós realizamos o experimento para a verificação da formação dos NETs nos neutrófilos retirados dos animais tratados com MSCs, nós observamos uma diminuição da formação dos NETs quando comparado com os animais não tratados. Nós realizamos ainda a dosagem de DNA extracelular no BALF e a redução no grupo tratado foi significativa. Nós ainda realizamos um ensaio de apotose celular para verificar que este DNA extracelular encontrado não provinha de um aumento de células apoptóticas

e/ou necróticas devido a LPA. Nenhuma diferença foi encontrada entre os grupos o que corrobora com os nossos resultados e demonstra que este DNA é proveniente da liberação dos NETs. Nós ainda tentamos realizar a análise de formação dos NETs diretamente no tecido pulmonar, entretanto, por limitações da técnica a vizualização do que realmente eram formações de NETs no tecido pulmonar era pouco específica, então optamos por não utilizar estes resultados.

Para concluirmos este trabalho nós ainda resolvemos investigar se estes efeitos benéficos provocados pelo tratamento MSCs era capaz de melhorar a função pulmonar através da avaliação da mecânica respiratória. Infelizmente, nosso modelo não se mostrou efetivo para que observássemos qualquer diferença entre os grupos, estudos recentes com metodologia semelhante ao nosso trabalho também não obtiveram nenhuma diferença nos parâmetros de mecânica respiratória em 24h[89]. Possivelmente estudos futuros realizando curvas de tempo possam elucidar melhor esta avaliação neste modelo.

Em um último momento para um terceiro artigo nós retomamos o estudo das MSCs na sepse e realizamos uma análise de expressão de mRNA de receptores tipo toll em diferentes órgãos (córtex cerebral, cólon, rim, fígado e pulmão). Os receptores tipo toll são receptores de reconhecimento de padrões que desempenham um papel fundamental na detecção de invasão microbiana e no início de respostas imunes inatas e adaptativas. Nós conduzimos a análise de quatro receptores diferentes (TLR2, 3, 4, 9) e não foi possível observar nenhuma alteração entre o grupo tratado com MSCs e o grupo não tratado em nenhum dos órgãos analisados. Nós tivemos algumas limitações nesse estudo, dentre elas, o tempo em que realizamos a análise. Devido ao nosso modelo ser um modelo muito grave de sepse possivelmente em 12h seria complicado encontrar alguma alteração, talvez a realização dos experimentos em tempos mais curtos possa ser possível observar alguma diferença. Entretanto, o estudo é válido pois até o presente momento não temos publicada nenhuma análise de diversos receptores tipo toll em um modelo de sepse experimental e a influência do tratamento com MSCs.

Por fim, de acordo com todos os nossos resultados, ficou evidenciado claramente no trabalho que as MSCs atuam durante a sepse modulando o sistema imune através da via das MAPKs e consequentemente reduzindo a produção e liberação de mediadores

inflamatórios. Além disso, ficou clara a efetividade das MSCs no tratamento da LPA, através da diminuição de mediadores inflamatórios e redução do estresse oxidativo ocasionando assim uma inibição da formação dos NETs. Cabe salientar que mais estudos devem ser realizados para aprofundar o conhecimento de outros mecanismos pelos quais estas células atuam para que futuramente possamos utilizar estas células como uma possível alternativa para o tratamento da sepse e da LPA em pacientes.

8. Referências

1. Bone RC. The pathogenesis of sepsis. Ann International Med 1991; 115: 457-469.

2. Majano G. The ancient riddle of sepsis. J Infec Dis 1991; 163: 937.

3. Tilney NL, Bailey GL, Morgan AP. Sequential system failure after rupture of AAA: an unsolved problem in postoperative care. Ann Surg 1973; 178: 117-122.

4. Baue AE. Multiple, progressive or sequential systems failure: a syndrome of the 1970s. Arch Surg 1975; 110: 779-781.

5. American College of Chest Physicians/Society of Critical Care Medicine Consensus Conference: Definitions for sepsis and organ failure and guidelines for the use of innovative therapies in sepsis. Chest 1992; 101: 1644-1655.

6. Levy MM, Fink MP, Marshall JC, Abraham E, Angus D, Cook D, et al. CCM/ESICM/ACCP/ATS/SIS International Sepsis Definitions Conference. Crit Care Med 2003; 31:1250-1256.

7. Hari MS, Phillips GS, Levy ML, Seymour CW, Liu VX, Deutschman CS, et al. New Definition and Assessing New Clinical Criteria for Septic Shock For the Third International Consensus Definitions for Sepsis and Septic Shock (Sepsis-3). JAMA 2016 ;315(8):775-87.

8. Seymour CW, Liu VX, Iwashyna TJ, Brunkhorst FM, Rea TD, Scherag A, et al. Assessment of Clinical Criteria for Sepsis For the Third International Consensus Definitions for Sepsis and Septic Shock (Sepsis-3). JAMA 2016; 315(8):762-74.

9. Martin GS, Mannino DM, Eaton S, Moss M. The epidemiology of sepsis in the United States from 1979 through 2000. N Eng J Med 2003; 348:1546-1554.

10. Bochud PY, Calandra T. Pathogenesis of sepsis: new concepts and implications for future treatment. BMJ 2003; 326: 262-266.

11. Jacobs RF, Sowell MK, Moss M, Fiser DH. Septic shock in children: bacterial etiologies and temporal relationships. Pediatr Infect Dis J 1990; 9:196-200.

12. Silva E, et al. Brazilian Sepsis Epidemiological Study. Crit Care 2004; 8: 251-260.

13. Martin GS. Sepsis, severe sepsis and septic shock: changes in incidence, pathogens and outcomes. Expert Rev Anti Infect Ther 2012; 10(6): 701–706.

14. Martin GS, Mannino DM, Eaton S, Moss M. The epidemiology of sepsis in the United States from through 2000. N Engl J Med 2003; 348(16):1546–1554.

15. Weil BR, Markel TA, Herrmann JL, Abarbanell AM, Kelly ML, Meldrum DR. Stem Cells in Sepsis. Ann Surg 2009; 250: 19 –27.

16. Takeuchi O, Akira S. Pattern recognition receptors and inflammation. Cell 2010; 140: 805 - 820.

17. Schulte W, Bernhagen J, Bucala R. Cytokines in sepsis: potent immunoregulators and potential therapeutic targets--an updated view. Mediators Inflamm 2013; 2013: 1659-1674.

18. Ward PA, Gao H. Sepsis, complement and the dysregulated inflammatory response. J Cell Mol Med 2009; 13: 4154 - 4160.

19. Fullerton JN, O'Brien AJ, Gilroy DW. Pathways mediating resolution of inflammation: when enough is too much. J Pathol 2013; 231: 8-20.

20. Hinshaw LB. Sepsis / Septic shock: Participation of the microcirculation: Na abbreviated review. Crit Care Med 1996; 24: 1072-1078.

21. Rubanyi GM. Fatores derivados do endotélio no choque. Clín Bras Med Intensiva 1996; 3: 13-26.

22. Moldawer LL. Biology of proinflammatory cytokines and their antagonists. Crit Care Med 1994; 22: S3-S7.

23. Fong Y et al. The biologic characteristics of cytokines and their implication in surgical injury. Surg Gynecol Obstet 1990; 170: 363-378.

24. Zhang W, Liu HT. MAPK signal pathways in the regulation of cell proliferation in mammalian cells. Cell Research 2002; 12(1): 9-18.

25. MAPK phosphatases — regulating the immune response. Liu Y, Shepherd EG, Nelin LD. Nat Rev Immunol 2007; 7(3):202-212.

26. Frazier WJ, Xue J, Luce WA, Liu Y. MAPK Signaling Drives Inflammation in LPS-Stimulated Cardiomyocytes: The Route of Crosstalk to G-Protein- Coupled Receptors. PLoS ONE 2012; 7(11): e50071.

27. Carvalho PRA, Trotta EA. Avanços no diagnóstico e tratamento da sepse. Jornal de Pediatria. 2003; 79(2): S195-S204.

28. Bochud PY, Glauser MP, Calandra T. Antibiotics in sepsis. Intens Care Med 2001; 27: 33-48.

29. Sáez-Llorens X, McCracken GH. Sepsis syndrome and septic shock in pediatrics: current concepts of terminology, pathophysiology, and management. J Pediatr 1993; 123: 497-508.

30. Huet O, Chin-Dusting JPF. Septic shock: desperately seeking treatment. Clinical Science 2014; 126, 31–39.

31. Bernard AM, Bernard GR. The Immune Response: Targets for the Treatment of Severe Sepsis. International Journal of Inflammation 2012; 2012: 697592.

32. Friedenstein AJ, Petrakova KV, Kurolesova AI, et al: Heterotopic of bone marrow. Analysis of precursor cells for osteogenic and hematopoietic tissues. Transplantation 1968; 6: 230-247.

33. Németh K, Leelahavanichkul A, Yuen PST, Mayer B, Parmelee A, Doi K, et al. Bone marrow stromal cells attenuate sepsis via prostaglandin E2—dependent reprogramming of host macrophages to increase their interleukin-10 production. Nat Med 2009; 15(1): 42–49.

34. Rey EG, Anderson P, González MA, Rico L, Büscher D, Delgado M. Human adult stem cells derived from adipose tissue protect against experimental colitis and sepsis. Gut 2009; 58: 929-939.

35. Tyndall A, Pistoia V. Mesenchymal stem cells combat sepsis. Nat Med 2009; 15(1): 18-19.

36. Abarbanell AM, Kelly ML, Meldrum DR. Stem Cells in Sepsis. Annals of Surgery 2009; 250(1): 19-27.

37. LL Lu, YJ Liu, SG Yang, QJ Zhao, X Wang, W Gong, et al. Isolation and characterization of human umbilical cord mesenchymal stem cells with hematopoiesis-supportive function and other potentials. Haematologica 2006; 91(8): 1017-26.

38. Zuk PA, Zhu M, Mizuno H, Huang J, Futrell JW, Katz AJ, et al. Multilineage cells from human adipose tissue: Implications for cell-based therapies. Tissue Eng 2001; 7: 211-228.

39. Mizuno H. Adipose derived Stem Cells for Tissue Repair and Regeneration: Tem Years of Research and a Literature Review. J Nippon Med Sch 2009; 76: 56-66.

40. Niemeyer P, Vohrer J, Schmal H, et al. Survival of human mesenchymal stromal cells from bone marrow and adipose tissue after xenogenic transplantation in immunocompetent mice. Cytotherapy. 2008; 1–12.

41. Nauta AJ, Fibbe WE. Immunomodulatory properties of mesenchymal stromal cells. Blood. 2007; 110: 3499 –3506.

42. Crisostomo PR, Markel TA, Wang Y, et al. Surgically relevant aspects of stem cell paracrine effects. Surgery. 2008;143: 577–581.

43. Wang M, Tsai BM, Crisostomo PR, et al. Pretreatment with adult progenitor cells improves recovery and decreases native myocardial proinflammatory signaling after ischemia. Shock. 2006;25:454–459.

44. Guo J, Lin GS, Bao CY, et al. Anti-inflammation role for mesenchymal stem cells transplantation in myocardial infarction. Inflammation. 2007;30: 97–104.

45. Markel TA, Crisostomo PR, Wang M, et al. Activation of individual tumor necrosis factor receptors differentially affects stem cell growth factor and cytokine production. Am J Physiol Gastrointest Liver Physiol. 2007;293: 657–662.

46. Gupta N, Su X, Popov B, et al. Intrapulmonary delivery of bone marrow derived mesenchymal stem cells improves survival and attenuates endotoxin- induced acute lung injury in mice. J Immunol 2007; 179:1855–1863.

47. Xu M, Uemura R, Dai Y, et al. In vitro and in vivo effects of bone marrow stem cells on cardiac structure and function. J Mol Cell Cardiol 2007; 42: 441–448.

48. Weil BR, Herrmann JL, Abarbanell AM, Manukyan MC, Poynter JA, Meldrum DR 2011. Intravenous infusion of mesenchymal stem cells is associated with improved myocardial function during endotoxemia. Shock 2011; 36: 235–241.

49. Mei SH, Haitsma JJ, Dos Santos CC, Deng Y, Lai PF, Slutsky AS, et al. Mesenchymal stem cells reduce inflammation while enhancing bacterial clearance and improving survival in sepsis. Am J Respir Crit Care Med 2010; 182: 1047–1057.

50. Pedrazza L, Lunardelli A, Luft C, Cruz CU, Mesquita FC, Bitencourt S et al. Mesenchymal stem cells decrease splenocytes apoptosis in a sepsis experimental model. Inflamm Res 2014; 63:719–728.

51. Rubenfeld GD, Caldwell E, Peabody E, Weaver J, Martin DP, Neff M, et al. Incidence and outcomes of acute lung injury. N Engl J Med 2005; 353:1685–1693.

52. Ashbaugh DG, Bigelow DB, Petty TL, and Levine BE. Acute respiratory distress in adults. Lancet 1967; 2:319–323.

53. Bernard GR, Artigas A, Brigham KL, Carlet J, Falke K, Hudson L, et al. Report of the American-European Consensus conference on acute respiratory distress syndrome: definitions, mechanisms, relevant outcomes, and clinical trial coordination. Consensus Committee. J Crit Care 1994; 9: 72–81.

54. Pepe PE, Potkin RT, Reus DH, et al. Clinical predictors of the adult respiratory distress syndrome. Am J Surg 1982; 144(1): 124-13.

55. Tomashefski JF Jr. Pulmonary pathology of acute respiratory distress syndrome. Clin Chest Med 2000; 21(3): 435-466.

56. Goss CH, Brower RG, Hudson LD, Rubenfeld GD, and Network A. Incidence of acute lung injury in the United States. Crit Care Med 2003; 31: 1607–1611.

57. Ware LB, and Matthay MA. The acute respiratory distresssyndrome. N Engl J Med 2000; 342: 1334–1349.

58. Parsons PE, Eisner MD, Thompson BT, Matthay MA, Ancukiewicz M, Bernard GR, Wheeler AP. Lower tidal volume ventilation and plasma cytokine markers of inflammation in patients with acute lung injury. Crit Care Med 2005; 33: 1–6, 230–232.

59. Stuber F, Wrigge H, Schroeder S, Wetegrove S, Zinserling J, Hoeft A, Putensen C. Kinetic and reversibility of mechanical ventilation-associated pulmonary and systemic inflammatory response in patients with acute lung injury. Intensive Care Med. 2002; 28: 834–841.

60. Levitt JE, Gould MK, Ware LB, and Matthay MA. Analytic review: the pathogenetic and prognostic value of biologic markers in acute lung injury. J Intensive Care Med. 2009; 24:151–167.

61. Ware LB, Matthay MA, Parsons PE, Thompson BT, Januzzi JL, Eisner MD, Pathogenetic and prognostic significance of altered coagulation and fibrinolysis in acute lung injury/acute respiratory distress syndrome. Crit Care Med. 2007; 35:1821– 1828.

62. Pugin J, Verghese G, Widmer MC and Matthay MA. The alveolar space is the site of intense inflammatory and profibrotic reactions in the early phase of acute respiratory distress syndrome. Crit Care Med. 1999; 27:304–312.

63. Zemans RL, Colgan SP, and Downey GP. Transepithelial migration of neutrophils: mechanisms and implications for acute lung injury. Am J Respir Cell Mol Biol 2009; 40: 519–535.

64. Halliwell B, Gutteridge JMC. Free radicals in biology and medicine. 3.ed. New York: Oxford University Press Inc, 1999. 22-16.

65. Halliwell B. Proteasomal dysfunction; a common feature of all neurodegenerative diseases? Implications for the environmental origins of neurodegeneration. Antioxidants & Redox Signaling 2006; 8 (11-12): 2007-2019.

66. Larramendy M, Mello-Filho AC, Martins EA, et al. Iron-mediated induction of sister-chromatid exchanges by hydrogen peroxide and superoxide anion. Mutat Res 1987; 178(1): 57-63.

67. Shaw RW, Hansen RE, Beinert H. The oxygen reactions of reduced cytochrome c oxidase. Position of a form with an unusual EPR signal in the sequence of early intermediates. Biochim Biophys Acta 1979; 548(2): 386-396.

68. Bowler RP, Velsor LW, Duda B, et al. Pulmonary edema fluid antioxidants are depressed in acute lung injury. Crit Care Med 2003; 31(9):2309-2315.

69. Dalle-Donne I, Aldini G, Carini M, Colombo R, Rossi R, Milzani A. Protein carbonylation, cellular dysfunction and disease progression. Journal of Cellular and Molecular Medicine 2006; 10(2): 389-406.

70. Gessner C, Hammerschmidt S, Kuhn H, et al. Exhaled breath condensate nitrite and its relation to tidal volume in acute lung injury. Chest 2003; 124(3): 1046-1052.

71. Brinkmann V, Reichard U, Goosmann C, Fauler B, Uhlemann Y, Weiss DS, et al. Neutrophilextracellular traps kill bacteria. Science. 2004; 303(5663):1532-1535.

72. Fuchs TA, Abed U, Goosmann C, Hurwitz R, Schulze I, Wahn V, et al. Novel cell death program leads to neutrophil extracellular traps. J Cell Biol. 2007; 176(2):231-241.

73. Meng W, Paunel-Görgülü A, Flohé S, Hoffmann A, Witte I, Mackenzie C, et al. Depletion of neutrophil extracellular traps in vivo results in hypersusceptibility to polymicrobial sepsis in mice. Crit Care. 2012; 16(4): R137.

74. Yildiz C, Palaniyar N, Otulakowski G, Khan MA, Post M, Kuebler WM, Tanswell K, Belcastro R, Masood A, Engelberts, Kavanagh BP. Mechanical ventilation induces neutrophil extracellular trap formation. Anesthesiology 2015; 122: 864–875.

75. Rossaint J, Herter JM, Van Aken H, Napirei M, Döring Y, Weber C, Soehnlein O, Zarbock A. Synchronized integrin engagement and chemokine activation is crucial in neutrophil extracellular trap-mediated sterile inflammation. Blood 2014; 123: 2573–84

76. De Campos T. Ventilation with lower tidal volumes as compared with traditional tidal volumes for acute lung injury and the acute respiratory distress syndrome. The Acute Respiratory Distress Syndrome Network. N Engl J Med 2000; 342: 1301–1308.

77. Bernard GR, Luce JM, Sprung CL, Rinaldo JE, Tate RM, Sibbald WJ et al. High-dose corticosteroids in patients with the adult respiratory distress syndrome. N Engl J Med 1987; 317: 1565–1570.

78. Luce JM, Montgomery AB, Marks JD, Turner J, Metz CA, and Murray JF. Ineffectiveness of high-dose methylprednisolone in preventing parenchymal lung injury and improving mortality in patients with septic shock. Am Rev Respir Dis. 1988; 138:62–68.

79. Steinberg KP, Hudson LD, Goodman RB, Hough CL, Lanken PN, Hyzy R, et al. Efficacy and safety of corticosteroids for persistent acute respiratory distress syndrome. N Engl J Med 2006 20; 354(16):1671-84.

80. Morris PE, Papadakos P, Russell JA, Wunderink R, Schuster DP, Truwit JD, et al. A double-blind placebo-controlled study to evaluate the safety and efficacy of L-2-oxothiazolidine-4-carboxylic acid in the treatment of patients with acute respiratory distress syndrome. Crit Care Med 2008; 36:782–788.

81. Payen D, Vallet B. Results of the French prospective multicentric randomized double-blind placebo-controlled trial on inhaled nitric oxide in ARDS. Intensive Care Med 1999; 25: S166.

82. Abraham E, Baughman R, Fletcher E, Heard S, Lamberti J, Levy H, et al. Liposomal prostaglandin E1 (TLC C-53) in acute respiratory distress syndrome: a controlled, randomized, double-blind, multicenter clinical trial. TLC C-53 ARDS Study Group. Crit Care Med 1999; 27: 1478–1485.

83. Vincent JL, Brase R, Santman F, Suter PM, McLuckie A, Dhainaut JF, et al. A multi-centre, doubleblind, placebo-controlled study of liposomal prostaglandin E1 (TLC C-53) in patients with acute respiratory distress syndrome. Intensive Care Med. 2001; 27: 1578–1583.

84. Ortiz LA, Dutreil M, Fattman C, Pandey AC, Torres G, Go K, Phinney DG. Interleukin 1 receptor antagonist mediatesthe antiinflammatory and antifibrotic effect of mesenchymal stem cells during lung injury. Proc Natl Acad Sci USA. 2007; 104: 11002–11007.

85. Xu J, Woods CR, Mora AL, Joodi R, Brigham KL, Iyer S, Rojas M. Prevention of endotoxin-induced systemic response by bone marrow-derived mesenchymal stem cells in mice. Am J Physiol Lung Cell Mol Physiol. 2007; 293: L131– L141.

86. 86 marrow-derived mesenchymal stem cells improves survival and attenuates endotoxin-induced acute lung injury in mice. J Immunol. 2007; 179: 1855–1863.

87. Nunes FB, Pires MGS, Filho JCFA, Wachter PH, Oliveira JR. Physiopathological studies in septic rats and the use of fructose-1,6-bisphosphate as cellular protection. Crit Care Med 2002; 30(9): 2069–74.

88. Jiang D, Muschhammer J, Qi Y, Kügler A, Devries JC, Saffarzadeh M, et al. Suppression of Neutrophil-Mediated Tissue Damage—A Novel Skill of Mesenchymal Stem Cells. Stem Cells 2016; 34: 2393-2406.

89. Kling MK, Rodriguez EL, Pfarrer C, Mühlfeld C, Brandenberger C. Aging exacerbates acute lung injury-induced changes of the air-blood barrier, lung function, and inflammation in the mouse. Am J Physiol Lung Cell Mol Physiol 2017; 312: 1–12.

9. Anexo

Artigo original realizado durante o doutorado-sanduiche em Barcelona/Espanha em parceria com o Laboratório de Biologia Molecular, Departament de Ciències Fisiològiques, Institut d'Investigació Biomèdica de Bellvitge (IDIBELL), Universitat de Barcelona. Publicado em agosto de 2016, no periódico *Oncotarget* com fator de impacto 5,008.

The HERC2 ubiquitin ligase is essential for embryonic development and regulates motor coordination

Monica Cubillos-Rojas[1], Taiane Schneider[1], Ouadah Hadjebi[1], Leonardo Pedrazza[1,2], Jarbas Rodrigues de Oliveira[2], Francina Langa[3], Jean-Louis Guénet[3], Joan Duran[4], Josep Maria de Anta[4], Soledad Alcántara[4], Rocio Ruiz[5,6], Eva María Pérez-Villegas[6], Francisco J. Aguilar-Montilla[6], Ángel M. Carrión[6], Jose Angel Armengol[6], Emma Baple[7], Andrew H. Crosby[7], Ramon Bartrons[1], Francesc Ventura[1] and Jose Luis Rosa[1]

[1] Departament de Ciències Fisiològiques, IDIBELL, Campus de Bellvitge, Universitat de Barcelona, L'Hospitalet de Llobregat, Barcelona, Spain

[2] Laboratório de Pesquisa em Biofísica Celular e Inflamação, Pontifícia Universidade Católica do Rio Grande do Sul, Porto Alegre, Rio Grande do Sul, Brazil

[3] Département de Biologie du Développement, Institut Pasteur, Paris, France

[4] Departament de Patologia i Terapèutica Experimental, Campus de Bellvitge, Universitat de Barcelona, L'Hospitalet de Llobregat, Barcelona, Spain

[5] Departamento de Bioquímica y Biología Molecular, Facultad de Farmacia, Universidad de Sevilla, Sevilla, Spain

[6] Departamento de Fisiología, Anatomía y Biología Celular, Universidad Pablo de Olavide, Sevilla, Spain

[7] Institute of Biomedical and Clinical Science, University of Exeter Medical School, RILD Wellcome Wolfson Centre, Exeter, UK

Correspondence to: Jose Luis Rosa, email: joseluisrosa@ub.edu

Keywords: ubiquitin, p53, angelman syndrome, purkinje cells, behavioural analysis

Received: June 07, 2016 *Accepted*: August 01, 2016 *Published*:

ABSTRACT

A mutation in the *HERC2* gene has been linked to a severe neurodevelopmental disorder with similarities to the Angelman syndrome. This gene codifies a protein with ubiquitin ligase activity that regulates the activity of tumor protein p53 and is involved in important cellular processes such as DNA repair, cell cycle, cancer, and iron metabolism. Despite the critical role of HERC2 in these physiological and pathological processes, little is known about its relevance *in vivo*. Here, we described a mouse with targeted inactivation of the *Herc2* gene. Homozygous mice were not viable. Distinct from other ubiquitin ligases that interact with p53, such as MDM2 or MDM4, p53 depletion did not rescue the lethality of homozygous mice. The HERC2 protein levels were reduced by approximately one-half in heterozygous mice. Consequently, HERC2 activities, including ubiquitin ligase and stimulation of p53 activity, were lower in heterozygous mice. A decrease in HERC2 activities was also observed in human skin fibroblasts from individuals with an Angelman-like syndrome that express an unstable mutant protein of HERC2. Behavioural analysis of heterozygous mice identified an impaired motor synchronization with normal neuromuscular function. This effect was not observed in p53 knockout mice, indicating that a mechanism independent of p53 activity is involved. Morphological analysis showed the presence of HERC2 in Purkinje cells and a specific loss of these neurons in the cerebella of heterozygous mice. In these animals, an increase of autophagosomes and lysosomes was observed. Our findings establish a crucial role of HERC2 in embryonic development and motor coordination.

INTRODUCTION

Angelman syndrome (AS) is a severe neurodevelopmental disorder that occurs in approximately one out of every 12,000 births. Patients with AS exhibit developmental delay, speech impairments, intellectual disability, epilepsy, abnormal electroencephalograms, puppet-like ataxic movements, prognathism, tongue protrusion, paroxysms of laughter, abnormal sleep patterns, hyperactivity, and a high prevalence of autism [1,2]. Genetic studies revealed that AS is associated with maternal deletions of chromosome 15q11-q13, paternal chromosome 15 uniparental disomy, or rare imprinting defects that affect the transcription of genes within the 15q11-q13 region. Specific loss-of-function mutations in the maternally inherited *UBE3A* gene which resides within this chromosomal region have been identified in a subset of affected individuals [3]. The *UBE3A* gene encodes an E3 ubiquitin ligase called UBE3A or E6-associated protein (E6AP). More recently, a mutation in the *HERC2* gene has been linked to neurodevelopmental delay and dysfunction in both AS and autism-spectrum disorders among the Old Order Amish [4,5]. Molecular analysis associated a missense mutation in the *HERC2* gene (c.1781C>T, p.Pro594Leu) with the disease phenotype. Although the *HERC2* gene also resides in the 15q11-q13 region, it seems that it is not imprinted [6]. *HERC2* encodes an ubiquitin ligase that binds to UBE3A and stimulates its ubiquitin ligase activity [7]. Deregulation of the activity of UBE3A is well recognized as contributing to the development of AS [2,3]. Thus, disruption of HERC2 function by this mutation is associated with a reduction in UBE3A activity resulting in neurodevelopmental delay with Angelman-like features [4,5].

Genetic variations in the *HERC2* gene are associated with eye pigmentation. Although multiple genes contribute to eye colour in humans, most variation can be attributed to a strong interaction between *HERC2* and adjacent *OCA2* on chromosome 15 [8]. A distal regulatory element of the *OCA2* promoter is within intron 86 of the *HERC2* gene and three different sequence variants of *HERC2* have been identified, such as predictors of eye colour in humans [9,10].

HERC2 belongs to the *HERC* gene family that encodes a group of proteins that contain multiple structural domains. All members have at least one copy of an N-terminal region showing homology to the cell cycle regulator RCC1 and a C-terminal HECT (homologous to the E6-AP carboxyl terminus) domain found in a number of E3 ubiquitin protein ligases. These two domains define the HERC family (HERC = HECT + RCC1) [11]. In humans, six members form the HERC family. They are classified into two groups: large (HERC1-2) and small (HERC3-6) proteins. Structurally, small HERC proteins contain the two characteristic domains HECT and RCC1, whereas large HERC proteins are giant proteins (approximately 5,000 amino acid residues) containing additional domains, including several RCC1 domains. Functionally, the HERC protein family regulates ubiquitination and ISGylation processes associated with membrane trafficking, immune response, DNA repair, cell stress response and cancer biology [11-20]. Recently, several substrates of HERC2 have been identified. HERC2 targets ubiquitin-dependent proteasomal degradation to xeroderma pigmentosa A (XPA) during circadian control of nucleotide excision repair [21] and the breast cancer suppressor BRCA1 during the cell cycle [22]. These data, together with the interaction of HERC2 with RNF8 [23], indicate a regulatory role for HERC2 in DNA repair by nucleotide excision and by homologous recombination of DNA double-strand breakage. More recently, other substrates, such as NEURL4, USP33 or FBXL5, have been reported that also indicate the participation of HERC2 in other important cellular processes such as centrosome architecture, β-adrenergic receptor recycling, RalB signaling, cancer cell migration, and iron metabolism [24-26].

HERC2 may also interact with proteins in a manner independent of proteasomal degradation. The tumor suppressor p53 is a transcription factor that coordinates the cellular response to several kinds of stress through the regulation of a wide range of genes [27,28]. In response to stress, p53 transcriptional activation is dependent of its oligomerization state [29]. Thus, p53 mutations that impair its oligomerization have been associated with a rare hereditary cancer predisposition disorder called Li-Fraumeni syndrome [30,31]. HERC2 interacts with p53 and modulates its transcriptional activity by regulating its oligomerization [32]. RNA interference experiments showed that HERC2 knock-down inhibited p53 oligomerization affecting its transcriptional activity. Under these conditions, up-regulation of cell growth and increased focus formation were observed, suggesting an important role of HERC2 in proliferation [32]. In agreement with these observations, an association of frameshift mutations of *HERC2* with gastric and colorectal carcinoma has been described [18]. Despite the critical role of HERC2 in cellular processes regulated by p53, little is known about its physiological relevance. The mutation of HERC2 found among the Old Order Amish with features similar to Angelman syndrome also suggests an important role for HERC2 in neurodevelopment [4,5]. To determine the physiological importance of HERC2, we decided to generate a mouse with targeted inactivation of the *Herc2* gene.

RESULTS

Characterization of the *Herc2*^{530} mice

To study the physiological role of HERC2, we generated a novel mutant allele at the *Herc2* locus by using a gene trapped embryonic stem (ES) cell line from The Sanger Institute. These ES cells, here called *Herc2*^{530}, contain a pGT0lxr expression vector with a strong splice acceptor site integrated within intron 2 of the mouse *Herc2* gene, which results in the expression of a truncated mRNA. PCR experiments with genomic DNA from the tails of mice generated with these ES cells confirmed the integration of the trap between exon 2 and 3 (Figure 1A).

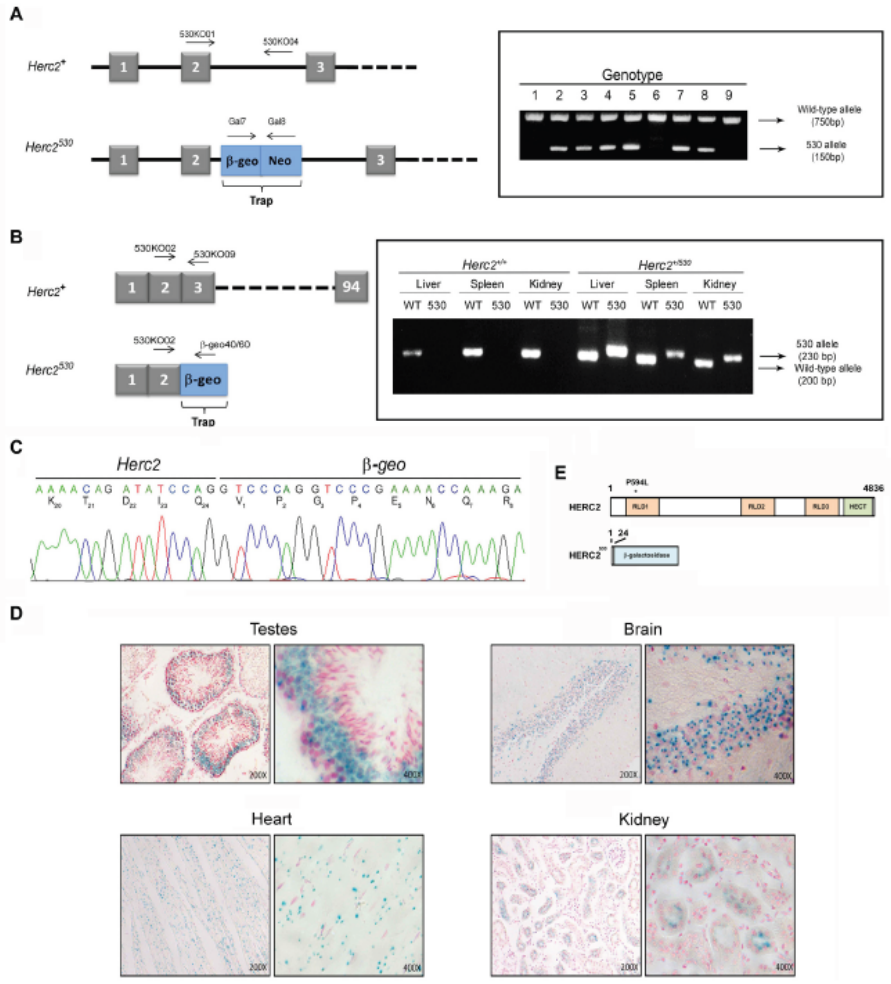

Figure 1: Generation of the *Herc2*^{530} mice. A. Schematic representation of the *Herc2* wild-type allele (*Herc2*$^{+}$) and *Herc2*^{530} allele and the designed primers to identify both alleles (left). The *Herc2*^{530} allele contains the pGT0lxr vector that expresses the fusion of β-galactosidase and neomycin transferase within intron 2. The integration of the trap was determined by genotyping using the indicated primers (right), 530KO01/530KO04 for the wild-type allele and Gal7/Gal8 for the 530 allele. **B.** Exon structure of *Herc2*$^{+}$ and *Herc2*^{530} (left). RT-PCR experiments with mRNA from liver, spleen and kidney of *Herc2*$^{+}$ and *Herc2*^{530} mice was performed using the indicated primers. **C.** PCR products from B were sequenced. The trap was inserted after exon 2, for which the mutant protein contains the first 24 amino acids of the HERC2 and β-galactosidase protein. **D.** β-galactosidase expression in *Herc2*^{530} mice. The activity of β-galactosidase was determined in the testes, brain, heart and kidney of *Herc2*^{530} mice and detected by *X-gal* staining. **E.** Scheme of HERC2 protein and the expected product from the *Herc2*^{530} allele. The P594L pathological mutation is indicated (*). RLD: RCC1-like domain.

RT-PCR experiments with mRNA from different tissues showed the formation of a truncated mRNA of *Herc2* fused to β-*galactosidase* (β-geo) (Figure 1B). Sequencing analysis confirmed these results and revealed the fusion of β-galactosidase after amino acid residue 24 of HERC2 (Figure 1C). β-galactosidase activity was determined in several tissues (Figure 1D), confirming the expression of a fused transcript of the first 24 amino acid residues of HERC2 with β-galactosidase. Because mouse HERC2 protein has 4,836 amino acid residues, we can consider that the HERC2 new mutant allele $Herc2^{530}$ is functionally deleted (Figure 1E).

Herc2 is an essential gene during embryonic development

91 offspring born from the intercross heterozygous mice were genotyped by PCR. Among these mice, 34 (37%) were wild-type for *Herc2*, and 57 (63%) were heterozygous for $Herc2^{+/530}$ (Figure 2A). We could not

A

Analysis of mice from a $Herc2^{+/+}$ x $Herc2^{+/530}$ cross

Variable	Expected frecuency, % (n)	Observed frecuency, % (n)
$Herc2^{+/+}$	25 (23/91)	37 (34/91)
$Herc2^{+/530}$	50 (45/91)	63 (57/91)
$Herc2^{530/530}$	25 (23/91)	0/91

B

Analysis of progeny from a $Herc2^{+/530}$ x $Herc2^{+/530}$ cross

Stage	Observed placentas	Placentas with embryo	Placentas without embryo	Genotypes		
				$Herc2^{+/+}$	$Herc2^{+/530}$	$Herc2^{530/530}$
E10.5	8	5	3	2	3	0
E8.5	11	8	3	1	7	0
E7.5	15	7	8	4	3	0

C

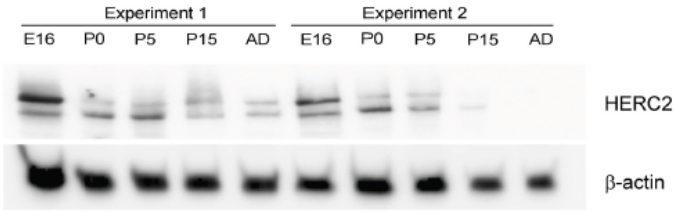

Figure 2: Analysis of progeny from the $Herc2^{+/530}$ cross. A. Analysis of offspring born from the intercross of $Herc2^{+/530}$ mice. Ninety-one animals were genotyped by PCR of genomic DNA isolated from mouse tails. The expected frequencies for $Herc2^{+/+}$ and $Herc2^{+/530}$ were obtained; however, no homozygous mice ($Herc2^{530/530}$) were identified. **B.** Analysis of embryonic lethality in $Herc2^{530/530}$ mice. Embryos from $Herc2^{+/530}$ pregnant females at different stages were isolated and genotyped. The $Herc2^{+/+}$ and $Herc2^{+/530}$ genotypes were identified, but not the $Herc2^{530/530}$. The placentas without embryos could not be genotyped. **C.** Analysis of HERC2 protein levels during development. Lysates from brains at different stages were analyzed by immunoblotting for HERC2 and β-actin. E16 (embryonic day), P0, P5 and P15 (post-natal day 0, 5 and 15, respectively) and AD (adult animal).

identify any viable homozygous *Herc2*$^{530/530}$. These data suggested an embryonic lethality for null mice. To determine the time of embryonic lethality in *Herc2*$^{530/530}$ mice, genomic DNA was isolated from embryos harvested at different stages (E7.5, E8.5 and E10.5) of pregnancy from *Herc2*$^{+/530}$ mice. We isolated 34 placentas and observed 14 (41%) without embryos (Figure 2B). Among the embryos, we identified both wild-type and heterozygous mice, but not homozygous mice. At day 7.5 and 8.5 in placentas without embryos, we observed some residuals. At day 10.5, these residuals were completely resorbed. Most likely, these residuals were rests of embryos homozygous for *Herc2*^{530}. These results indicate that the expression of at least a normal *Herc2* copy is essential for the completion of embryonic development before day 7.5.

Genes important for development are usually highly expressed during embryonic stages. To determine the expression pattern of the HERC2 protein during development, we analyzed the levels of the endogenous protein in samples from brains at embryonic day E16, postnatal days P1, P5 and P15, and adult mice (8 weeks). Anti-HERC2 antibodies detected a double band that decreased during development, with the highest levels in the embryonic stage and lower levels in the adult animal (Figure 2C). Similar expression profiles were observed for other members of the HERC family, such as HERC1 or HERC3 (data not shown), suggesting an important role of the HERC proteins during embryonic development.

p53 inactivation did not rescue embryonic lethality of homozygous *Herc2*^{530} mice

Growth curves and survival rates were analyzed in *Herc2*$^{+/530}$ mice. The growth curve was not significantly altered in *Herc2*$^{+/530}$ mice during the time studied (Figure 3A). The survival rate was also similar to wild-type mice during the period studied (Figure 3B).

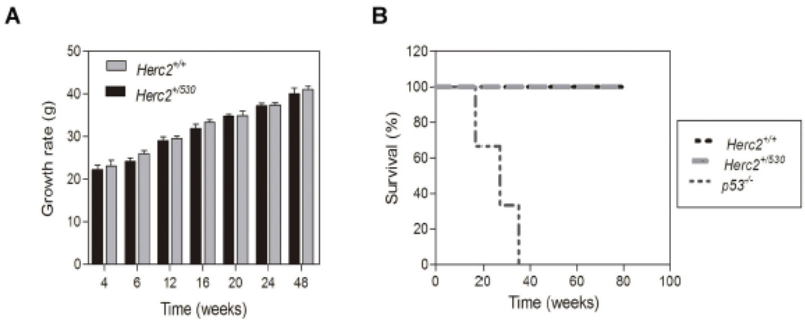

C

Analysis of mice from a *Herc2*$^{+/530}p53^{+/-}$ x *Herc2*$^{+/530}p53^{+/-}$ cross

Variable	*Herc2*$^{+/+}$	*Herc2*$^{+/530}$	*Herc2*$^{530/530}$	Total
p53$^{+/+}$	3	21	0	24
p53$^{+/-}$	10	49	0	59
p53$^{-/-}$	2	8	0	10
Total	15	78	0	93

Figure 3: *p53* inactivation did not rescue the lethality of *Herc2*$^{530/530}$ homozygous mice. Graphs of growth rate **A.** and survival **B.** from *Herc2*$^{+/+}$ and *Herc2*$^{+/530}$ mice. Growth and survival were analyzed in male mice (n>10) at the indicated weeks. The survival for *p53*$^{-/-}$ mice also was analyzed. **C.** The analysis of mice from a cross of double heterozygous *Herc2*$^{+/530}$ *p53*$^{+/-}$ animals. The offspring was genotyped by PCR of genomic DNA with the appropriate primers, indicating that the embryonic lethal phenotype of *Herc2*$^{530/530}$ embryos was not rescued by crossing with *p53*$^{-/-}$ mice.

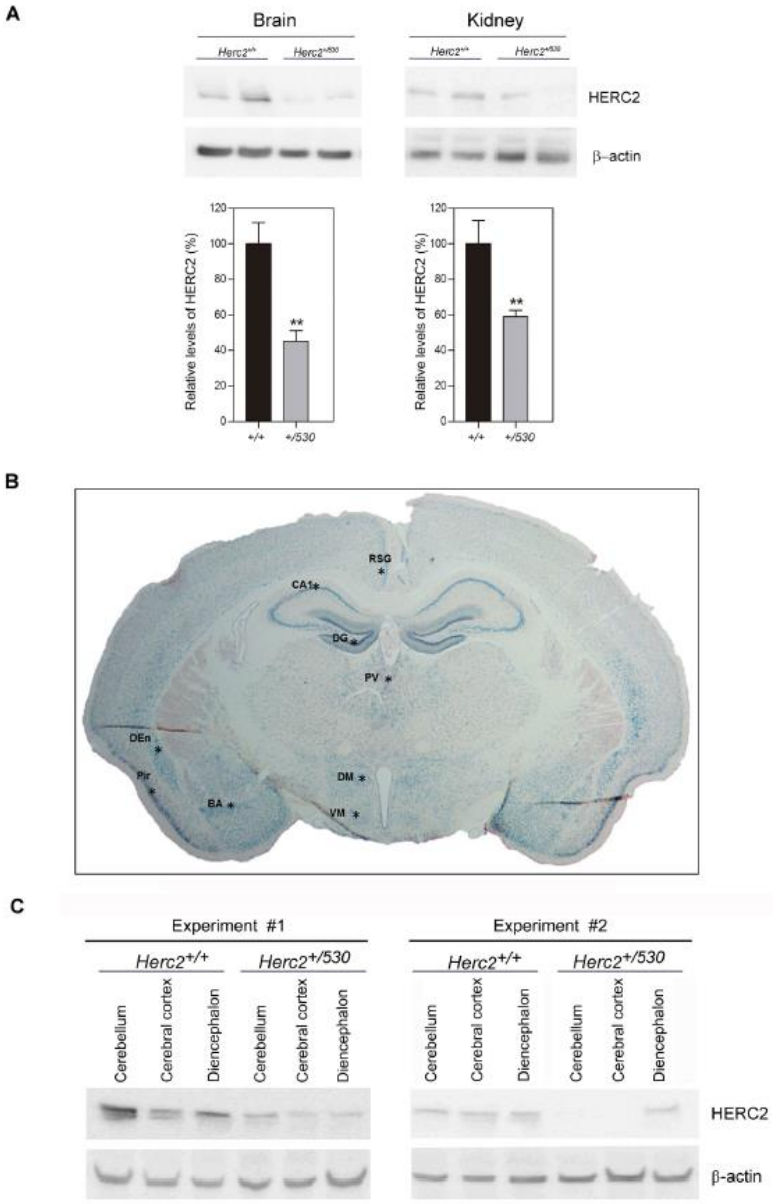

Figure 4: *Herc2*$^{+/530}$ mice show reduced levels of HERC2 protein. A. HERC2 protein levels were analyzed by immunoblotting using specific antibodies against HERC2 in several tissues from 8 week old mice. The levels of HERC2 were quantified (n = 8) and normalized with respect to β-actin levels. **B.** β-galactosidase expression in brain from *Herc2*^{530} mouse. The β-galactosidase activity was detected ubiquitously in all areas using *X-gal* staining. However, there were forebrain cortical and subcortical areas in which β-galactosidase labeling was the most intense (asterisks). **C.** The levels of HERC2 were analyzed by immunoblotting in lysates of cerebellum, cerebral cortex and diencephalon from *Herc2*$^{+/+}$ and *Herc2*$^{+/530}$ mice at P4 (post-natal day 4). BA, basal amygdala. CA1, pyramidal cell layer of the hippocampal cornu ammonis 1. DEn, dorsal endopiriform nucleus. DG, granular cell layer of hippocampal dentate gyrus. DM, dorsomedial nucleus of the hypothalamus. Pir, piriform cortex. PV, paraventricular thalamic nucleus. RSG, retrosplenial granular cortex. VM, ventromedial nucleus of the hypothalamus.

It had been previously demonstrated that knockout mice for the E3 ubiquitin ligases of p53, such as *MDM2* or *MDM4*, are lethal in embryonic stages due to growth inhibition and apoptosis. Interestingly, this lethality could be rescued by concomitant p53 depletion [33-35]. Because HERC2 is an E3 ubiquitin ligase that regulates p53 activity [32], we asked whether p53 inactivation might also rescue the lethality of *Herc2*$^{530/530}$ homozygous mice. We crossed double heterozygous *Herc2* and *p53* mice (*Herc2*$^{+/530}$ *p53*$^{+/-}$ mice) to obtain double homozygous mice. We analyzed the genotype of the offspring by performing an adequate PCR assay on of genomic DNA samples but did not observe any viable *Herc2*$^{530/530}$ mouse (Figure 3C). These data suggest the non-involvement of p53 in the embryonic death caused by the depletion of *Herc2*.

Partial inactivation of the *Herc2* gene is sufficient to reduce HERC2 protein levels and activity

We analyzed protein levels of HERC2 in *Herc2*$^{+/530}$ animals by immunoblotting. We observed that the levels of HERC2 were decreased approximately 50% in the brain and kidney of *Herc2*$^{+/530}$ animals (Figure 4A). The analysis of β-galactosidase activity in *Herc2*$^{+/530}$ mice allows the analysis of *Herc2* expression in more detail. Ubiquitous expression of HERC2 was observed in all tissues analyzed (Figure 1D). In the brain, this expression was higher in the hippocampus (pyramidal cell layer and granular layer of dentate gyrus), hypothalamic nucleus (dorsomedial and ventromedial), amygdaloid nucleus (basal and medial), piriform cortex, dorsal endopiriform nucleus, entorhinal cortex, retrospenial cortex, paraventricular thalamic nucleus, and cerebellum (Figure 4B and data not shown).

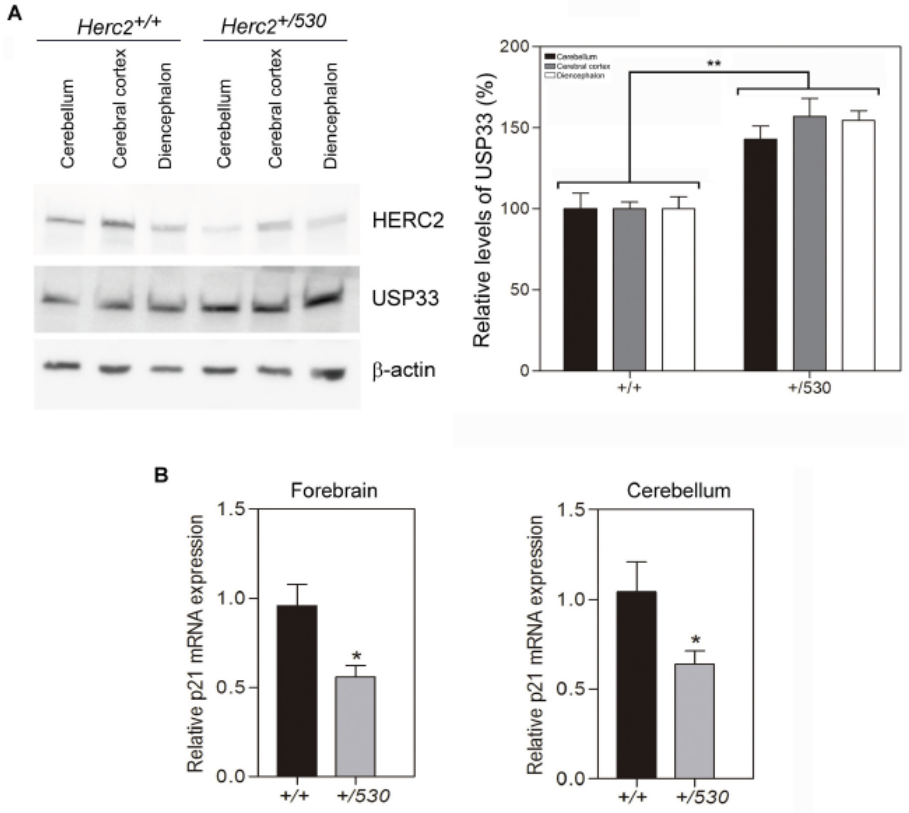

Figure 5: *Herc2*$^{+/530}$ mice show reduced activity of HERC2. A. USP33, a substrate of ubiquitination of HERC2, was analyzed in lysates (cerebellum, cerebral cortex and diencephalon) from 8 week old mice by immunoblotting. Higher levels of USP33 were observed in all areas of *Herc2*$^{+/530}$ mice. Levels of USP33 were quantified and normalized with respect to β-actin levels. **B.** *Herc2*$^{+/530}$ mice show reduced levels of *p21* mRNA. RT quantitative PCR analyses were performed in forebrain and cerebellum from *Herc2*$^{+/+}$ and *Herc2*$^{+/530}$ mice to quantify *p21* gene expression ($n = 10$). The levels of expression were normalized with respect to *GAPDH* gene expression.

Table 1: Behavioural tests of *Herc2*$^{+/530}$ mice

Cognitive task	Behavioural tests		Test Values: mean ± error (n)		*P* value
			Herc2$^{+/+}$	*Herc2*$^{+/530}$	
Anxiety	Time outside of the dark box (s)		235 ± 13 (9)	232 ± 9 (8)	0.83
	Immobile time suspended by the tail (s)		205 ± 14 (9)	173 ± 14 (19)	0.11
Learning and Memory	Object recognition memory (DI)	STM	0.24 ± 0.08 (6)	0.23 ± 0.05 (10)	0.87
		LTM	0.26 ± 0.09 (6)	0.32 ± 0.06 (10)	0.60
	Step through passive avoidance test (Latency)	STM	2.92 ± 0.24 (6)	2.21 ± 0.37 (15)	0.12
		LTM	2.84 ± 0.31 (7)	3.04 ± 0.32 (19)	0.66
Motor function	Open field (total activity)		1649 ± 108 (8)	1612 ± 199 (16)	0.87
	Rotarod (#Falls)		1.14 ± 0.46 (7)	4.21 ± 0.90 (19)	**0.0058
	Forelimb Grip strength (s)		7.00 ± 0.98 (6)	7.96 ± 0.78 (8)	0.46

STM: Short Term Memory; LTM: Long Term Memory; DI: Discrimination index; n: number of animals

These observations were confirmed by immunoblotting. We dissected the cerebellum, cerebral cortex and diencephalon, detecting HERC2 protein in all these areas (Figure 4C). The levels of HERC2 protein were reduced in *Herc2*$^{+/530}$ animals (Figure 4C) with respect to control mice (*Herc2*$^{+/+}$).

These data show that the levels of HERC2 protein are reduced almost 50% in *Herc2*$^{+/530}$ mice tissues and suggest that the HERC2 activity must also decrease in the brain of heterozygous animals. Two activities have been associated with HERC2 protein; an E3 ubiquitin ligase activity which regulates protein levels of USP33, BRCA1 or XPA [21,22,25], and an activity as a stimulator of the p53 oligomerization that regulates the transcriptional activity of p53 [32]. To analyze the activity of E3 ubiquitin ligase, we performed immunoblotting experiments in the mouse brain areas with antibodies against substrates ubiquitinated by HERC2. Only the USP33 protein was detected by immunoblotting in these mouse samples (Figure 5A). Interestingly, in *Herc2*$^{+/530}$ mice, the levels of USP33 were higher than in control mice. To examine the activity stimulating p53 oligomerization and transcriptional activity, we analyzed the levels of *p21* mRNA by RT quantitative PCR analysis. A decrease in *p21* mRNA levels was observed in *Herc2*$^{+/530}$ mice (Figure 5B). Altogether, these data show that the partial inactivation of the *Herc2* gene in *Herc2*$^{+/530}$ mice is sufficient to reduce HERC2 protein levels and activity.

A homozygous mutation in human *Herc2* causes an Angelman-like syndrome and reduces the activity of the HERC2 protein

HERC2 has been implicated in a human disorder with some features similar to Angelman syndrome. The substitution of proline by leucine at amino acid position 594 in HERC2 caused HERC2^{P594L} instability and almost total loss of the protein in homozygosis [4,5]. Based on our data from heterozygous animals, we hypothesized that these patients would have lower levels of HERC2 activity. To test this hypothesis, we analyzed the levels of USP33 protein from fibroblasts derived from an affected individual and a healthy control. We observed a high increase of USP33 levels in fibroblasts from a patient (Figure 6A). To confirm that HERC2 activity was diminished, we also analyzed the levels of p21 protein. We observed a decrease in the p21 protein levels in fibroblasts from this patient (Figure 6A). However, the p53 and α-tubulin levels did not significantly change. The *p21* mRNA levels also confirmed the decrease in p53 transcriptional activity in fibroblasts from the patient (Figure 6B). The level of p53 protein is regulated by the proteasome. In the presence of the proteasome inhibitor MG132, we observed a similar stabilization of p53 protein levels in fibroblasts from the patient and the control (Figure 6C). Under these conditions, we also detected a decrease in p21 protein levels in fibroblasts from the patient (Figure 6C), indicating a decrease in its p53 activity. These data show the low activity of HERC2 in individuals carrying the HERC2^{P594L} mutation.

In conclusion, the low HERC2 activity found in *Herc2*$^{+/530}$ mice (Figure 5) and in individuals with the HERC2^{P594L} mutation (Figure 6A-6C) correlated with an increase in levels of the USP33 protein and a decrease in levels of the p21 protein. These data suggest that in conditions with low levels of HERC2 protein, cells could contain more USP33 and less p21. To confirm this point, human U2OS cells were depleted of HERC2 using interference RNA, and USP33 and p21 were analyzed by immunoblotting (Figure 6D). HERC2 knockdown increased levels of the USP33 protein and decreased levels of the p21 protein.

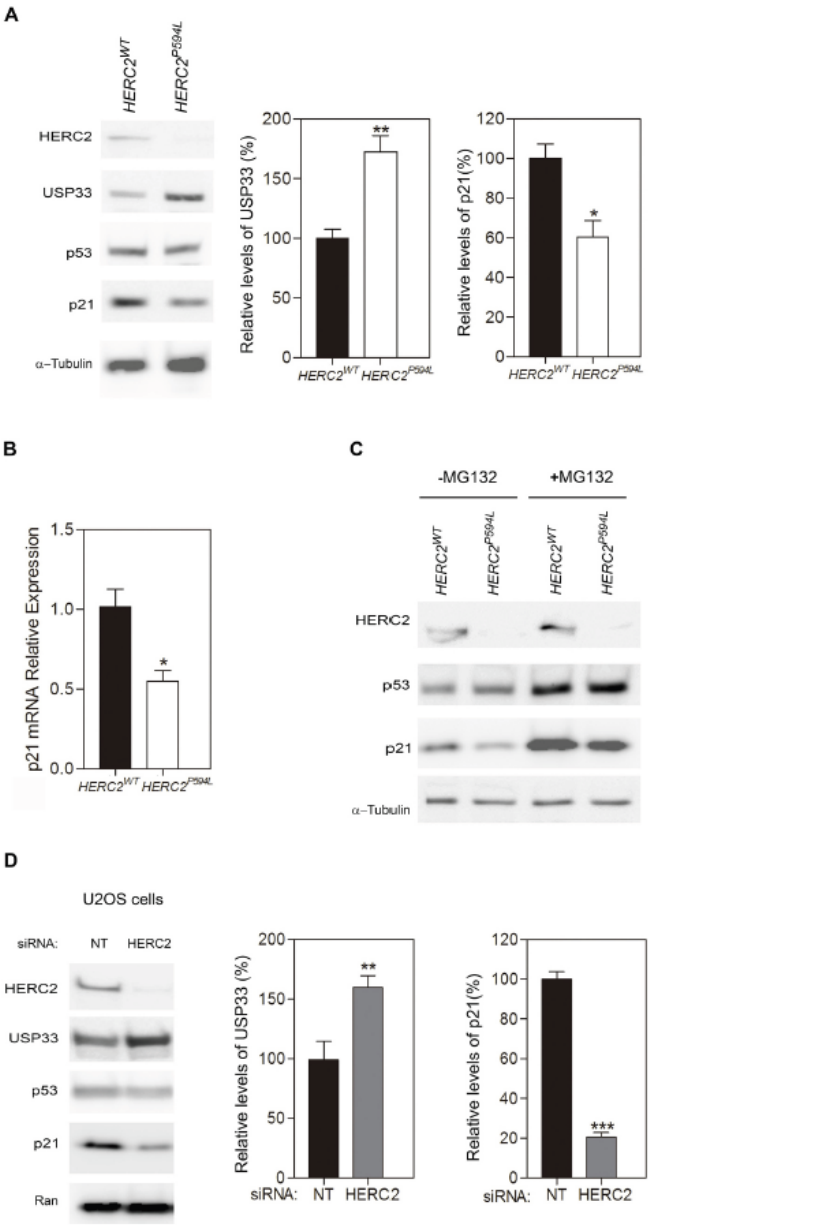

Figure 6: A homozygous mutation in human *HERC2* that causes an Angelman-like syndrome reduces the activity of the HERC2 protein. A. Fibroblasts derived from individuals with HERC2 wild-type or HERC2 with the mutation P594L were analyzed by immunoblotting for the indicated antibodies. Levels of USP33 and p21 proteins were quantified and normalized with respect to α-tubulin levels. **B.** Levels of *p21* mRNA were analyzed by RT quantitative PCR analysis and normalized with respect to *18S* gene expression. **C.** The levels of HERC2, p53, p21 and α-tubulin proteins were analyzed in the presence or absence of the proteasome inhibitor MG132. **D.** U2OS cells were transfected with non-targeting (NT) or HERC2 siRNAs and analyzed by immunoblotting against the indicated proteins. The levels of USP33 or p21 were quantified and normalized with respect to Ran levels.

HERC2 regulates motor coordination

Individuals carrying the HERC2^{P594L} mutation present a severe developmental delay with an unstable gait [4,5]. We wondered whether *Herc2*$^{+/530}$ mice with a reduction of approximately 50% in HERC2 protein could have some features found in HERC2^{P594L} patients. To examine this question, behavioural tests to measure different cognitive tasks were performed in *Herc2*$^{+/530}$ and wild-type mice. Except for the rotarod test, no significant

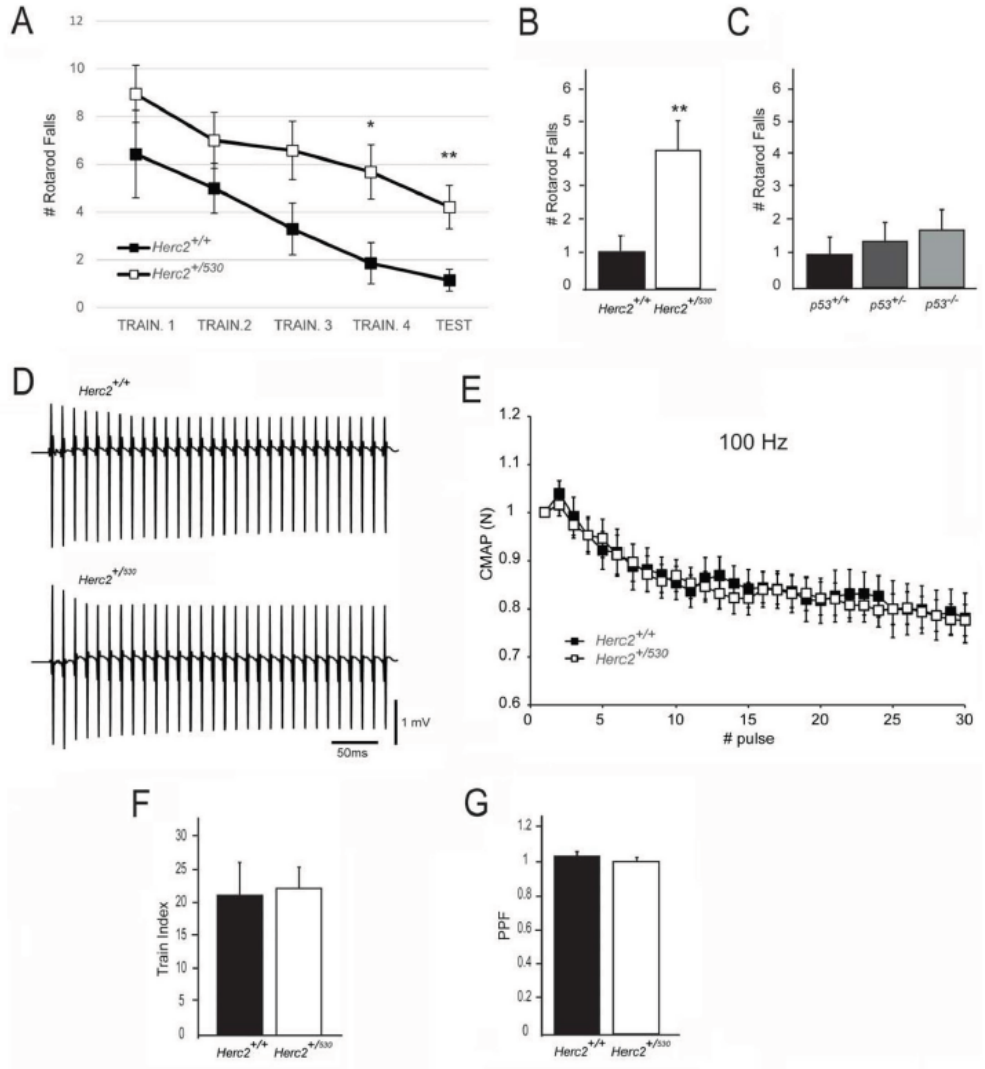

Figure 7: Impaired motor coordination in *Herc2*$^{+/530}$ mice. A.-B. The number of falls from the rotarod increases in *Herc2*$^{+/530}$ mice at 6 months of age in comparison with control littermates. **C.** No difference was found in *p53*$^{+/-}$ and *p53*$^{-/-}$ mice in comparison with WT. (D-E) EMG measurements of CMAP amplitudes in the MG of control and *Herc2*$^{+/530}$ mice show normal neurotransmission efficacy in postnatal heterozygous mice. **D.** Representative recordings during a train of stimuli at 100 Hz in a control and a *Herc2*$^{+/530}$mouse. **E.** Depression of CMAP amplitudes (normalized to the first response) during a train of stimuli of 300 ms at 100 Hz in control (n = 7) and heterozygous mice (n = 18). The train index **F.**, corresponding to the depression at the end of the train, and PPF (Pair -Pulse Facilitation) **G.**, are similar between groups.

differences between the two groups were found (Table 1; video). *Herc2*$^{+/530}$ mice displayed a statistically significant increase in rotarod falls compared to wild-type mice (*Herc2*$^{+/+}$: 1.14 ± 0.46, $n = 7$ and *Herc2*$^{+/530}$: 4.21 ± 0.90, $n = 19$, $p = 0.0058$) (Figure 7A-7B), suggesting a role for HERC2 in motor coordination. Because HERC2 regulates p53 activity, we asked whether p53 inactivation could produce effects similar to *Herc2*$^{+/530}$ mice. We performed the rotarod test in *p53*$^{+/-}$ and *p53*$^{-/-}$ mice. No significant differences were observed compared to wild-type mice (Figure 7C). These data indicate that the impaired motor coordination in *Herc2*$^{+/530}$ mice is specific and independent of p53. Next, we analyzed whether muscular function was affected in *Herc2*$^{+/530}$ mice. The electrical neuromuscular properties of the *Herc2*$^{+/530}$ mice were studied *in vivo* by performing electromyography (EMG) on the medial gastrocnemius (MG) muscle using short train stimuli at 100 Hz (Figure 7D). The depression at the end and the facilitation at the beginning of a train of 30 stimuli were similar in mutant and wild-type mice when measured by normalization of the CMAP (Compound Muscular Action Potentials) amplitude ($p = 0.8$ and $p = 0.85$, respectively) (Figure 7E-7G). These results indicate a normal muscular function.

The cerebellum regulates motor coordination, and alterations in its structure have been associated with impaired motor coordination. To examine whether the deficit of motor synchronization in *Herc2*$^{+/530}$ mice was caused by an alteration of cerebellar structure, we performed immunohistochemistry analysis of the specific marker of Purkinje cells calbindin-D28 k (CaBP) (Figure 8). CaBP immunoreactive Purkinje cell somata form a continuous cell layer in the cerebellar cortex of *Herc2*$^{+/+}$ mice (Figure 8A-8C). In *Herc2*$^{+/530}$ mice, parasagittal zones devoid of immunoreactivity throughout the cerebellum indicative of Purkinje cell loss were observed (arrows and arrowheads in Figure 8D-8F). These symmetrical Purkinje cell-deprived bands -characterized by the presence of wide spaces lacking cell somata in the Purkinje cells layer (asterisks in Figure 8H) and dendritic debris through the molecular layer (mol in Figure 8H)-, were distributed differently along a medio-lateral gradient (see comparison between Figure 8D-8F from a *Herc2*$^{+/530}$ mouse and Figure 8A-8C from a *Herc2*$^{+/+}$ mouse). Thus, vermal and paravermal Purkinje cells were less affected than in the cerebellar hemispheres. In the vermis and paravermis, the loss of Purkinje cells was distributed in narrow gaps (arrows in Figure 8D and 8E), while at the hemispheres, the areas of Purkinje cells loss reached a great extension (arrowheads in Figure 8D and 8F), in which remain some surviving Purkinje cells (small arrows in Figure 8F). Epifluorescence microscopy analysis showed that HERC2 immunoreactivy in Purkinje cells colocalize with CaBP (Figure 9). In *Herc2*$^{+/530}$ mice, HERC2 immunohistochemistry confirmed the loss of Purkinje cells in narrow gaps at the vermis/paravermis or in a greater extension at the hemispheres (Figure 9C-9E).

CaBP immunohistochemistry also revealed the presence of pathological signs in *Herc2*$^{+/530}$ Purkinje cells. Rounded thickenings resembling axonal torpedoes were observed in Purkinje cell axons, which contrast with the fine grained morphology of normal Purkinje cells axonal plexuses (see arrows in the comparison between *Herc2*$^{+/+}$ and *Herc2*$^{+/530}$ in Figure 10A-10C). Phenotypic alterations of *Herc2*$^{+/530}$ Purkinje cells were also observed in the 1.5 µm thick sections stained with toluidine blue (Figure 10D-10E). Disappeared Purkinje cells somata were substituted by glial Golgi-epithelial cells (Figure 10D: arrows, Purkinje cells; small arrows, Golgi-epithelial cells). High magnification allowed to detect degenerative dark accumulations within the cytoplasm of the soma (arrowheads in Figure 10E) and the dendrites (arrows in Figure 10E) of the Purkinje cells. Electron microscopy analysis of cerebella confirmed these degenerative signs in *Herc2*$^{+/530}$ mice (Figure 10F-10H and 11). The cytoplasm of *Herc2*$^{+/530}$ Purkinje cells contained a high number of lysosomes and electron-dense debris (Figure 10F-10H, asterisks), and autophagosomes with different degrees of evolution (Figure 10G, arrows). Damaged cisterns of Golgi apparatus and numerous cisterns of the rough endoplasmic reticulum fused to the cytoplasmic face of the nuclear membrane were also observed (not shown). The difference between mice *Herc2*$^{+/+}$ and *Herc2*$^{+/530}$ was even most evident in the principal Purkinje cell dendrites (Pcd in Figure 11). Thus, numerous degenerative signs were present in *Herc2*$^{+/530}$ Purkinje cells dendrite (Figure 11B and 11E), while were almost absent in wild-type ones (Figure 11A, 11C and 11D). These degenerative signs were found in 2 and 9 month-old animals (Figure 10F-10H), with a slight increase of these alterations in the older mice (not shown). These data show that the partial inactivation of HERC2 in *Herc2*$^{+/530}$ mice causes Purkinje cell loss, which explain motor incoordination detected here in rotarod test. The increase of autophagosomes and lysosomes observed in *Herc2*$^{+/530}$ Purkinje cells (Figure 10 and 11) led us to wonder whether HERC2 may be involved in the regulation of autophagy. To this end, we have analyzed the adaptor-substrate p62/SQSTM1 by laser confocal microscopy. HERC2 immunostaining colocalized with p62 (Figure 12). This colocalization, it was observed both in wild-type animals as in *Herc2*$^{+/530}$ animals (Figure 12, arrows and arrowheads in the merged). *In Herc*$^{+/+}$ *mice*, p62 immunostaining showed a punctate labeling pattern that concentrated in Purkinje cells somata (Figure 12, arrows). This pattern was altered in *Herc2*$^{+/530}$ animals; thus, in addition to the somatic labeling, p62 immunostaining was also evident within the dendritic trees and the axonal torpedoes of Purkinje cells (Figure 12, arrows and arrowheads) indicating a dysregulation of autophagy in *Herc2*$^{+/530}$ Purkinje cells. Altogether,

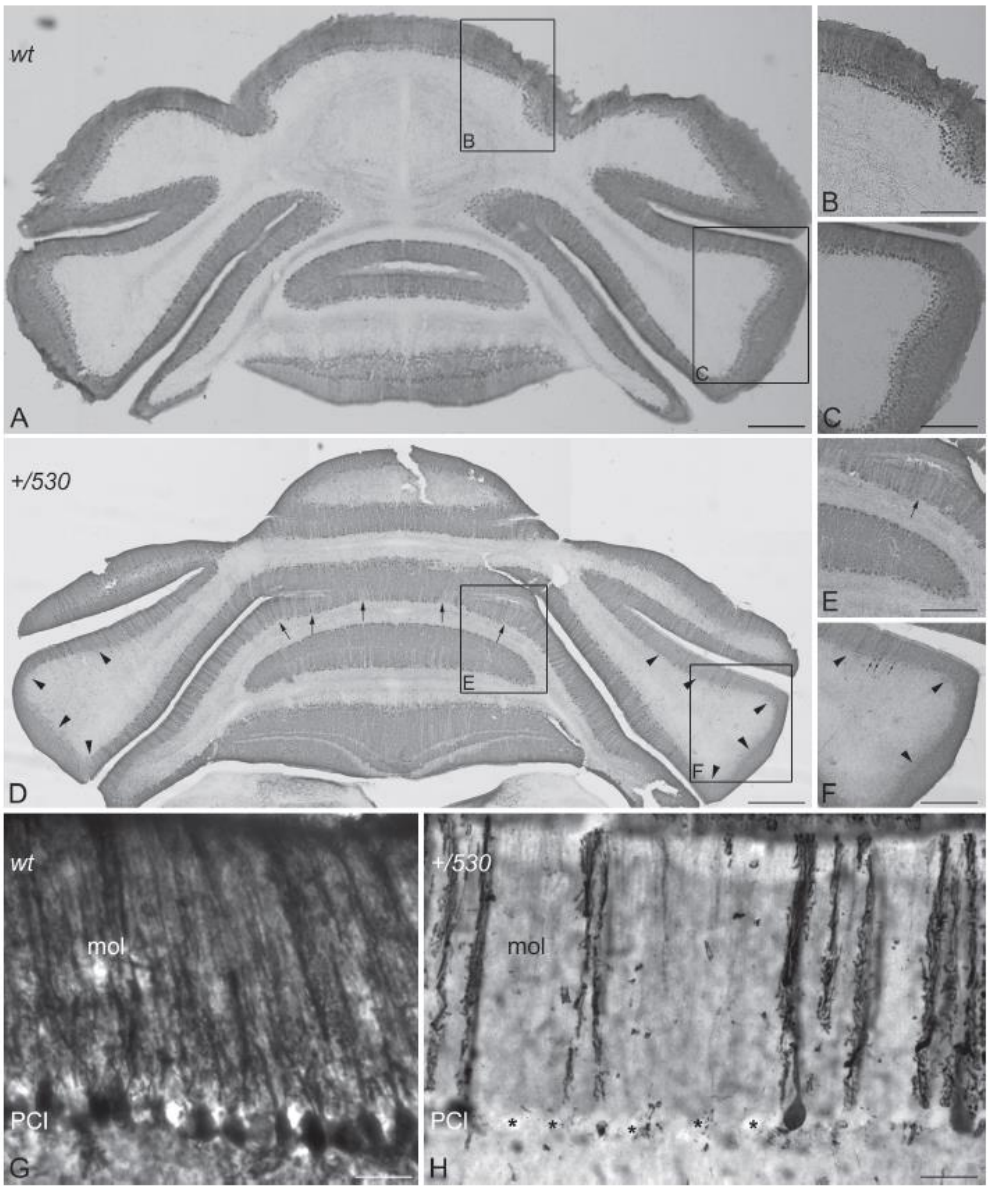

Figure 8: Purkinje cells loss in *Herc2*$^{+/530}$ mice. Microphotographs of coronal sections through the cerebellar cortex of 9 months old wild-type (*wt*, A-C, G) and 9 months old *Herc2*$^{+/530}$ mice (*+/530*, D-F, H). Calbindin immunohistochemistry shows as Purkinje cell somata form a continuous cell layer in the *Herc2*$^{+/+}$ (*wt*) cerebellum **A.-C.** However, parasagittal zones lacking of immunoreactivity throughout the *Herc2*$^{+/530}$ cerebellum indicative of Purkinje cell loss are observed (arrows and arrowheads, in **D.-F.**). These symmetrical Purkinje cells deprived bands, characterized by the presence of wide spaces lacking Purkinje cell somata (H, asterisks) and dendritic debris through the molecular layer (H, mol), distribute differently according a medio-lateral gradient. In the vermis and paravermal zones the immunonegative zones are sagittaly distributed in narrow gaps (D-E, arrows); while at the hemispheres the areas devoid of Purkinje cells, also bilateral, reach a greater extension (D, F, arrowheads) in which remain some surviving Purkinje cells (F, small arrows). **G**, illustrates the *Herc2*$^{+/+}$ (*wt*) immunostaining of normal Purkinje cells; note as dendritic trees fulfill the molecular layer (G, mol), while Purkinje cells somata align in a continuous row. PCl, Purkinje cells layer. Bars = 600 μm (A, D), 400 μm (B-C, E-F), and 30 μm **G.-H.**

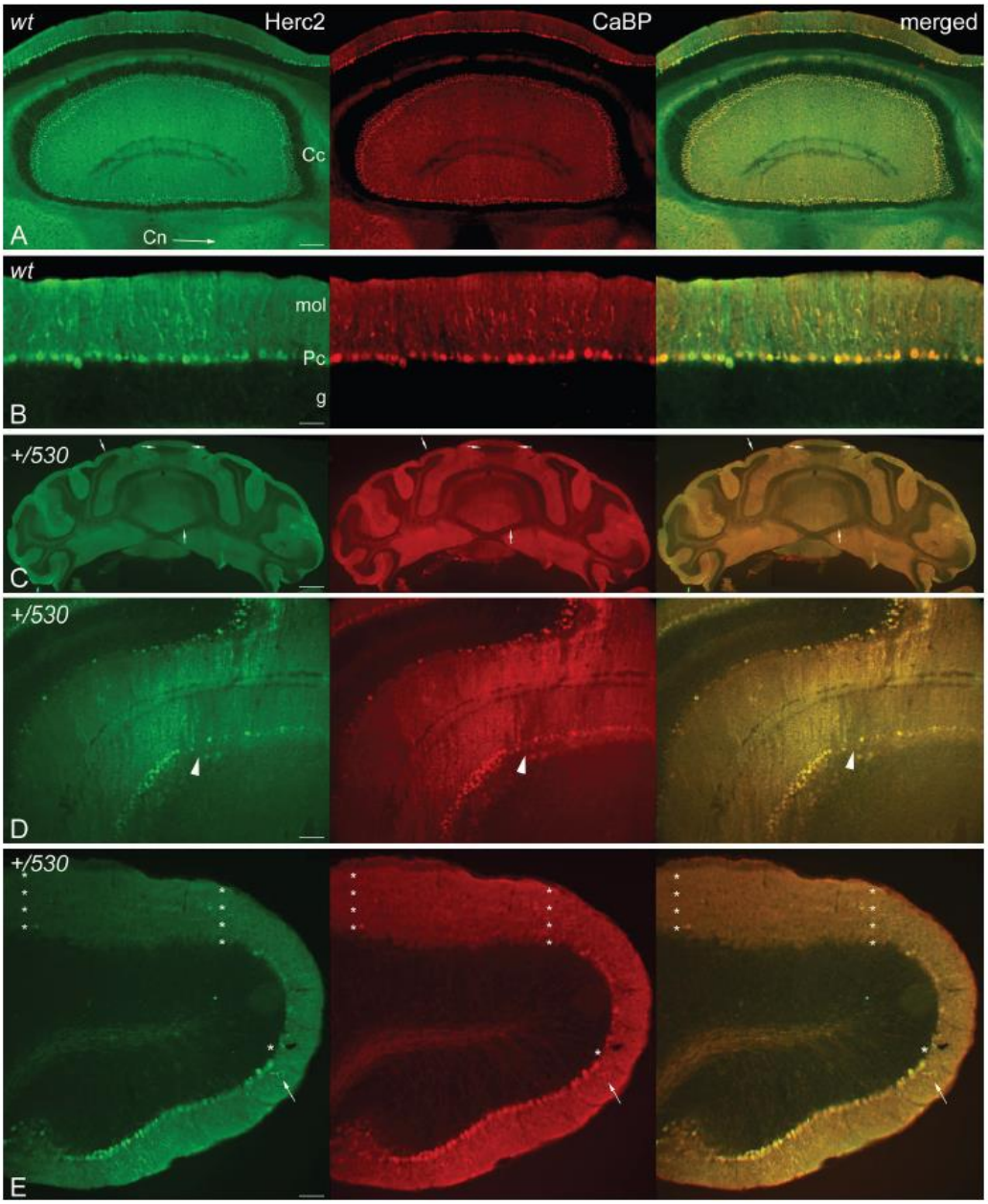

Figure 9: HERC2 is present in Purkinje cells. Microphotographs of coronal sections through the cerebellar cortex of 9 months old *Herc2*$^{+/+}$ (*wt*, **A.-B.**) and 9 months old *Herc2*$^{+/530}$ mice (*+/530*, **D.-E.**). Epifluorescence microscopy analysis shows that HERC2 is expressed in all the adult Purkinje cells colocalizating with the general marker of Purkinje cell calbindin (CaBP) (A-E) in the cerebellar cortex (A, Cc,), and their axonal endings in the cerebellar nuclei (A, Cn, arrow). *Herc2*$^{+/530}$ cerebellum displays parasagittal bands of Purkinje cells loss in the vermis and paravermal zones (**C.**, arrows; D, arrowheads), and areas of extensive Purkinje cell loss in the cerebellar paraflocculus (asterisks). The arrows in E illustrate the co-expression of both proteins in the Purkinje cell dendritic tree. Bars = 750µm (C), 200 µm (A), 100µm (D), 75µm (E), and 50 µm (B).

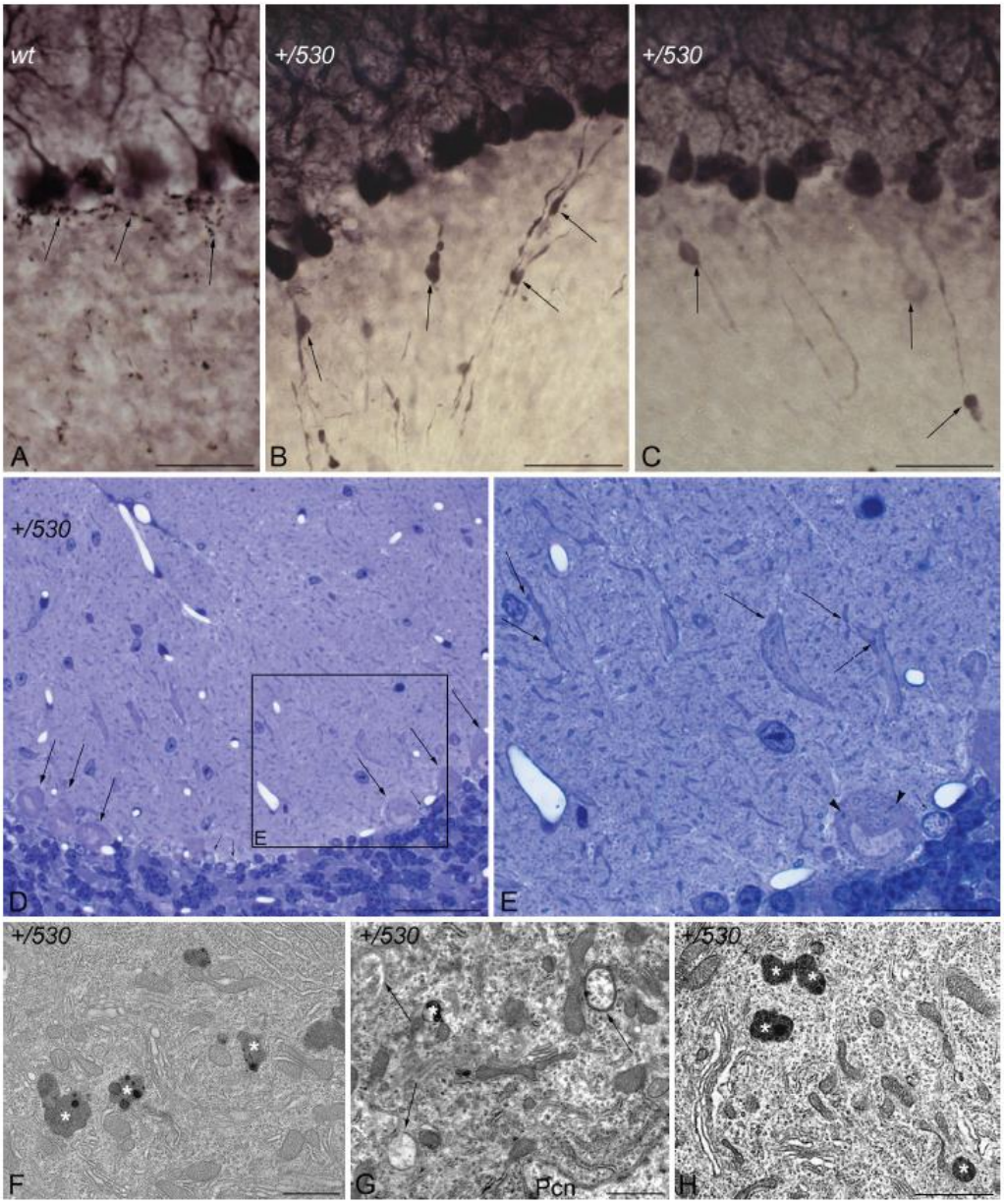

Figure 10: Purkinje cell degeneration in *Herc2*$^{+/530}$ mice. Microphotographs of transmitted light **A.-E.** and electron microscopy **F.-H.** of parasagittal sections through the cerebellar cortex of 9 months *Herc2*$^{+/+}$ (*wt*, A), and 2 (H) and 9 months old *Herc2*$^{+/530}$ mice (*+/530*, **B.-G.**). Calbindin immunohistochemistry reveals the presence of rounded thickenings resembling to axonal torpedoes in *Herc2*$^{+/530}$ Purkinje cell axons (B-C, arrows), which contrast with the fine grained morphology of normal Purkinje cells axonal plexuses (A, arrows). 1.5 µm thick sections illustrated Purkinje cells (D, arrows) limiting a zone in which disappeared Purkinje cells were substituted by glial Golgi-epithelial cells (small arrows in D and E). High magnification allows detect degenerative dark accumulations within the cytoplasm of the soma (E, arrowhead) and the dendrites (E, arrows) of the Purkinje cells. *Herc2*$^{+/530}$ Purkinje cells cytoplasm possesses lysosomes, electron-dense debris (F-H, asterisks), and autophagosomes with different degrees of evolution (G, arrows). Pcn, Purkinje cell nucleus. Bars = 50 µm (A-D), 25 µm (E), and 1 µm (F-H).

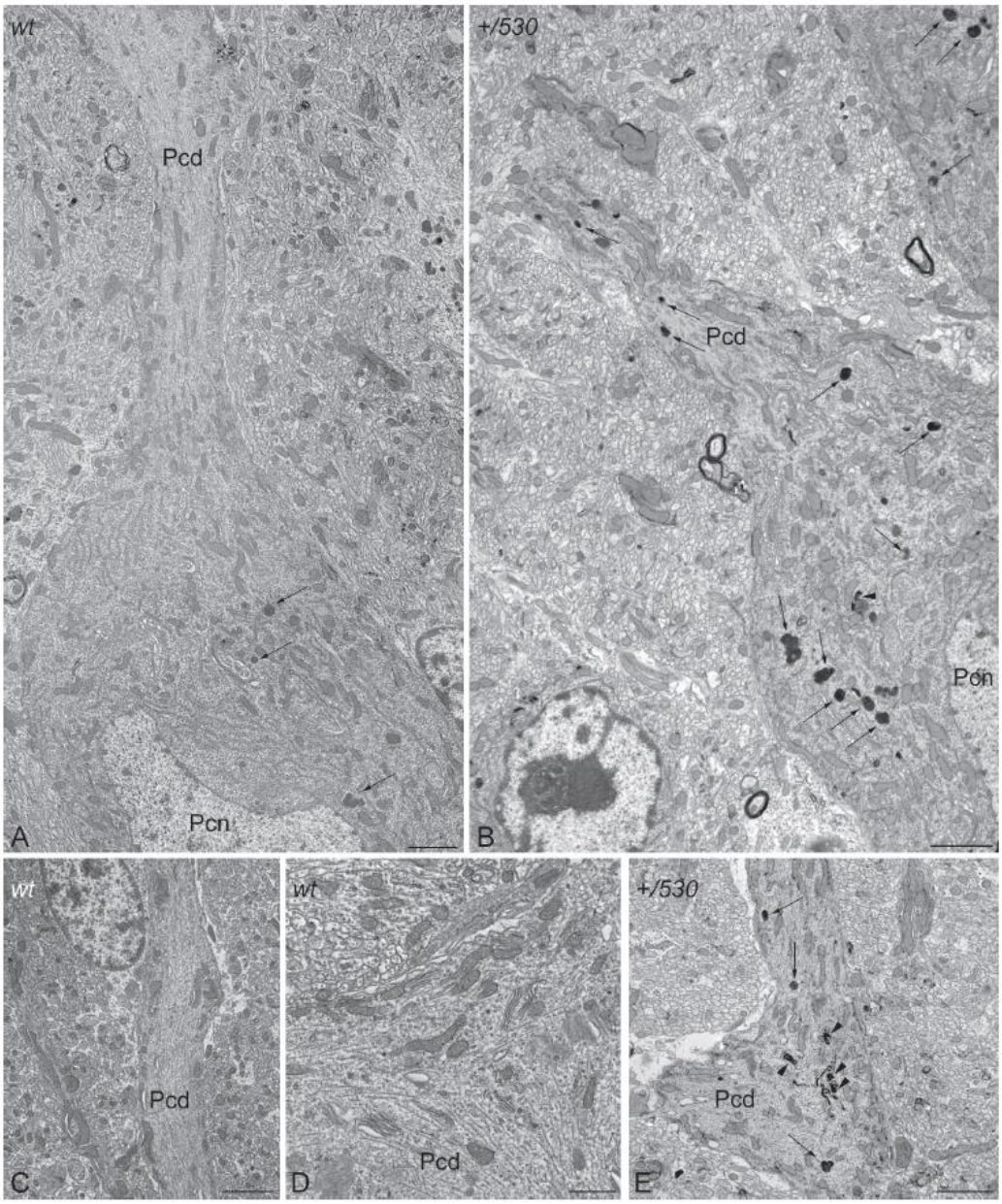

Figure 11: Ultrastructural analysis of *Herc2*$^{+/530}$ mice indicates accumulation of autophagosomes and lysosomes in Purkinje cells. Electron photomicrographs of parasagittal sections through the cerebellar vermis of 9 months old *Herc2*$^{+/+}$ (*wt*, **A.**, **C.-D.**) and 9 months old *Herc2*$^{+/530}$ mice (*+/530*, **B.**, **E.**). An important difference in the presence of autophagic (arrowheads), and lysosomal (arrows) organelles can be observed between wild-type (A) and *Herc2*$^{+/530}$ (B) Purkinje cells cytoplasm. The difference is even most evident in the principal Purkinje cell dendrites. Thus, numerous degenerative signs are present in *Herc2*$^{+/530}$ Purkinje cells dendrite (E), while are almost absent in wild-type ones (C-D). Pcd, Purkinje cell dendrite. Pcn, Purkinje cell nucleus. Bars = 2 μm (A-C, E), and 1 μm (D).

these findings suggest that HERC2 plays an active role in regulating the Purkinje cells homeostasis, whose deregulation elicits alterations in motor coordination.

DISCUSSION

We have generated a new mutant allele of the HERC2 ubiquitin ligase, *Herc2*^{530}, which has led us to identify *Herc2* as an essential gene for embryonic development. The *HERC2* gene encodes an unusual long polypeptide chain of almost 5,000 amino acid residues. The maintenance during evolution of this single and long polypeptide chain suggests an important physiological role for the giant HERC2 protein. Here, we showed that the inactivation of *Herc2* causes embryonic lethality before 7.5 days. At that time, we observed a high number of abnormal placentas, probably indicating resorption of unviable embryos. Although we have not studied the cause of this embryonic lethality, a possibility could be defective implantation. The unviability of embryos when HERC2 is inactivated would be indicative of the difficulty of finding human individuals homozygous for mutations of this gene.

To our knowledge, only the HERC2^{P594L} mutation found in the Amish community has been reported in humans [4,5]. In these individuals, the HERC2 protein is unstable and low levels are detected, although apparently high enough to avoid embryonic lethality. Ubiquitin ligases that interact with p53, such as MDM2 or MDM4, had also been identified as essential during embryonic phases. The absence of MDM2 induces embryonic lethality in mice at the peri-implantation (E4-E5.5) stage of development, whereas mice deficient for MDM4 die in mid-gestation (E7.5-E8.5) [33-35]. The lethality during these phases was rescued by a double knockout of the ubiquitin ligase and p53 [33-35]. Because HERC2 is also an ubiquitin ligase that interacts and regulates p53 activity [32], we analyzed whether the double knockout of HERC2 and p53 could also rescue the lethality. Our results show that the double knockout did not rescue the embryonic lethality, indicating a p53-independent role for HERC2 in development. Moreover, these data also confirm, at a genetic level, the different functions of MDM2 (or MDM4) and HERC2 in p53 regulation.

HERC2 acts as an ubiquitin ligase tagging for degradation by the proteasome of substrates such as XPA,

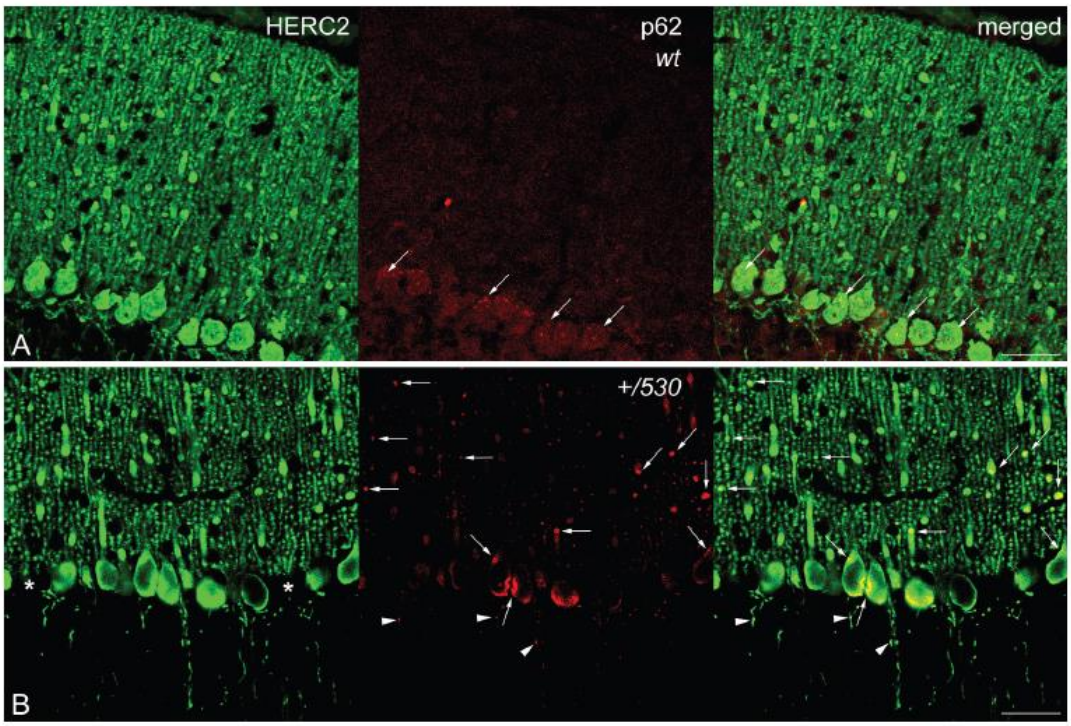

Figure 12: p62/SQSTM1 in *Herc2*$^{+/530}$ mice. Laser confocal microphotographs of coronal sections through the cerebellar cortex of the vermis of 9 months *Herc2*$^{+/+}$ (*wt*, A) and 9 months old *Herc2*$^{+/530}$ (*+/530*, B) mice double labeled with HERC2 and p62 antibodies. Colocalizations of HERC2 and p62 are indicated by arrows in dendrites and cell somata **A.**, **B.**, and by arrowheads in the axonal torpedoes of *Herc2*$^{+/530}$ Purkinje cells (B). Asterisks in B indicate the absence of Purkinje cell bodies. Bar = 50 µm (A-B).

BRCA1, NEURL4, FBXL5 or USP33 [21,22,24-26]. HERC2 may also positively regulate p53 activity through stimulation of its oligomerization [32]. The analysis of levels of USP33 and p21 led us to analyze these two activities, respectively. These activities had been reported in culture cell but not in physiological conditions. The generation of *Herc2*$^{+/530}$ mice containing approximately one-half of the HERC2 protein (Figure 4) led us to analyze the role of HERC2 *in vivo*. *Herc2*$^{+/530}$ mice had higher levels of USP33 protein and lower levels of p21 mRNA (Figure 5). These results show for the first time the inhibition of HERC2 activity in physiological conditions. Individuals from the Amish community with a punctual mutation in HERC2, HERC2^{P594L}, suffer a developmental disorder with features similar to Angelman syndrome [4,5]. These individuals produce an instable HERC2^{P594L} protein. Skin fibroblasts obtained from these individuals also had higher levels of USP33 protein and lower levels of p21, in agreement with a loss of HERC2 activity. We showed how these results can be extrapolated to other human cells through interference RNA experiments. HERC2 knockdown caused an increase in the levels of USP33 protein and a decrease in the levels of p21. In conclusion, we show how the loss of HERC2 protein correlates with the loss of its activities, confirming the involvement of HERC2 in cellular processes regulated by USP33 [25] and p53 [32].

The tumor suppressor gene *p53* is mutated in approximately 50% of human sporadic cancers and in inherited cancer predispositions, such as Li-Fraumeni syndrome [27,28]. Homozygous *p53*$^{-/-}$ mice are highly prone to cancer, particularly T-cell lymphoma and sarcoma [36,37]. Experiments with heterozygous *p53*$^{+/-}$ mice indicate that a mere reduction in p53 levels may be sufficient to promote tumorigenesis [38]. The p53 transcriptional activation is dependent of its oligomerization state [29], and p53 mutations that impair its oligomerization have been associated with the Li-Fraumeni syndrome [30,31]. Because HERC2 interacts with p53 and modulates its transcriptional activity by regulating its oligomerization [32] and *Herc2*$^{+/530}$ mice have less p53 activity (Figure 5), we would expect *Herc2*$^{+/530}$ mice to show an increased susceptibility to developing spontaneous tumors. However, we have not observed a greater number of tumors in *Herc2*^{530} mice (data not shown). In agreement with these data, an increased susceptibility to develop spontaneous tumors in individuals from the Amish community with the HERC2^{P594L} punctual mutation [4,5] and lower p53 activity (Figure 6) has not been reported. The hypothesis that loss of transcription in p53 is the driving force selected during tumorigenesis needs to be reevaluated, as it is far from straightforward. For example, mice expressing p53 mutants transcriptionally defective for growth arrest, senescence and apoptosis, are not prone to cancer [39,40]. Moreover, cells from mice deficient for the three p53 target genes, *p21*, *Puma* and *Noxa,* are deficient in their ability to undergo p53-mediated cell-cycle arrest, apoptosis, and senescence, although the animals remain tumor-free [41].

Our study identifies a new function for the HERC2 ubiquitin ligase as a regulator of motor coordination through regulation of Purkinje cells homeostasis. HERC2 protein is expressed in Purkinje cells (Figure 9). The decrease of its protein levels correlates with the loss of Purkinje cells in the vermis and hemispheres of the cerebellum that would explain the motor incoordination detected in *Herc2*$^{+/530}$ mice with rotarod experiments (Figure 7 and 8). The Purkinje cell loss is bilateral and symmetrical as in other mutations characterized by the Purkinje cells loss [42], demonstrating the specificity of the degenerative process. This loss is not homogeneously distributed; thus, the loss of Purkinje cells appears as discrete gaps in the continuous staining of the molecular layer of the vermis, while at the hemispheres, the loss reaches a great extension (Figure 8). Despite their homogenous shapes and common morphological features, these results suggest some difference between Purkinje cells and is in agreement with previous observations indicating that these neurons do not constitute a biochemically homogenous population [42,43]. Pathological signs, such as varicose enlargements resembling axonal torpedoes and widespread accumulations of dense cytoplasmic material, were observed in Purkinje cells of *Herc2*$^{+/530}$ mice. Proliferation of Golgi epithelial cells is also indicative of Purkinje cell degeneration. Electron microscopy analysis of *Herc2*$^{+/530}$ cerebella showed Purkinje cells containing numerous degenerating signs in autophagosomes, lysosomes and Golgi cisterns (Figure 10 and 11, and data not shown). These results resemble those obtained from a different mutant mouse called *tambaleante* [44,45]. In these animals, a progressive and specific loss of Purkinje cell was observed with a very similar pattern of neurodegenerative signs. Interestingly, the Purkinje cell degeneration in *tambaleante* mutant mice is a consequence of a missense mutation in HERC1 [44], the structural homolog of HERC2. In this regard, it seems that the functional alteration of one of them it is not compensated by the other. In agreement with this independent role of HERC1 and HERC2, the essential role of HERC1 for normal development and for neurotransmission at the mouse neuromuscular junction [46] was not observed in *Herc2*$^{+/530}$ mice (Figure 7). Thus, both ubiquitin ligases seem to have a crucial and independent role in Purkinje cell physiology. This functional similarity of HERC1 and HERC2 was unexpected, because despite their structural homology, endogenous proteins do not interact between them, do not have common known interactors, have different subcellular locations and were involved in different pathways of cell signaling [11,12,32]. However,

an interaction between the first 1,000 amino acid residues of HERC2 and HERC1 has recently been detected using mass spectrometry analysis [47], suggesting a possible interaction in some unknown circumstances.

A functional role of cerebellar p53 protein in adult walking synchronization has been reported [48]. Because HERC2 positively regulates p53 activity [32] and *Herc2*$^{+/530}$ mice had less HERC2 activity, it was plausible that the impaired motor synchronization in *Herc2*$^{+/530}$ mice was caused by a decrease in p53 activity. For this reason, we analyzed motor coordination in p53 knockout mice. We did not observe significant differences with rotarod experiments in these animals (Figure 7). Our results are in agreement with other studies where no differences in motor synchronization were detected by Tomasevic *et al.* [49] in p53 knockout mice. These authors described a role for p53 in the recovery of neuromotor function after a traumatic brain injury but not before the injury [49]. Thus, the motor coordination regulated by HERC2 seems to be independent of p53 activity.

Pioneering studies associated mutations at the mouse *Herc2* locus induced by ethylnitrosourea or ionizing radiation with a runty, jerky, sterile phenotype (*rjs*), also known as the juvenile development and fertility phenotype (*jfd2*), characterized by reduced size, jerky gait, fertility problems, including spermatocyte and oocyte abnormalities, defective maternal behaviour, and reduced lifespan with juvenile lethality [50-52]. More recently, a mutation in the *HERC2* gene has been linked to the neurodevelopmental delay and dysfunction seen in Angelman syndrome and autism-spectrum disorders among the Amish community [4,5]. Now, our study demonstrates an important role of HERC2 in the regulation of motor coordination through Purkinje cells homeostasis that would explain some features observed in *rjs/jdf2* mice and individuals with the HERC2^{P594L} mutation. It is important to note that, different to the above studies, the impaired motor synchronization is observed in mice with only a mutated allele of *Herc2* (*Herc2*$^{+/530}$ mice), indicating the relevance of HERC2 activity in motor function coordination.

Studies of spontaneous mouse mutants have implicated autophagy in the death of Purkinje neurons. *Lurcher* mice with mutations in the delta2 glutamate receptor, *pcd* mice with loss of *nna1* expression or *tambaleante* mice with mutation in the HERC1 protein show an increase of autophagy associated with Purkinje cell death [44,53-55]. While conditional inactivation of autophagy genes such as *Atg5* or *Atg7* from Purkinje cells in mice yields Purkinje cell degeneration and death [56,57]. This dual role of the autophagy in Purkinje cells degeneration seems to indicate that these neurons are very sensitive to the dysregulation of autophagy. Although more studies will be necessary to establish the role precise of HERC2 in autophagy, our results are in agreement with these previous observations in other mouse models, and reveal a dysregulation of autophagy in *Herc2*$^{+/530}$ Purkinje cells. A recent study also suggests the involvement of HERC2 in Parkinson's disease [58], it would be interesting to analyze in future studies the HERC2 role in the midbrain dopaminergic neurons of *Herc2*$^{+/530}$ mice.

In summary, the generation of a mutant mouse of *Herc2* led us to identify the HERC2 ubiquitin ligase as essential for embryonic development and an important regulator of motor coordination. These results may also explain some features observed among the Old Order Amish with a homozygous missense mutation in *HERC2*. Future studies will be necessary to identify additional partners involved in HERC2 physiology and its role in human diseases.

MATERIALS AND METHODS

Animals

The ES cell line AR0530 from The Sanger Institute containing a gene trap β-galactosidase/neomycin (β-geo-Neo) cassette that has integrated between exons 2 and 3 in the *Herc2* gene was used. We choose this ES cell line to study *Herc2* gene expression by β-galactosidase activity and to avoid the variability of the already existing *Herc2* mutations (deletions, point mutations, DNA rearrangements) [50]. ES cells were injected into 4.5 day C57BL/6J blastocysts, which were then implanted into pseudopregnant females. The resulting 90-95% coat color chimeras were crossed with C57BL/6 mice to generate the heterozygous animals *Herc2/Herc2*^{530} (*Herc2*$^{+/530}$). *p53* knockout mice B6.129S2-*Trp53*^{tm1Tyj}/J from Jackson laboratories [37] were kindly provided by Dr. J. Martin-Caballero. All animal experiments were performed in accordance with guidelines approved by the Ethical Committee for Animal Experimentation of the University of Barcelona.

Genotyping

Tail DNA or embryo samples were purified using the NucleoSpin Tissue kit (MACHEREY-NAGEL) according to the manufacturer's protocol. PCR amplification was performed using the primers: 530KO1 5'GGCTGCCCAGTCTCGCCTTG3' and 530KO04 5'CTGTCACCTCTCCGGGAGAAC3' for the amplification of the *Herc2* wild-type allele; Gal7 5'TTTCCATATGGGGATTGGTG3' and Gal8 5'TGTCTGTTGTGCCCAGTCAT3' for the *Herc2* 530 allele; and p53036 5'ACAGCGTGGTGGTACCT3' and p53037 5'TATACTCAGAGCCGGCCT p53038 5' CTATCAAGGCATAGCGTTGG for the genotype of p53. The PCR settings were 94°C for 3 minutes, 94°C for 1 minute, annealing at 60°C for 1 minute and elongation at

72°C for 1 minute, for 35 cycles.

RT-PCR

To assess trap expression, total RNA was isolated from mice tissues or cells using TRIsure reagent (Bioline). Two µg of total RNA was reverse-transcribed using the cDNA Reverse Transcription kit (Applied Biosystems) and random primers. To assess the trap insertion, PCR was carried out with primers: 530KO02 5'CAGGTCTGACCACCCGGAGG3'; 530KO09 5'GGGAGTTCTCGATTTTGTGC3'; and β-geo40/60 5'AGGGTTTTCCCAGTCACGAC3'. The PCR settings were 94°C for 3 minutes, 94°C for 1 minute, annealing at 55°C for 30 seconds and elongation at 72°C for 45 seconds, for 30 cycles. Additionally, cDNA was sequenced using BigDye 3.1 on an ABI 3130XL genetic analyzer (Applied Biosystems). To analyze the expression of *p21,* RT quantitative PCR was carried out using the ABI Prism 7900 HT fast-real Time PCR system and commercially available Taqman assays (Applied Biosystems): *CDKN1A* (mouse p21: Mm04205640_g1; human p21: Hs00355783_m1); *GAPDH* (mouse GAPDH: Mm99999915_g1; human GAPDH: Hs99999905_m1); and *18S (*Hs99999901_s1). The PCR data were captured and analyzed using the Sequence Detector software (SDS version 2.3, Applied Biosystems).

Histology and immunochemistry

X-gal staining of β-galactosidase activity. Mice were anesthetized and perfused via the left ventricle with 2% paraformaldehyde in a phosphate buffer (0.12 M). All tissues were dissected and fixed in the same solution for 3 hours at 4°C, and later were cryopreserved by immersion in 30% sucrose for 48 h at 4°C. Whole tissues were then embedded into an 8% gelatin and 15% sucrose solution, frozen in liquid nitrogen and stored at -80°C. Before staining for β-galactosidase activity, the tissues were sliced (7-10 µm), prepared on polylysinated slides, and permeabilized with PBS-0.3% Triton. After washing in PBS, the slices were incubated in staining solution (2 mM *X-gal*, 4 mM $K_4Fe(CN)_6$, 4 mM $K_3Fe(CN)_6$, 2 mM $MgCl_2$ in PBS) overnight while shaking in the dark at 4°C. After washing in PBS, the slices were stained with neutral red and mounted for microscopic observation.

The protocol to study the cerebellar Purkinje cells was reported previously [46]. Briefly, two and nine month old mice were deeply anaesthetised with pentobarbital (80 mg/kg i.p.), and perfused transcardially with 4% paraformaldehyde in 0.12 M phosphate buffer (PB, pH 7.2). After dissection, the brains were post-fixed overnight in the same fixative and transferred to 30% sucrose in PB until they sank. Sagittal and coronal sections of the cerebellum (40 µm thick) were cut on a freezing microtome, and collected in PBS. The sections were incubated overnight with a polyclonal anti-calbindin D-28k antibody (1:10,000). After washing, the sections were incubated for one hour in a biotinylated secondary antibody (1:500) followed by incubation for one hour in the ABC elite kit (1:400). A mixture of 0.3% DAB-0.6% nickel sulfate-0.1% hydrogen peroxide in PBS was used to reveal the immunoreaction. For double labeling analyses the sections were incubated overnight with the following primary antibodies mixtures: polyclonal anti-HERC2 (1:400)/monoclonal anti-calbindin D-28k (1:1000), and polyclonal anti-HERC2 (1:400)/monoclonal anti-p62 (1:100). After washing, the sections were incubated for one hour in a mixture of Alexa Fluor® 488 donkey-anti-rabbit (1:500) and Alexa Fluor® 594 donkey-anti-mouse (1:500). Images were acquired in a Zeiss Axio-Imager M1 microscope. Laser confocal analyses were made on an Olympus FluoView 1000 upright microscope.

Electron microscopy

Two and nine month old mice were deeply anaesthetized with pentobarbital (80 mg/kg i.p.), and perfused transcardially with a mixture of 1% paraformaldehyde and 1% glutaraldehyde in 0,12 M phosphate buffer (PB, pH 7.2). Thereafter, the brains were dissected out and immersed overnight in the same fixative. Sagittal slices of the cerebella were cut and immersed in 2% OsO_4 in PB, stained in a block with ethanolic 0.5% uranyl acetate, dehydrated with an increased gradient of ethanol, and embedded in Durcupan (Fluka®). Semithin and ultrathin sections were obtained on a Leica EM UC7 ultramicrotome. Semithin sections were stained with 1% toluidine blue. Ultrathin sections were collected in copper grids (150 and 300 mesh) and observed without counterstaining in a Zeiss Libra EM at 80 kV (CITIUS).

Behavioural tests

Anxiety

To evaluate mice anxiety, two different protocols were used [59]. Tail suspension: mice were suspended above the floor by fixing the end of the tail to wire netting and immobility was scored by manual observation during a 5 min test session. Time outside the dark box: mice were placed in a rectangular arena (55x40x40 cm^3) with a dark box with a door. The time inside/outside the box was scored by manual observation during a 5 min test session.

Learning and memory

Object recognition memory

Mice were tested as described previously [60]. Briefly, mice were placed in a rectangular arena (55x40x40 cm^3) and two identical objects were placed in the arena during the training phase. Subsequently, the animal's memory of one of the original objects was assessed by comparing the amount of time spent exploring the novel object as compared with that spent exploring the familiar one. The relative exploration of the novel object was expressed as a discrimination index [DI 5 $(t_{novel} - t_{familiar})/(t_{novel} + t_{familiar})$].

Step-through passive avoidance test

The test was performed as described previously [60]. Briefly, in the habituation phase, the mice were handled and allowed to move freely for 1 min in a chamber (47x18x26 cm^3, manufactured by Ugo Basile). In the training phase, the mice were confined to the light compartment and then 30 s later, the door separating the dark-light compartments was opened. Once mice entered the dark compartment, the door closed automatically and the mice received an electrical stimulation (0.5 mA, 5 s) delivered through the metal floor. In the retention tests, the latency to enter into a dark compartment (escape latency) is a measure of information learning or memory retention. To compare the results obtained in different experiments, the fold change in escape latency with respect to the latency obtained in the training session is calculated.

Motor function

Motor activity in the open field

To evaluate locomotor and exploratory activity, mice were placed for 5 minutes in an open field (38×21×15 cm) (Cybertec S.A.). This apparatus consisted of a walled platform containing infrared emitters and sensors (IR) coupled to an altimeter, and the movement sensor was connected to a computer that recorded the number of times the mouse interrupted the IR beams/min.

Fore limb grip strength

To evaluate fore limb strength, mice were held above a horizontal wire and lowered to allow the fore limbs to grip the wire. The ability of the mice to remain attached by the fore limbs was scored during 10 s.

Rotarod

To habituate mice to the rotarod (Ugo Basile Biological Research Apparatus), the animals were placed on the roller at a speed of 20 rpm until they could remain on it for one minute without falling off. To assay motor coordination, animals were then tested at a rotational speed of 20 rpm, accelerating to 60 rpm in increments of 5 rpm, and quantifying the number of falls at each increase in speed.

Electrophysiological analysis of the medial gastrocnemius (MG) muscle in mice

Compound muscular action potentials (CMAPs) were recorded in anesthetized mice (tribromethanol 2 %, 0.15 ml/10 g body weight, i.p.) as described previously [46,61]. Briefly, the recording needle electrode was placed into the medial part of the MG muscle and the reference electrode was situated at the base of the fifth phalanx. A ground electrode was placed at the base of the tail. Stimulating needle electrodes were placed at the sciatic notch and the head of the fibula. Stimulation protocols of supramaximal current pulses (0.05 ms duration, 5-10 mA amplitude) were applied as a short train of 100 Hz pulses generated by an isolated pulse stimulator (Pulse Train Stimulator Cibertec cs-20). The outputs recorded were differentially amplified (P511 AC Amplifier Astro-Med, INC), digitally acquired at 10,000 samples/s (CED 1401 Plus; Cambridge Electronic Designed, Cambridge, UK) and stored on a computer for later analysis. The analysis consisted of measuring the amplitude from the positive to the negative peak of the CMAPs recorded during a train of stimuli, normalizing the amplitude to the first response.

Cell culture and transfection

Human fibroblasts and ethical statements were previously described [5]. U2OS cells were obtained from ATCC. Cells were cultured at 37°C in Dulbecco's modified Eagle's medium (DMEM) supplemented with 10% fetal bovine serum, 100 units/ml penicillin, 100 µg/ml streptomycin and 2 mM glutamine. Transfection of cells with siRNAs (Non Targeting, NT: UAGCGACUAAACACAUCAA; HERC2, H2: GACUGUAGCCAGAUUGAAA) purchased from GenePharma was carried out using calcium phosphate. Transfected cells were analyzed 72 hours post-transfection. MG132 (Z-Leu-Leu-Leu-al) (Sigma-Aldrich) was added to the cells for 6 hours to a final concentration of 10 µM.

Antibodies used

The following antibodies were used: anti-HERC2 monoclonal (BD Biosciences); anti-HERC2 polyclonal [32]; anti-p21 (C-19); anti-p62 (SQSTM1 (D-3): sc-28359); anti β-actin (Santa Cruz Biotechnology, Inc.); anti-calbindin D-28k polyclonal (Cb-38a, Swant); anti-calbindin D-28k monoclonal (Cb-955, Sigma); anti-p53

Ab-5 (DO-7) (Neo Markers); anti-USP33 (Proteintech); anti-Ran [62]; anti α-tubulin (Ab-1, Calbiochem); Alexa Fluor® 488 donkey-anti-rabbit (A21207), and Alexa Fluor® 594 donkey-anti-mouse (A21203) (Invitrogen); horseradish peroxidase-conjugated secondary antibodies (Invitrogen); biotin-conjugated secondary antibodies (Vector); and the Avidine-Streptavidine Elite Kit (Vector).

Lysate and immunoblot

Mice were euthanized by cervical dislocation. The organs were collected and frozen in liquid nitrogen and stored at -80°C until analysis. Tissues, human fibroblasts or U2OS cells were prepared in lysis buffer (consisting of 50 mM TrisHCl, pH 7.5, 150 mM NaCl, 0.5% NP40, 50 mM β-glycerophosphate, 50 mM NaF, 1 mM sodium vanadate, 1 mM phenyl-methylsulfonyl fluoride, 5 μg/mL leupeptin, 5 μg/mL aprotinin, 1 μg/mL pepstatin-A and benzamidine 100 μg/mL) and the tissues were homogenized in a motor-driven Polytron PT3000. The lysates were incubated on ice for 20 minutes and centrifuged at 13,000 g for 10 minutes at 4°C. Total protein levels were measured by BCA (Pierce). Equal amounts of supernatant proteins were analyzed using the Tris-acetate PAGE system [63]. Band intensities were analyzed using a gel documentation system (LAS-3000, Fujifilm). Proteins levels were normalized and expressed as a percentage of controls.

Statistical analysis

The results are expressed as mean±SEM. The data were analyzed by one-way analysis of variance (ANOVA) or Student's *t*-test. For comparison of significance, Tukey's test was used as a post hoc test according to the statistical program GraphPad Prism. Differences were considered significant at p values of less than 0.05: $*p < 0.05$, $**p < 0.01$, and $***p < 0.001$.

ACKNOWLEDGMENTS

We would like to thank The Sanger Institute for the ES cell line AR0530, J. Martin-Caballero for *p53*$^{-/-}$ mice, and A. Gimeno, E. Adanero, A. Angelo, E. Castaño and B. Torrejon for technical assistance. We also acknowledge S. Sánchez-Tena for valuable discussion throughout this study, and G. Alvarez de Toledo for the facilities to use the FluoView 1000 laser confocal scanning microscope. RR held a Juan de la Cierva contract JCI-2011-08888 from the MINECO and VPPI-US from the University of Sevilla. TS and LP were supported by fellowships from the CAPES Foundation (Ministry of Education from Brazil) and from CNPq-Programa Ciências sem Fronteiras (Ministry of Science, Technology and Innovation Education of Brazil), respectively. This article is based upon work from COST Action (PROTEOSTASIS BM1307), supported by COST (European Cooperation in Science and Technology).

CONFLICTS OF INTEREST

All authors have not conflicts of interest to disclose.

GRANT SUPPORT

This work was supported by grants from Spanish Ministerio de Ciencia e Innovación [BFU2011-22498 to J.L.R. and BFU2014-56313P to F.V.] and Brazilian Scientific Program "Ciências sem Fronteiras" from the Ministry of Science, Technology and Innovation Education of Brazil [313600/2013-9 to J.L.R. and 400422/2013-1 to J.R.O.].

Editorial note

This paper has been accepted based in part on peer-review conducted by another journal and the authors' response and revisions as well as expedited peer-review in Oncotarget.

REFERENCES

1. Williams CA, Beaudet AL, Clayton-Smith J, Knoll JH, Kyllerman M, Laan LA, Magenis RE, Moncla A, Schinzel AA, Summers JA, Wagstaff J. Angelman syndrome 2005: updated consensus for diagnostic criteria. Am J Med Genet A. 2006; 140: 413-418.
2. Mabb AM, Judson MC, Zylka MJ, Philpot BD. Angelman syndrome: insights into genomic imprinting and neurodevelopmental phenotypes. Trends Neurosci. 2011; 34: 293-303.
3. Williams CA, Driscoll DJ, Dagli AI. Clinical and genetic aspects of Angelman syndrome. Genet Med. 2010; 12: 385-395.
4. Puffenberger EG, Jinks RN, Wang H, Xin B, Fiorentini C, Sherman EA, Degrazio D, Shaw C, Sougnez C, Cibulskis K, Gabriel S, Kelley RI, Morton DH, et al. A homozygous missense mutation in HERC2 associated with global developmental delay and autism spectrum disorder. Hum Mutat. 2012; 33: 1639-1646.
5. Harlalka G V, Baple EL, Cross H, Kuhnle S, Cubillos-Rojas M, Matentzoglu K, Patton MA, Wagner K, Coblentz R, Ford DL, Mackay DJ, Chioza BA, Scheffner M, et al. Mutation of HERC2 causes developmental delay with Angelman-like features. J Med Genet. 2013; 50: 65-73.
6. Cassidy SB, Schwartz S, Miller JL, Driscoll DJ. Prader-Willi syndrome. Genet Med. 2012; 14: 10-26.
7. Kühnle S, Kogel U, Glockzin S, Marquardt A, Ciechanover A, Matentzoglu K, Scheffner M. Physical and functional interaction of the HECT ubiquitin-protein ligases E6AP and

HERC2. J Biol Chem. 2011; 286: 19410-19416.

8. Pośpiech E, Draus-Barini J, Kupiec T, Wojas-Pelc A, Branicki W. Gene-gene interactions contribute to eye colour variation in humans. J Hum Genet. 2011; 56: 447-455.
9. Mengel-From J, Børsting C, Sanchez JJ, Eiberg H, Morling N. Human eye colour and HERC2, OCA2 and MATP. Forensic Sci Int Genet. 2010; 4: 323-328.
10. White D, Rabago-Smith M. Genotype-phenotype associations and human eye color. J Hum Genet. 2011; 56: 5-7.
11. Garcia-Gonzalo FR, Rosa JL. The HERC proteins: functional and evolutionary insights. Cell Mol Life Sci. 2005; 62: 1826-38.
12. Hadjebi O, Casas-Terradellas E, Garcia-Gonzalo FR, Rosa JL. The RCC1 superfamily: From genes, to function, to disease. Biochimica et Biophysica Acta - Molecular Cell Research. 2008; 1783: 1467-1479.
13. Dastur A, Beaudenon S, Kelley M, Krug RM, Huibregtse JM. Herc5, an interferon-induced HECT E3 enzyme, is required for conjugation of ISG15 in human cells. J Biol Chem. 2006; 281: 4334-4338.
14. Kroismayr R, Baranyi U, Stehlik C, Dorfleutner A, Binder BR, Lipp J. HERC5, a HECT E3 ubiquitin ligase tightly regulated in LPS activated endothelial cells. J Cell Sci. 2004; 117: 4749-4756.
15. Hochrainer K, Kroismayr R, Baranyi U, Binder BR, Lipp J. Highly homologous HERC proteins localize to endosomes and exhibit specific interactions with hPLIC and Nm23B. Cell Mol Life Sci. 2008; 65: 2105-2117.
16. Diouf B, Cheng Q, Krynetskaia NF, Yang W, Cheok M, Pei D, Fan Y, Cheng C, Krynetskiy EY, Geng H, Chen S, Thierfelder WE, Mullighan CG, et al. Somatic deletions of genes regulating MSH2 protein stability cause DNA mismatch repair deficiency and drug resistance in human leukemia cells. Nat Med. 2011; 17: 1298-1303.
17. Bekker-Jensen S, Rendtlew Danielsen J, Fugger K, Gromova I, Nerstedt A, Lukas C, Bartek J, Lukas J, Mailand N. HERC2 coordinates ubiquitin-dependent assembly of DNA repair factors on damaged chromosomes. Nat Cell Biol. 2010; 12: 12-80.
18. Yoo NJ, Park SW, Lee SH. Frameshift mutations of ubiquitination-related genes HERC2, HERC3, TRIP12, UBE2Q1 and UBE4B in gastric and colorectal carcinomas with microsatellite instability. Pathology. 2011; 43: 753-755.
19. Zhou H, Shi R, Wei M, Zheng W-L, Zhou JY, Ma WL. The expression and clinical significance of HERC4 in breast cancer. Cancer Cell Int. 2013; 13: 113.
20. Sánchez-Tena S, Cubillos-Rojas M, Schneider T, Rosa JL. Functional and pathological relevance of HERC family proteins: a decade later. Cell Mol Life Sci. 2016; 73: 1955-1968.
21. Kang T-H, Lindsey-Boltz L a, Reardon JT, Sancar A. Circadian control of XPA and excision repair of cisplatin-DNA damage by cryptochrome and HERC2 ubiquitin ligase. Proc Natl Acad Sci U S A. 2010; 107: 4890-4895.
22. Wu W, Sato K, Koike A, Nishikawa H, Koizumi H, Venkitaraman AR, Ohta T. HERC2 is an E3 ligase that targets BRCA1 for degradation. Cancer Res. 2010; 70: 6384-6392.
23. Oestergaard VH, Pentzold C, Pedersen RT, Iosif S, Alpi A, Bekker-Jensen S, Mailand N, Lisby M. RNF8 and RNF168 but not HERC2 are required for DNA damage-induced ubiquitylation in chicken DT40 cells. DNA Repair (Amst). 2012; 11: 892-905.
24. Al-Hakim AK, Bashkurov M, Gingras AC, Durocher D, Pelletier L. Interaction Proteomics Identify NEURL4 and the HECT E3 Ligase HERC2 as Novel Modulators of Centrosome Architecture. Mol Cell Proteomics. 2012; 11: M111.014233.
25. Chan NC, Den Besten W, Sweredoski MJ, Hess S, Deshaies RJ, Chan DC. Degradation of the deubiquitinating enzyme USP33 is mediated by p97 and the ubiquitin ligase HERC2. J Biol Chem. 2014; 289: 19789-19798.
26. Moroishi T, Yamauchi T, Nishiyama M, Nakayama KI. HERC2 targets the iron regulator FBXL5 for degradation and modulates iron metabolism. J Biol Chem. 2014; 289: 16430-16441.
27. Brady CA, Attardi LD. P53 at a Glance. J Cell Sci. 2010; 123: 2527-2532.
28. Kruse JP, Gu W. Modes of p53 Regulation. Cell. 2009; 137: 609-622.
29. Itahana Y, Ke H, Zhang Y. p53 Oligomerization is essential for its C-terminal lysine acetylation. J Biol Chem. 2009; 284: 5158-5164.
30. Davison TS, Yin P, Nie E, Kay C, Arrowsmith CH. Characterization of the oligomerization defects of two p53 mutants found in families with Li-Fraumeni and Li-Fraumeni-like syndrome. Oncogene. 1998; 17: 651-656.
31. Lomax ME, Barnes DM, Hupp TR, Picksley SM, Camplejohn RS. Characterization of p53 oligomerization domain mutations isolated from Li-Fraumeni and Li-Fraumeni like family members. Oncogene. 1998; 17: 643-649.
32. Cubillos-Rojas M, Amair-Pinedo F, Peiró-Jordán R, Bartrons R, Ventura F, Rosa JL. The E3 ubiquitin protein ligase HERC2 modulates the activity of tumor protein p53 by regulating its oligomerization. J Biol Chem. 2014; 289: 14782-14795.
33. Jones SN, Roe AE, Donehower LA, Bradley A. Rescue of embryonic lethality in Mdm2-deficient mice by absence of p53. Nature. 1995; 378: 206-208.
34. Parant J, Chavez-Reyes A, Little NA, Yan W, Reinke V, Jochemsen AG, Lozano G. Rescue of embryonic lethality in Mdm4-null mice by loss of Trp53 suggests a nonoverlapping pathway with MDM2 to regulate p53. Nat Genet. 2001; 29: 92-95.

35. Montes de Oca Luna R, Wagner DS, Lozano G. Rescue of early embryonic lethality in mdm2-deficient mice by deletion of p53. Nature. 1995; 378: 203-206.
36. Donehower LA, Harvey M, Slagle BL, McArthur MJ, Montgomery CA, Butel JS, Bradley A. Mice deficient for p53 are developmentally normal but susceptible to spontaneous tumours. Nature. 1992; 356: 215-221.
37. Jacks T, Remington L, Williams BO, Schmitt EM, Halachmi S, Bronson RT, Weinberg RA. Tumor spectrum analysis in p53-mutant mice. Curr Biol. 1994; 4: 1-7.
38. Donehower L a, Lozano G. 20 Years Studying P53 Functions in Genetically Engineered Mice. Nat Rev Cancer. 2009; 9: 831-41.
39. Li T, Kon N, Jiang L, Tan M, Ludwig T, Zhao Y, Baer R, Gu W. Tumor suppression in the absence of p53-mediated cell-cycle arrest, apoptosis, and senescence. Cell. 2012; 149: 1269-1283.
40. Brady CA, Jiang D, Mello SS, Johnson TM, Jarvis LA, Kozak MM, Broz DK, Basak S, Park EJ, McLaughlin ME, Karnezis AN, Attardi LD. Distinct p53 transcriptional programs dictate acute DNA-damage responses and tumor suppression. Cell. 2011; 145: 571-583.
41. Valente LJ, Gray DHD, Michalak EM, Pinon-Hofbauer J, Egle A, Scott CL, Janic A, Strasser A. p53 efficiently suppresses tumor development in the complete absence of its cell-cycle inhibitory and proapoptotic effectors p21, Puma, and Noxa. Cell Rep. 2013; 3: 1339-1345.
42. Dusart I, Guenet JL, Sotelo C. Purkinje cell death: differences between developmental cell death and neurodegenerative death in mutant mice. Cerebellum. 2006; 5: 163-173.
43. Hawkes R, colonnier M, Leclerc N. Monoclonal antibodies reveal sagittal banding in the rodent cerebellar cortex. Brain Res. 1985; 333: 359-365.
44. Mashimo T, Hadjebi O, Amair-Pinedo F, Tsurumi T, Langa F, Serikawa T, Sotelo C, Guenet JL, Rosa JL. Progressive Purkinje cell degeneration in tambaleante mutant mice is a consequence of a missense mutation in HERC1 E3 ubiquitin ligase. PLoS Genet. 2009; 5: e1000784.
45. Ruiz R, Pérez-Villegas EM, Bachiller S, Rosa JL, Armengol JA. HERC 1 Ubiquitin Ligase Mutation Affects Neocortical, CA3 Hippocampal and Spinal Cord Projection Neurons: An Ultrastructural Study. Front Neuroanat. 2016; 10: 42.
46. Bachiller S, Rybkina T, Porras-García E, Pérez-Villegas E, Tabares L, Armengol JA, Carrión AM, Ruiz R. The HERC1 E3 Ubiquitin Ligase is essential for normal development and for neurotransmission at the mouse neuromuscular junction. Cell Mol Life Sci. 2015; 72: 2961-2971.
47. Galligan JT, Martinez-Noël G, Arndt V, Hayes S, Chittenden TW, Harper JW, Howley PM. Proteomic analysis and identification of cellular interactors of the giant ubiquitin ligase HERC2. J Proteome Res. 2015; 14: 953-966.
48. Campana ALM, Rondi-Reig L, Tobin C, Lohof AM, Picquet F, Falempin M, Weitzman JB, Mariani J. p53 inactivation leads to impaired motor synchronization in mice. Eur J Neurosci. 2003; 17: 2135-2146.
49. Tomasevic G, Raghupathi R, Scherbel U, Wieloch T, McIntosh TK. Deletion of the p53 tumor suppressor gene improves neuromotor function but does not attenuate regional neuronal cell loss following experimental brain trauma in mice. J Neurosci Res. 2010; 88: 3414-3423.
50. Walkowicz M, Ji Y, Ren X, Horsthemke B, Russell LB, Johnson D, Rinchik EM, Nicholls RD, Stubbs L. Molecular characterization of radiation- and chemically induced mutations associated with neuromuscular tremors, runting, juvenile lethality, and sperm defects in jdf2 mice. Mamm Genome. 1999; 10: 870-878.
51. Ji Y, Walkowicz MJ, Buiting K, Johnson DK, Tarvin RE, Rinchik EM, Horsthemke B, Stubbs L, Nicholls RD. The ancestral gene for transcribed, low-copy repeats in the Prader-Willi/Angelman region encodes a large protein implicated in protein trafficking, which is deficient in mice with neuromuscular and spermiogenic abnormalities. Hum Mol Genet. 1999; 8: 533-542.
52. Lehman AL, Nakatsu Y, Ching A, Bronson RT, Oakey RJ, Keiper-Hrynko N, Finger JN, Durham-Pierre D, Horton DB, Newton JM, Lyon MF, Brilliant MH. A very large protein with diverse functional motifs is deficient in rjs (runty, jerky, sterile) mice. Proc Natl Acad Sci U S A. 1998; 95: 9436-9441.
53. Yue Z, Horton A, Bravin M, DeJager PL, Selimi F, Heintz N. A novel protein complex linking the δ2 glutamate receptor and autophagy: Implications for neurodegeneration in lurcher mice. Neuron. 2002; 35: 921-933.
54. Selimi F, Lohof AM, Heitz S, Lalouette A, Jarvis CI, Bailly Y, Mariani J. Lurcher GRID2-induced death and depolarization can Be dissociated in cerebellar Purkinje cells. Neuron. 2003; 37: 813-819.
55. Chakrabarti L, Eng J, Ivanov N, Garden GA, La Spada AR. Autophagy activation and enhanced mitophagy characterize the Purkinje cells of pcd mice prior to neuronal death. Mol Brain. 2009; 2: 24.
56. Nishiyama J, Miura E, Mizushima N, Watanabe M, Yuzaki M. Aberrant membranes and double-membrane structures accumulate in the axons of Atg5-null Purkinje cells before neuronal death. Autophagy. 2007; 3: 591-596.
57. Komatsu M, Wang QJ, Holstein GR, Friedrich VL, Iwata J, Kominami E, Chait BT, Tanaka K, Yue Z. Essential role for autophagy protein Atg7 in the maintenance of axonal homeostasis and the prevention of axonal degeneration. Proc Natl Acad Sci U S A. 2007; 104: 14489-14494.
58. Imai Y, Kobayashi Y, Inoshita T, Meng H, Arano T, Uemura K, Asano T, Yoshimi K, Zhang CL, Matsumoto G, Ohtsuka T, Kageyama R, Kiyonari H, et al. The Parkinson's Disease-Associated Protein Kinase LRRK2 Modulates Notch Signaling through the Endosomal Pathway. PLoS Genet. 2015; 11:e1005503.

59. Romero-Granados R, Fontán-Lozano Á, Aguilar-Montilla FJ, Carrión ÁM. Postnatal proteasome inhibition induces neurodegeneration and cognitive deficiencies in adult mice: a new model of neurodevelopment syndrome. PLoS One. 2011; 6: e28927.

60. Suárez-Pereira I, Canals S, Carrión AM. Adult newborn neurons are involved in learning acquisition and long-term memory formation: the distinct demands on temporal neurogenesis of different cognitive tasks. Hippocampus. 2015; 25: 51-61.

61. Ruiz R, Tabares L. Neurotransmitter release in motor nerve terminals of a mouse model of mild spinal muscular atrophy. J Anat. 2014; 224: 74-84.

62. Rosa JL, Casaroli-Marano RP, Buckler AJ, Vilaro S, Barbacid M. p619, a giant protein related to the chromosome condensation regulator RCC1, stimulates guanine nucleotide exchange on ARF1 and Rab proteins. EMBO J. 1996; 15: 4262-4273.

63. Cubillos-Rojas M, Amair-Pinedo F, Tato I, Bartrons R, Ventura F, Rosa JL. Simultaneous electrophoretic analysis of proteins of very high and low molecular mass using Tris-acetate polyacrylamide gels. Electrophoresis. 2010; 31: 1318-1321.

Pontifícia Universidade Católica do Rio Grande do Sul
Pró-Reitoria Acadêmica
Av. Ipiranga, 6681 - Prédio 1 - 3º. andar
Porto Alegre - RS - Brasil
Fone: (51) 3320-3500 - Fax: (51) 3339-1564
E-mail: proacad@pucrs.br
Site: www.pucrs.br/proacad